Utilising novel clinically relevant mouse models to test new therapeutic interventions for peripheral artery diseases

Thesis submitted by

James Andrew Phie

BSc (Hons)

For the degree of Doctor of Philosophy

In the College of Medicine and Dentistry

James Cook University, Townsville, Australia

(February 2020)

STATEMENT OF SOURCES DECLARATION

Every reasonable effort has been made to gain permission and acknowledge the owners of copyright material. I would be pleased to hear from any copyright owner who has been omitted or incorrectly acknowledged.

Name

James Phie

Signature

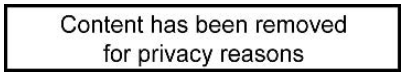

Date

16.02.2020

ACKNOWLEDGEMENTS

First and foremost, I would like to thank my primary advisor, Professor Jonathan Golledge. Thank you Jon for the inexhaustible effort that you apply to each and every project that I am involved in, and for all your help in preparing this thesis and related publications. Thank you for your lightning fast response times. Your efficiency and work ethic are both terrifying and inspiring. Thank you for your kind words of encouragement and for supporting me in many different ways throughout my PhD.

I owe many thanks to my co-advisors, Dr Robert Kinobe, Dr Smriti Krishna, Dr Joseph Moxon, and Dr Corey Moran. Robert, you have been a mentor and advisor to me for the better part of a decade, and I would not be the scientist I am today without your continued encouragement and support. Your advice and feedback have been instrumental in the writing of this thesis and in my career thus far. Smriti, thank you for always being there, answering my endless questions about the academic world and for all the time you have dedicated to teaching me laboratory techniques. Joe, thank you for all of your in-depth and insightful feedback on all of my projects, and for all the mentorship and advice you have given me over the years. Corey, it has been a pleasure to work with and learn from you over my PhD candidature. Thank you for your help troubleshooting experimental issues, brainstorming ideas and setting up animal models, and for all your thoughtful advice.

I owe many thanks to the past and current members of the Queensland Research Centre for Peripheral Vascular Disease. Thanks are due to Dr Susan Morton, Dr Malindu Fernando, Mrs Sharon Lazzaroni, Dr Shiv Thanigaimani, Dr Eric Biros, and Ms Kathleen Pola. I owe thanks to my colleague Dr Pacific Huynh. Thank you for your enthusiasm assisting with my PhD projects, and for all the salads, food gifts and lunchtime musings.

Thanks to Dr Melissa Crowe, Dr Diana Mendez and the rest of the doctoral cohort program. The work you do with this program has provided invaluable help and support to myself and countless other candidates. Thank you to Dr Ann Kraeuter for lending the open field assessment facilities and for teaching me how to use the open field analysis software, animal handling and gavage skills. Thank you to Dr Sandip Kamath for draft feedback and mentorship early on in my candidature, and to Mr Kunal Pratap for helpful discussion and recommendations for laboratory assays.

Thank you to Associate Professor Suzy Munns for all the time you have dedicated to mentoring me, and for introducing me to the joys of teaching. Thanks also to Associate Professor Damien Paris for helpful discussion and advice, and to Emeritus Professor Rhondda Jones for your support and invaluable advice on the statistical analyses used in this thesis.

Thank you to Dr Lynn Woodward, Mr Chris wright, Mrs Susan Wright, Mrs Emma Anderson and Mr Lachlan Pomfrett. Your assistance throughout the years cannot be understated.

Thank you to Jack Williams for all of your support through the final wing of this journey.

Finally, thank you to my parents, Ross and Donna Phie. Thank you for all that you have done and all that you continue to do. Thank you for supporting me through all my endeavours. I would not be where I am today without your unconditional love and support.

STATEMENT OF THE CONTRIBUTION OF OTHERS TO THE THESIS

Nature of Assistance	Contribution to thesis	Name and title of co-contributors
Intellectual support	Project design and aims, planning, manuscript drafting and editing, drafting of thesis	Professor Jonathan Golledge Dr Smriti Krishna Dr Joseph Moxon Dr Corey Moran Dr Robert Kinobe
	Advice on statistics	Dr Joseph Moxon Emeritus Professor Rhondda Jones
Financial support	Stipends	JCU Australian Postgraduate Award Top-up scholarship from the College of Medicine and Dentistry
	Research costs	Primary advisor funds AITHM award JCU graduate research school grants
	Conference travel	JCU College of Medicine and Dentistry minimum resources fund Australian Vascular Biology Society travel award
Technical support	Animal surgeries	Dr Smriti Krishna Dr Pacific Huynh Dr Robert Kinobe
	Experimental procedures for animal studies	Dr Smriti Krishna Dr Pacific Huynh Dr Corey Moran Dr Susan Morton Dr Aluísio Andrade-Lima

STATEMENT OF THE CONTRIBUTION OF OTHERS TO PUBLISHED CHAPTERS

Chapter	Details of publications which chapter is based	Nature and extent of the intellectual input of each author, including the candidate
Chapter 4	**Phie, James**, Krishna, Smriti M., Moxon, Joseph V., Omer, Safraz M., Kinobe, Robert, and Golledge, Jonathan. *Flavonols reduce aortic atherosclerosis lesion area in apolipoprotein E deficient mice: a systematic review and meta-analysis.* PLoS ONE, 2017. 12 (7). e0181832. pp. 1-13.	James Phie developed the research question. James Phie performed all analyses and was provided statistical help by Joseph Moxon. Smriti Krishna and Safraz Omer independently performed the same analyses and results from all three observers were collated. James Phie wrote the first draft of the paper which was revised with editorial input from Smriti Krishna, Joseph Moxon, Robert Kinobe and Jonathan Golledge. James Phie prepared all figures and tables.
Chapter 6	**Phie, James**, Moxon, Joseph V., Krishna, Smriti M., Kinobe, Robert, Morton, Susan K., and Golledge, Jonathan. A diet enriched with tree nuts reduces severity of atherosclerosis but not abdominal aneurysm in angiotensin II-infused apolipoprotein E deficient mice. Atherosclerosis, 2018. 277. pp. 28-33.	The authors co-developed the research question. James Phie and Jonathan Golledge planned outcome measures and study design. James Phie performed all experiments with the help of Joseph Moxon, Smriti Krishna, Robert Kinobe and Susan Morton. James Phie performed statistical data analyses with assistance from Joseph Moxon. James Phie prepared the first draft of the paper with editorial input from all co-authors. James Phie prepared all figures and tables.

ABSTRACT

Lower limb peripheral artery disease and abdominal aortic aneurysm are two of the commonest forms of vascular disease. These diseases often occur concurrently and both currently lack effective pharmacological treatments. Animal studies have reported positive results from many therapeutic interventions in vascular disease models, however these interventions were not beneficial when administered to patients in subsequent randomized controlled trials. This suggests that the translatability of current vascular animal models needs to be improved for successful drug discovery. This thesis used mouse models with a focus on clinically relevant study design to test potentially promising therapeutics for the treatment of vascular diseases.

A two-stage surgical procedure was used to induce lower limb ischemia by gradual occlusion of the femoral artery with ameroid constrictors and subsequent ligation and resection of the femoral artery. Blood flow to the lower limb was significantly lower than baseline for the duration of the experiments. This allowed for assessment of interventions in stable ischemia without recovery, which is more comparable to chronic limb ischemia that occurs in patients. Patients with chronic limb ischemia typically suffer from reduced exercise performance and pain on exertion, resulting from reduced blood flow and inflammation. The nutraceutical, quercetin, was previously reported to improve exercise performance and blood flow, and reduce pain and inflammation in mice. A dietary intervention containing quercetin, at doses translatable to human patients, was tested in the established two-stage lower limb ischemia model. Quercetin did not significantly improve exercise performance, or reduce pain in this model. Furthermore, blood flow was not improved despite significant increases in the pro-angiogenic signalling molecule nitric oxide in the plasma. Additionally, quercetin did not significantly reduce plasma cytokines (Interleukin-6, 10, 12 or tumour necrosis factor alpha) in the stable limb ischemia model.

The angiotensin II subcutaneous infusion model of abdominal aortic aneurysm is the most commonly used aneurysm model, and is suitable for testing preventative interventions. Aneurysms formed with the angiotensin II model had high rupture rates, which are a key feature of human abdominal aortic aneurysms. Quercetin and omega-3 fatty acids have both been reported to reduce the development of abdominal aortic aneurysm in animal models. Tree nuts contain both quercetin and omega-3 fatty acids, and preventative dietary intervention with nuts has been associated with reduction in atherosclerosis lesion

area in mice, and reduced risk of lower limb peripheral artery disease development in humans. Macadamia and pecan nuts were administered, at doses translatable to human patients, for 56 days including 28 days prior to angiotensin II infusion, and for 28 days alongside angiotensin II infusion. Despite promising effects of nut constituents in abdominal aortic aneurysm prevention, a diet enriched with macadamia and pecan nuts did not significantly reduce aneurysm development or aortic rupture. However, similar to previous reported studies, the dietary intervention with nuts significantly reduced atherosclerotic plaque development in the aortic arch and brachiocephalic artery.

While the angiotensin II model has been effective for testing prevention treatments, a newly developed model using topical aortic application of elastase and 0.2% w/v 3-aminopropionitrile fumarate salt in drinking water was deemed more suitable for testing treatment interventions in pre-established disease. As previously reported, we found that the model caused long-term, continually growing aneurysms that were prone to developing intraluminal thrombi and aortic rupture, which are both important features of human abdominal aortic aneurysm. Additionally, similar to patients, it was found that the inflammasome was significantly upregulated in the elastase and 3-aminopropionitrile fumarate model as evidenced by increases in caspase-1 activity and aortic Interleukin-1 beta concentration.

Colchicine, an FDA approved drug for the treatment of gout, is a potent inhibitor of the inflammasome. Data from recent studies reported that colchicine reduced ST-segment-elevation myocardial infarction size in patients, and studies are underway testing the effects of colchicine in atherosclerosis. No studies have assessed the effects of colchicine in abdominal aortic aneurysm, however. Surgeries were performed with topical elastase application and 3-aminopropionitrile fumarate salt was administered in drinking water for 21 days prior to administration of either colchicine or vehicle, which were administered daily via gavage for a total of 70 days. We found that treatment with colchicine did not reduce the growth and rupture rate of small abdominal aortic aneurysms in this model, despite significantly reducing caspase-1 activity. Furthermore, treatment with colchicine did not reduce gene and protein expression of inflammatory cytokines (Interleukin-1 beta, interleukin-18, tumour necrosis factor alpha or interferon gamma) or amount of cluster of differentiation 68 (Macrophages) and cluster of differentiation 3 (T cells) present within the aorta or intraluminal thrombus.

Particular emphasis has been placed on the experimental model design and timing and route of administration of interventions in order to improve clinical relevance of the disease models. As a result, the therapeutics tested above did not improve major outcomes of peripheral artery disease despite previous *in vitro* and *in vivo* evidence suggesting that these treatments may potentially be beneficial. These data emphasize that study design and the experimental model chosen has a marked impact on whether interventions have a positive effect. These results suggest careful consideration should made when designing animal studies in order to ensure that results are translatable to patients.

TABLE OF CONTENTS

Statement of sources declaration ii

Acknowledgements iii

Statement of the contribution of others to the thesis v

Statement of the contribution of others to published chapters vi

Abstract vii

Table of contents x

List of abbreviations xvi

List of figures xix

List of tables xxii

Preface xxiii

Publications arising from thesis chapters xxiv

CHAPTER 1 General introduction 1

1.1 Peripheral artery diseases 1

1.2 Lower limb PAD and intermittent claudication 1

1.2.1 Pathophysiology of lower limb PAD leading to IC 1

1.2.2 Current management strategies for IC 4

1.2.3 Current animal models of IC 5

1.2.4 Selection of a suitable mouse model of IC 7

1.3 AAA 10

1.3.1 Formation and pathophysiology of AAA 10

1.3.2 Current management strategies for AAA 11

1.3.3 Current animal models of AAA 12

1.3.4 Selection of suitable mouse models of AAA 16

1.4 Pre-clinical study design features and impact on translatability of results 19

1.5 Potential therapeutic interventions for IC and small AAA 20

1.5.1 The flavonoid quercetin as a potential treatment for IC 20
1.5.2 Nut supplementation as a potential preventative for AAA 28
1.5.3 Colchicine as a potential treatment for AAA 29
1.6 Summary of thesis focus and aims 30
CHAPTER 2 General materials and methods 32
2.1 Animals 32
2.2 Isoflurane anaesthesia 32
2.3 Ultrasound assessment of aortic diameter 33
2.4 Tail cuff plethysmography for measurement of blood pressure 33
2.5 Laser Doppler perfusion imaging 34
2.6 *Ex vivo* morphometric assessment of aortic diameter 34
2.7 Tail vein blood sampling 34
2.8 Cardiac puncture 35
2.9 Blood centrifugation for plasma 35
2.10 Sacrifice/Dissection 35
2.11 *En face* staining of aortic arch 35
2.11.1 Preparation of *en face* staining 35
2.11.2 Sudan IV staining procedure 36
2.11.3 Sudan IV data analysis 36
2.12 Histology 36
2.12.1 Fixing, processing and paraffin embedding 36
2.12.2 Storing and preparation of frozen sections 36
2.12.3 Haematoxylin and Eosin staining 37
2.12.4 Verhoeff Van Gieson's elastin staining 37
2.12.5 Picrosirius red staining 38
2.13 Brachiocephalic artery atherosclerosis lesion area determination 38
2.14 Protein extraction and quantification of aortic total protein concentration 38

2.15 Statistical analyses 39

CHAPTER 3 Reproducbility of outcome measures 41

3.1 Outline 41

3.2 Ultrasound measurements of cross-sectional aortic diameter 41

3.3 Blood pressure 42

3.4 Blood flow measurements using laser Doppler perfusion imaging 43

3.5 *Ex vivo* measurements of aortic diameter 43

3.6 Atherosclerosis lesion area in the brachiocephalic artery 44

CHAPTER 4 Flavonols reduce aortic atherosclerosis lesion area in mice: A systematic review and meta-analysis 46

4.1 Introduction 46

4.2 Materials and methods 47

4.2.1 Search strategy, inclusion and exclusion criteria 47

4.2.2 Data extraction and quality assessment tool 48

4.2.3 Statistical analysis 49

4.3 Results 49

4.3.1 Study selection 49

4.3.2 Study characteristics 51

4.3.3 Atherosclerosis lesion area 54

4.3.4 Plasma lipids 56

4.3.5 Oxidative stress 56

4.3.6 Quality assessment of included studies 56

4.3.7 Meta-analysis, sensitivity analyses and funnel plots 60

4.4 Discussion 64

CHAPTER 5 Quercetin does not improve exercise performance or blood flow in a novel model of sustained hind limb ischemia 68

5.1 Introduction 68

5.2 Materials and Methods 69

5.2.1 Mice 69
5.2.2 Study design and outcome assessment 69
5.2.3 Two-stage induction of HLI 71
5.2.4 Experimental groups 72
5.2.5 Assessment of exercise performance with a treadmill test 72
5.2.6 Assessment of physical activity with an open field test 72
5.2.7 Assessment of pressure sensitivity from pressure application 73
5.2.8 Assessment of blood flow with laser Doppler perfusion imaging 73
5.2.9 Preparation of plasma samples 73
5.2.10 Total plasma nitrate and nitrite concentration 73
5.2.11 Quantification of plasma cytokines 73
5.2.12 Sample size calculation 74
5.2.13 Statistical analyses 74
5.3 Results 75
5.3.1 Mice welfare 75
5.3.2 Quercetin did not improve exercise performance, reduce pressure sensitivity or improve physical activity 75
5.3.3 Quercetin did not improve hind limb blood supply despite increase in plasma total nitrates 77
5.3.4 Quercetin did not influence plasma cytokine concentrations 79
5.4 Discussion 80
CHAPTER 6 Tree nut supplementation reduces the severity of atherosclerosis but not AAA in mice 82
6.1 Introduction 82
6.2 Materials and Methods 83
6.2.1 Mice 83
6.2.2 Study design 83
6.2.3 Micro-osmotic pump implantation 84

6.2.4 Dietary interventions 84
6.2.5 Assessment of AAA severity 84
6.2.6 Assessment of blood pressure 85
6.2.7 Quantification of atherosclerosis severity 85
6.2.8 Sample size calculation 85
6.2.9 Statistical analyses 86
6.3 Results 86
6.3.1 A diet enriched with nuts did not influence Ang II-induced AAA incidence or severity 88
6.3.2 The diet enriched with nuts reduced the severity of atherosclerosis in the brachiocephalic artery but not the aortic arch of *ApoE*$^{-/-}$ mice 91
6.3.3 A diet enriched with nuts did not affect blood pressure 92
6.4 Discussion 94
CHAPTER 7 Colchicine does not reduce AAA growth in a novel E-BAPN induced mouse model 97
7.1 Introduction 97
7.2 Methods 98
7.2.1 Mice 98
7.2.2 Study design 98
7.2.3 Induction of AAA 100
7.2.4 Intervention and vehicle control groups 100
7.2.5 Ultrasound assessment of infrarenal aortic diameter 100
7.2.6 Morphometric assessment of infrarenal aortic diameter 100
7.2.7 Aneurysm severity 101
7.2.8 Histological assessment of elastin degradation and collagen content 101
7.2.9 Measurement of tissue cytokines and caspase-1 activity 101
7.2.10 Immunofluorescence 102
7.2.11 Sample size calculations 102

7.2.12 Statistical analyses 103
7.3 Results 103
7.3.1 Characteristics of the E-BAPN model 103
7.3.2 Tissue Caspase-1 activity and IL-1β concentration 106
7.3.3 Colchicine administration did not reduce the growth of established AAAs 106
7.3.4 Colchicine administration reduced Caspase-1 activity but did not reduce tissue inflammatory cytokine concentrations or RNA expression 109
7.4 Discussion 111
CHAPTER 8 General discussion and conclusions 114
8.1 Summary of main findings 114
8.2 Impact of experimental design on study results and the importance of clinical relevance 115
8.3 Thesis strengths and limitations 117
8.4 Implications and future research 118
8.5 Conclusions 119
References 120
APPENDIX 139
A. Copyright permission from publishers to use my primary authored material 139
B. LME model raw outputs 141

LIST OF ABBREVIATIONS

Ang II	Angiotensin II
AAA	Abdominal aortic aneurysm
AMP	Adenosine monophosphate
AMPK	AMPK-activated protein kinase
ANOVA	Analysis of variance
ApoE-/-	Apolipoprotein E deficient
ARRIVE	Animal research: reporting of *in vivo* experiments
CI	Confidence interval
CRP	C-reactive protein
CVD	Cardiovascular disease
DAPI	4′,6-diamidino-2-phenylindole
DNA	Deoxyribonucleic acid
EMIQ	Enzymatically modified isoquercitrin
EVAR	Endovascular aneurysm repair
HDL	High density lipoprotein
HDL-C	High density lipoprotein cholesterol
HIF-1	Hypoxia-inducible factor 1
HLI	Hind limb ischemia
HO-1	Heme oxygenase-1
IC	Intermittent claudication
IL-1β	Interleukin-1beta
IL-6	Interleukin-6
ILT	Intraluminal thrombus

IRA	Infrarenal aorta
LDL	Low density lipoprotein
LDL-C	Low density lipoprotein cholesterol
LME	Linear mixed effects
MMP	Matrix metalloprotinase
MUFA	Monounsaturated fatty acid
n-3	Omega-3
n-6	Omega-6
NADPH	Nicotinamide adenine dinucleotide phosphate
NLRP3	Nacht domain, leucine-rich repeat, and pyrin domain-containing protein 3
NO	Nitric oxide
OCT	Optimal cutting temperature
PAD	Peripheral artery disease
PBS	Phosphate buffered saline
PGC1α	peroxisome proliferator-activated receptor gamma coactivator 1-alpha
PRISMA	Preferred Reporting Items for Systematic Reviews and Meta-Analyses
PUFA	Polyunsaturated fatty acid
SD	Standard deviation
SEM	Standard error of the mean
SMD	Standard mean difference
SRA	Suprarenal aorta
TBS	Tris-buffered saline
TC	Total cholesterol
TG	Triglyceride

TMT	Treadmill test
TNF-α	Tumour necrosis factor-alpha
VEGF	Vascular endothelial growth factor

LIST OF FIGURES

Figure 1.1. Illustration of atherosclerotic occlusion leading to ischemia in the lower limb. 2
Figure 1.2. A variation of the HLI ligation model. 5
Figure 1.3. A two-stage surgical HLI model using hygroscopic ameroid constrictors. 7
Figure 1.4. Diagram depicting the major pathophysiological features of AAA. 11
Figure 1.5. Representative images of *ex vivo* aortas from the most commonly used mouse models of AAA. 14
Figure 1.6. Summary of the potential involvement of quercetin in pathways relating to blood flow and angiogenesis. 22
Figure 1.7. Summary of the potential involvement of quercetin in pathways relating to blood flow and angiogenesis, mitochondrial biogenesis, inflammation, pain and muscle damage. .24
Figure 3.1. Intra-observer and inter-observer reproducibility of maximum aortic diameter measured by ultrasound. 42
Figure 3.2. Intra-observer reproducibility of systolic, diastolic and mean arterial blood pressure measured by tail-cuff plethysmography. SBP, systolic blood pressure; DBP, diastolic blood pressure; MAP, mean arterial pressure. 43
Figure 3.3. Intra-observer and inter-observer reproducibility of blood flow measurements using laser Doppler perfusion imaging. 43
Figure 3.4. Intra-observer and inter-observer reproducibility of *ex vivo* maximum aortic diameter measurements. TA, thoracic aorta. 44
Figure 3.5. Intra-observer and inter-observer reproducibility of atherosclerosis lesion area measurements in the brachiocephalic artery. 44
Figure 4.1. Structural properties of the major flavonoid classes (examples in brackets) used in atherosclerosis research in *ApoE-/-* mice. 47
Figure 4.2. Preferred Reporting items of Systematic Review and Meta-analyses flow diagram. 50
Figure 4.3. Forest plot showing the effects of flavonoids on atherosclerosis lesion area. Sub-analyses were performed to test the effect of flavonols, flavan-3-ols, isoflavones and flavone glycosides on atherosclerosis lesion area. 61
Figure 4.4. Funnel plot for assessment of publication bias of included studies assessing the effects of flavonoids, flavonols and flavan-3-ols on atherosclerosis lesion area 63
Figure 5.1. Baseline limb perfusion and distance travelled on a treadmill for intervention groups prior to randomised assignment of intervention. 70

Figure 5.2. Study design and timing of quercetin dietary intervention and outcome assessments. 71
Figure 5.3. Body weight in mice receiving quercetin and controls throughout the experimental period. 75
Figure 5.4. The effect of quercetin on ambulatory performance, pressure sensitivity and voluntary activity. 76
Figure 5.5. The effect of quercetin on hind limb perfusion measured by LDPI and plasma nitrate and nitrite concentrations....78
Figure 5.6. Plasma cytokine concentration at baseline before HLI or quercetin administration, and at the endpoint following four weeks quercetin administration.....79
Figure 6.1. Animal study design from the beginning of the intervention with a diet enriched with macadamia and pecan nuts through until sacrifice. 84
Figure 6.2. Body weight and food consumption from the beginning of the intervention with a diet enriched with macadamia and pecan nuts through to sacrifice....87
Figure 6.3. The effect of a diet enriched with tree nuts on Ang II-induced AAA incidence and severity.....89
Figure 6.4. All aortas from mice receiving a diet enriched with tree nuts and control mice at experimental endpoint (day 56). 90
Figure 6.5. Diameter of the SRAs of mice that died of aortic rupture prior to the experimental end point (day 56) 91
Figure 6.6. The effect of a diet enriched with nuts on atherosclerosis lesion area. 92
Figure 6.7. The effect of a diet enriched with nuts on blood pressure prior to and following Ang II infusion.....93
Figure 7.1. Timing of surgery, intervention and ultrasound measurements during the animal study.....99
Figure 7.2. Maximum infrarenal aortic diameter in E-BAPN groups prior to randomisation to colchicine or vehicle gavage.....99
Figure 7.3. The effect of E-BAPN on infrarenal aortic diameter and structure....104
Figure 7.4. The effect of E-BAPN on the NLRP3 inflammasome. 106
Figure 7.5. The effect of oral colchicine administration on AAA incidence, severity and rupture rates. 107
Figure 7.6. Ex vivo images of E-BAPN treated aortas from vehicle and colchicine intervention groups. 108

Figure 7.7. The effect of oral colchicine intervention on tissue cytokines and inflammatory cell markers related to the NLRP3 inflammasome. 110

LIST OF TABLES

Table 1.1. Summary of pathophysiology of lower limb PAD leading to IC 4
Table 1.2. Features of the two-stage surgical HLI model selected for use in this thesis 10
Table 1.3. Characteristics of the most commonly used mouse models of AAA. 15
Table 1.4. Presence of clinically relevant features in AAA models. 18
Table 1.5. The potential beneficial effects of quercetin on the pathophysiology of lower limb PAD.....27
Table 2.1. Details of all experimental mice used within the chapters of this thesis 32
Table 4.1. Characteristics of studies included in this meta-analysis.....52
Table 4.2. Effect of different flavonoids on atherosclerosis lesion area in *ApoE*$^{-/-}$ mice and key aspects of the methods of the included studies. 55
Table 4.3. Study quality assessment tool. 58
Table 4.4. Leave one study out sensitivity analyses for the effects of flavonoids on atherosclerosis lesion area.....62
Table 7.1. Deaths during experimental period. 105

PREFACE

This thesis consists of eight chapters, four of which were originally written as stand-alone publications. The results and narratives presented in these chapters are similar to those that have been published, however the chapters have been modified in order to achieve consistent formatting, limit repetition and improve narrative flow.

PUBLICATIONS ARISING FROM THESIS CHAPTERS

Journal articles

Published

Phie, James, Moxon, Joseph V., Krishna, Smriti M., Kinobe, Robert, Morton, Susan K., and Golledge, Jonathan. A diet enriched with tree nuts reduces severity of atherosclerosis but not abdominal aneurysm in angiotensin II-infused apolipoprotein E deficient mice. Atherosclerosis, 2018. 277. pp. 28-33.

Phie, James, Krishna, Smriti M., Moxon, Joseph V., Omer, Safraz M., Kinobe, Robert, and Golledge, Jonathan. *Flavonols reduce aortic atherosclerosis lesion area in apolipoprotein E deficient mice: a systematic review and meta-analysis.* PLoS ONE, 2017. 12 (7). e0181832. pp. 1-13.

Submitted

Phie, James, Krishna, Smriti M, Kinobe, Robert, Moxon, Joseph V, Andrade-Lima, Aluísio, Morton, Susan K, Lazzaroni, Sharon M, Huynh, Pacific, and Golledge, Jonathan. *Quercetin does not improve exercise performance or physical activity in a novel model of sustained hind limb ischemia.*

In progress

Phie James, Huynh, Pacific, Moran, Corey, Kinobe, Robert, Krishna, Smriti M, Moxon, Joseph V, and Golledge, Jonathan. *Colchicine does not reduce aortic aneurysm growth in a novel elastase and BAPN induced mouse model.*

Presentations

Phie, James, Krishna, Smriti M., Kinobe, Robert, Moxon, Joseph V., Lima, Aluísio H.R.A., Morton, Susan K., Lazzaroni, Sharon M., Huynh, Pacific, and Golledge, Jonathan. *Quercetin does not improve exercise performance in old Apolipoprotein E deficient mice with sustained hind limb ischemia.* Joint Vascular Biology Meeting (JVBM), Sydney 2019. (Poster presentation).

Phie, James, Moxon, Joseph V., Krishna, Smriti M., Kinobe, Robert, Morton, Susan K., and Golledge, Jonathan. *Tree nuts protect against atherosclerosis but not abdominal aortic aneurysm in mice.* Joint Annual Scientific Meeting of Australian Atherosclerosis Society (AAS), Australian Vascular Biology Society (AVBS) and High Blood Pressure Research Council of Australia (HBPRCA), Adelaide 2018. (Poster presentation).

Phie, James, Krishna, Smriti M., Moxon, Joseph V., Omer, Safraz M., Kinobe, Robert, and Golledge, Jonathan. *Flavonols, but not flavan-3-ols, reduce aortic atherosclerosis lesion area in mice*. Festival of life sciences, Townsville 2017. (Poster presentation).

Phie, James, Krishna, Smriti M., Moxon, Joseph V., Omer, Safraz M., Kinobe, Robert, and Golledge, Jonathan. *Flavonols reduce atherosclerosis in mice: a systematic review and meta-analysis*. Townsville Hospital Health Research Showcase, Townsville 2017. (Poster presentation).

CHAPTER 1
GENERAL INTRODUCTION

1.1 Peripheral artery diseases

Peripheral artery diseases (PADs) consist primarily of occlusive and dilating diseases affecting the abdominal aorta and its branches [1, 2]. The two most common PADs are lower limb PAD and abdominal aortic aneurysm (AAA). Lower limb PAD is an occlusive disease that leads to limb pain and walking impairment (known as intermittent claudication, IC) [3]. Reduced daily physical activity [4, 5] is one of the biggest predictors of reduced quality of life in patients with IC [6, 7] and is associated with higher cardiovascular and all-cause mortality [8]. AAA is a dilating disease associated with decreased aortic wall strength that can lead to abdominal aortic rupture with mortality rates as high as 90% [9, 10]. These two forms of PAD exist concurrently, with studies suggesting up to 45% of people that have AAA suffer from lower limb PAD [11-13], however the pathogenesis of these diseases appears to be distinct [14, 15]. Due to the potential for therapeutics to have beneficial effects in one disease and potentially harmful effects in the other, novel interventions should be tested in both diseases. Despite the impact of these threatening diseases, cilostazol is the only specific pharmacological treatment available for IC and it is currently not recommended by the European guidelines for use in patients with IC due to side effects and lack of efficacy [16]. Additionally, early revascularisation surgery in patients with IC is reported to be associated with higher rates of amputation compared with initial conservative treatment [17]. There are currently no pharmacological treatments approved for the treatment of small AAA, which are currently monitored over time until surgery is deemed necessary [18]. In this thesis clinically relevant animal models will be used to investigate novel promising interventions for IC and small AAA development and growth.

1.2 Lower limb PAD and intermittent claudication

1.2.1 Pathophysiology of lower limb PAD leading to IC

Better understanding of the pathophysiology of lower limb PAD may facilitate the identification of new, more effective treatments to improve walking impairment in patients with IC. Lower limb PAD is primarily initiated by occlusion of arteries supplying the limbs by atherosclerosis and related thromboses (Figure 1.1) [19]. Lower limb PAD

has four main pathophysiological issues downstream of the atherosclerosis occlusion that are not well managed by current therapies. (i) The blood supply to the lower limb distal to the occlusion is further decreased due to endothelial dysfunction, which reduces flow-mediated vasodilation and hyperaemia [20, 21]. (ii) Mitochondrial function is reduced [22], (iii) there is a build-up of lactic acid and other metabolites within the skeletal muscle, and (iv) there is an increase in oxidative stress and inflammation in the lower limb [23]. These major pathophysiological issues are discussed in more depth below.

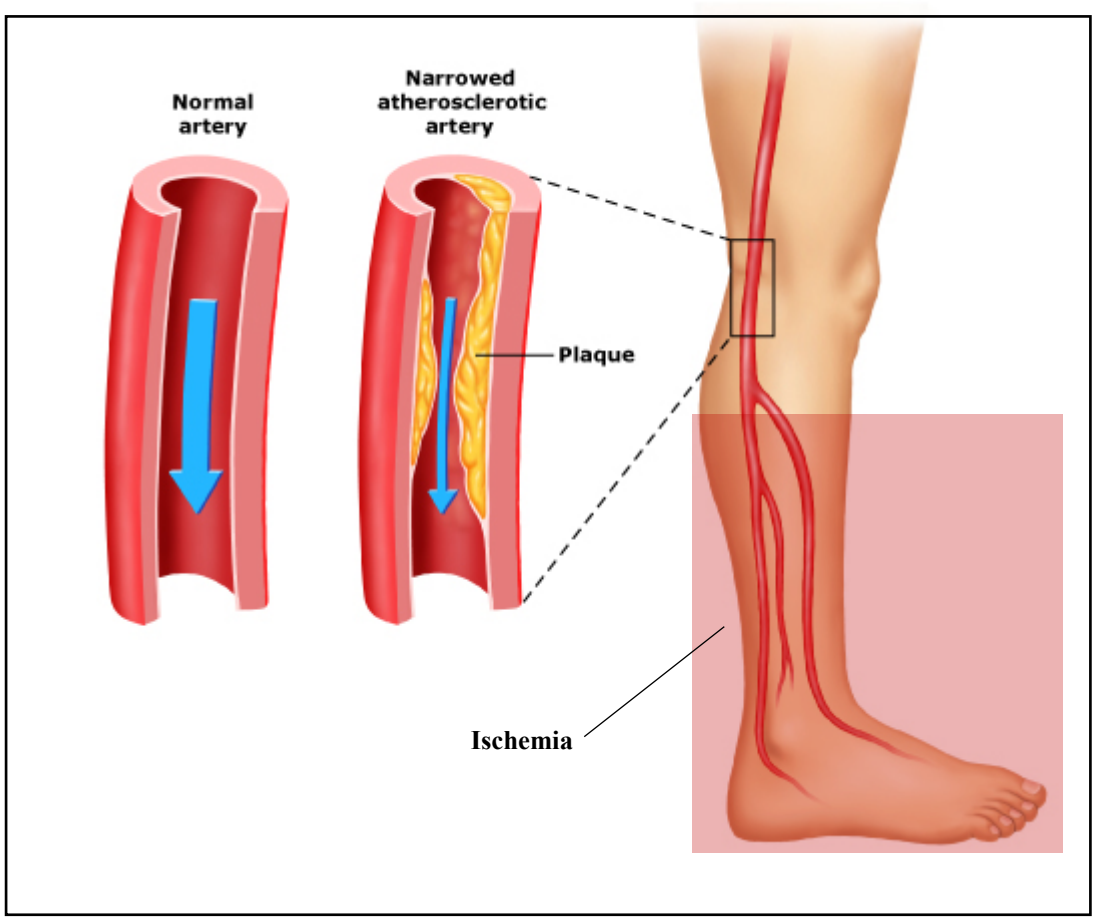

Figure 1.1. Illustration of atherosclerotic occlusion leading to ischemia in the lower limb. Adapted from Vranic [24].

Walking capacity in IC has recently been reported to be inversely associated with endothelial dysfunction [25]. Endothelial dysfunction is characterised by a reduced capacity for the endothelium to respond to changes in blood flow and other chemical signals [21]. Importantly, a decreased capacity for blood vessels to undergo endothelium dependent flow mediated vasodilation leads to limited exercise induced hyperaemia [25-27]. Furthermore, overall capillary density supplying the limb tissues in lower limb PAD patients has been reported to be lower, and basement membrane thickness higher, further

impairing nutrient exchange to the ischaemic muscle [28]. Endothelial dysfunction can therefore contribute to decreased blood flow and ischemia during exertion in patients with lower limb PAD. Therapies targetting the responsiveness of the endothelium to blood flow changes may be beneficial in reducing ischemia in patients with IC.

Ischemia in the limbs arising from a reduction in blood flow can lead to downstream chronic changes within the skeletal muscle. Calf skeletal muscle mitochondrial density has been reported to increase in patients with severely reduced blood flow, suggesting that skeletal muscle mitochondria undergo adaptations in response to decreased blood flow [29]. However, increases in mitochondrial density are not associated with an increase in 6-minute walk distance and 4-meter walking velocity in patients with IC, despite this being the case for subjects without IC [29-31]. This suggests that the mitochondrial changes that occur in lower limb PAD are maladaptive. Calf skeletal muscle fibres in patients with IC also have high amounts of uncleared, damaged mitochondria, which suggests an impairment of mitophagy which may explain why increases in mitochondria numbers do not lead to increases in exercise performance in patients with IC [32]. Targeting the pathophysiological dysfunction of mitochondria may therefore be one potential way to treat patients with IC.

The accumulation of lactic acid and increased expression of inflammatory cytokines in the lower limb skeletal muscle has been associated with increased pain on exertion and decreased exercise capacity in patients with IC. Pain during ischemia can arise due to a decrease in extracellular pH as a result of a build-up of lactate and other metabolic by-products [33, 34], although this may not be the primary cause of walking intolerance in patients with IC [35]. Interleukin-6 (IL-6) has also been reported to increase muscle pain in humans and mice [36, 37], and reduce maximum treadmill walking distance in patients with IC [20, 38].

Collectively, the above information suggests that lower limb PAD and IC arise from 4 pathophysiological issues, including reduced blood flow, reduced mitochondrial function, lactic acid buildup, and inflammation. By improving blood flow, improving mitochondrial function, and reducing inflammation, pain may be reduced and therefore exercise performance and quality of life may be improved in patients with IC (Table 1.1).

Table 1.1. Summary of pathophysiology of lower limb PAD leading to IC

Pathophysiology	Symptoms
Reduced blood flow	Reduced exercise performance [25-28]
Reduced mitochondrial function	Reduced exercise performance [29-32]
Build-up of lactic acid and other metabolites	Pain [33, 34]
Oxidative stress and Inflammation	Pain [20, 36-38]

1.2.2 Current management strategies for IC

Current management strategies for IC are aimed at increasing exercise capacity and reducing pain on exertion by reducing atherosclerotic plaque formation, thrombosis and establishing collateral circulation. Currently, IC is managed by controlling risk factors, exercise therapy and in more urgent situations angioplasty, stenting and open bypass surgery [27]. Current advised risk factor management for IC includes smoking cessation, lipid lowering, antithrombotic drugs, blood pressure control and anti-platelet therapies [39]. While their efficacy has been shown, these interventions alone are not enough to completely ameliorate the symptoms of IC [40]. Supervised exercise programs, and less successfully home exercise programs, have proven beneficial effects in patients with IC however compliance rates of 77% have been reported due to lack of willingness to participate or other medical conditions [27, 41]. Cilostazol has been reported to improve walking distance and is the only approved drug for the treatment of IC. However, the effects of this vasodilator and anti-coagulant drug are disappointing. Walking distance has been reported to be improved by up to 150 metres after three months of supervised exercise [42]. However, an average of only a 107 metre improvement in walking distance was reported for patients treated with cilostazol for six months [43]. Additionally, side effects are frequent with up to 30% of patients in a long term study experiencing headache, and up to 15% experiencing diarrhoea, palpitations and abnormal stool [44]. Due to these side effects and its limited efficacy, cilostazol is currently not recommended by the European guidelines for use in patients with IC [16]. Additionally, not all patients with IC are ideal candidates for surgery, and stenting and bypass surgeries have associated risks as restenosis and new plaque formation often occur [45]. The limitations

with currently available therapies for IC reveal a need for the development of new, better tolerated and more efficacious interventions. The discovery of novel therapeutic interventions for PADs requires proof-of-principle and mechanistic studies using suitable patient relevant animal models.

1.2.3 Current animal models of IC

Lower limb PAD and symptoms of IC are primarily modelled in animals by surgical induction of hind limb ischemia (HLI). HLI surgical models have been employed in multiple different animal species and knockout models [46]. Mouse models are the most commonly used due to the high availability of knockout models, multiple strains with varied attributes, their low cost and the high amount of research data available. Mouse models of HLI induced by atherosclerotic or thrombotic occlusion are rarely used due to their unreliable and inconsistent nature of ischemia induction [46]. For the purposes of this thesis, ligation and excision mouse models of HLI will be discussed.

In most mouse surgical models of HLI, an incision is made on the limb, the femoral artery is ligated proximally and distally, and the intervening section is resected (Figure 1.2) [47]. There is however a large heterogeneity in the methods of HLI induction, which has consequences for the severity of ischemia and the symptoms observed in mice [48].

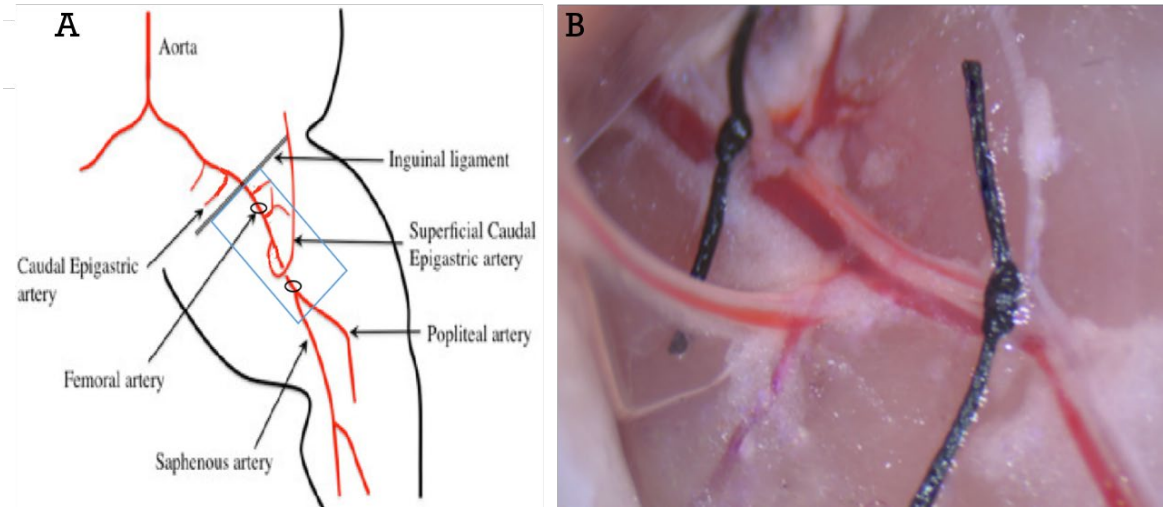

Figure 1.2. A variation of the HLI ligation model. (A) Diagrammatic representation of important vessels and ligation points in the mouse limb. Adapted from Suhara et al. 2018 [49]. The location of Figure 1.2B is indicated by the blue rectangle. Common proximal and distal ligation points are indicated by black circles. (B) A close-up of ligation sites and important vessels in the mouse hind limb.

Depending on the study, the femoral artery is ligated more proximal or distal, the femoral artery side branches including lateral circumflex and proximal caudal femoral arteries are ligated or left intact, and the amount of the femoral artery resected is longer or shorter [50]. In some experiments, the vein is also ligated which produces much more severe ischemia leading to toe discolouration, necrosis and possible limb auto-amputation [51]. Some studies have attempted resection of the genitocrural and sciatic nerves in addition to the femoral artery [51].

C57BL/6J, DBA/1J and BALB/c, three commonly used mouse strains, have been reported to have different susceptibility to ischemia following the same surgical HLI procedures [48, 52]. It has been hypothesised that the primary difference between strains is the number of pre-existing collateral vessels and their ability to develop new collateral circulation through angiogenesis and arteriogenesis [46, 53]. Older mice have also been reported to have a reduced rate of blood flow recovery [54].

Recently new subacute surgical HLI models which utilise hygroscopic ameroid constrictors to close the femoral artery have been developed (Figure 1.3) [55-57]. Ameroid constrictors slowly contract over 7-14 days which causes a slower onset of ischemia and less severe muscle necrosis [56-58]. Within these models, some studies have utilised one surgery whilst one study has utilised a two-stage surgical procedure in which the femoral artery is ligated and resected 14 days after ameroids are implanted [59]. Mice undergoing HLI induction over 14 days with ameroid constrictors recovered blood flow more slowly than those undergoing HLI by simple ligation and resection [57, 58].

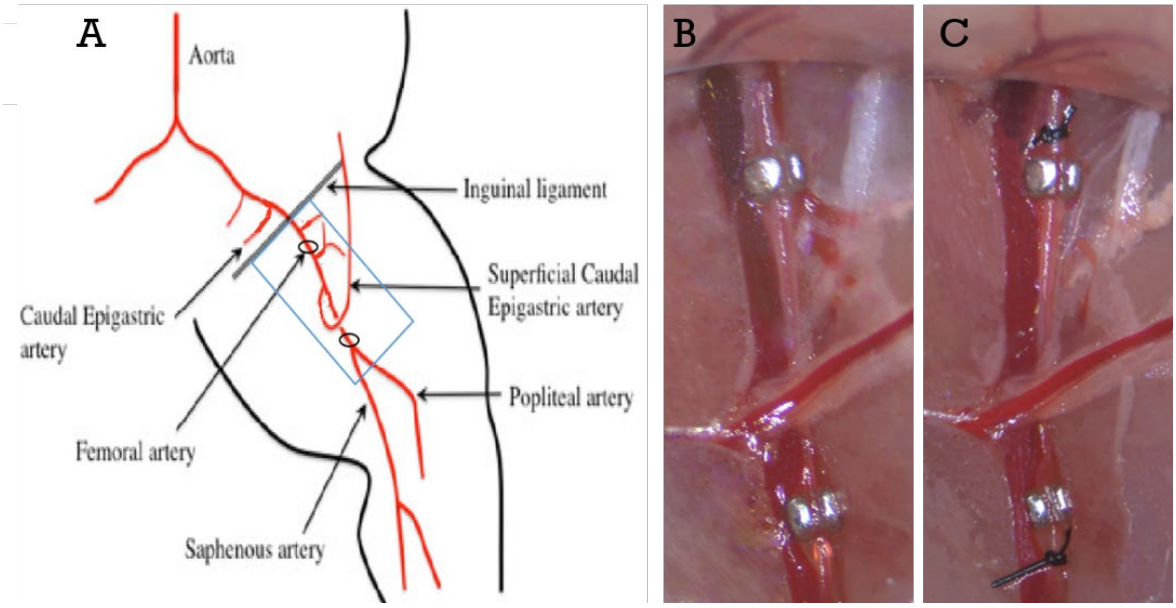

Figure 1.3. A two-stage surgical HLI model using hygroscopic ameroid constrictors. (A) Diagrammatic representation of important vessels and ligation points in the mouse limb. Adapted from Suhara et al. 2018 [49]. The location of Figure 1.3B and C is indicated by the blue rectangle. Location of the two ameroid constrictors are illustrated by black circles. (B) A close-up of ameroid constrictors inserted around the femoral artery in proximal and distal locations during the first surgery of the two-stage surgical model. (C) A close-up of ameroid constrictors with ligations made proximal to the proximal ameroid and distal to the distal ameroid immediately prior to resection of the intervening femoral artery. Second surgery of the two-stage surgical model, 14 days after the first surgery in figure B.

1.2.4 Selection of a suitable mouse model of IC

Selection of the appropriate model that can produce a sustained ischemia without spontaneous recovery, and of the appropriate moderate severity to induce IC but not limb gangrene and auto-amputation is important if results are to be clinically relevant.

A limitation of the ligation and resection variations of the HLI model are that control mice in many species exhibit marked blood flow recovery within the first 28 days post surgery [60]. This recovery is due to pre-existing and newly formed collateral circulation which circumvents the resected femoral artery to supply the lower limb. This is likely caused by changes in shear stress and endothelial nitric oxide synthase (eNOS) and platelet-derived growth factor (PDGF) mediated signalling of angiogenesis and arteriogenesis [61-63]. This recovery is unfortunately not seen to the same degree in patients. Patients develop lower limb PAD and symptoms of IC over many years, and therefore the rate of change in shear stress is minor. There is no substantial development

of collateral vessels in patients and those that do develop are not suitable for exercise due to exercise-induced vasoconstriction in these vessels [64]. The recovery of control mice within the first 28 days limits the duration of the experimental model, and as such it is not suitable to assess interventions for established disease.

The use of hygroscopic ameroid constrictors to close the femoral arteries over 7-14 days can produce a slower onset and more sustained ischemia compared with the ligation models [58]. This has been reported to be accompanied by lower upregulation of shear-stress dependent genes compared to acute ligation and resection models of HLI [58]. The slow onset of ischemia, the less acute severe symptoms, and less acute recovery observed in the HLI models utilising hygroscopic ameroid constrictors are all features of human IC. Resection of the femoral artery 14 days after occlusion with hygroscopic ameroid constrictors, in a two-stage surgical procedure, has been reported to produce an even more sustained ischemia [59]. These data suggest that this model may be more suitable and translatable for testing interventions of pre-existing disease.

The location of occlusion is another important consideration. As expected, occlusion and resection that starts more proximal and spans a longer region of the femoral artery causes the most prolonged ischemia [50, 65]. Occlusion and ligation of the femoral vein or nerve have questionable clinical relevance, since in patients IC is primarily due to occlusion in the femoral artery [19]. Additionally, ligation of the femoral vein and nerve cause more severe symptoms such as limb gangrene and autoamputation as opposed to IC. Therefore based on these findings the artery only will be occluded and resected, in the most proximal and distal regions, in the model used in this thesis.

The strain and age of the mouse can also be modified to achieve the desired combination of severity of ischemia and sustained reduction in blood flow. Previously it has been reported that DBA/1J mice experience more severe ischemia compared with C57BL/6J and BALB/c mice following the same acute HLI surgery [48]. BALB/c mice experience more intense ischemia and seven fold slower acute collateral blood flow compared with C57BL/6J mice [52]. Additionally, three month old C57BL/6J mice were reported to have two times greater blood flow recovery compared with 18 month old mice by day 14, despite having similar perfusion immediately after acute HLI surgery [54]. These findings suggest that mice with a C57BL/6J background may produce a moderate ischemia that is representative of IC. Furthermore, the use of C57BL/6J mice older than 3 months may

produce the same intensity of ischemia but have slower blood flow recovery as is observed in patients.

A drawback of current surgical models are the lack of PAD risk factors which are commonly present in patients. Atherosclerosis is the primary cause of lower limb PAD however models of HLI are surgically induced. Nonetheless, common risk factors for lower limb PAD may be incorporated into existing HLI models using genetic knockout mice [46]. Apolipoprotein E is important in the transport, metabolism and prevention of oxidation of cholesterol and low density lipoproteins. Apolipoprotein E deficient (*ApoE*$^{-/-}$) mice with a C57BL/6J background have atherosclerosis and dyslipidemia, which are two risk factors for PAD, by 12 weeks of age.

In this thesis, a two-stage surgical model of HLI using hygroscopic ameroid constrictors will be used, with proximal and distal occlusion and resection, with 6 month old *ApoE*$^{-/-}$ mice with C57BL/6J background, in order to produce a sustained HLI of similar severity to human IC with similar coexisting dyslipidemia (Table 1.2).

Table 1.2. Features of the two-stage surgical HLI model selected for use in this thesis

Feature	Rationale	References
Two-stage surgical model	Slow occlusion and reduced rate of spontaneous recovery of blood flow	[58, 59]
Proximal and distal occlusion and resection	Reduced rate of spontaneous recovery of blood flow	[50, 65]
Femoral artery only	Moderate ischemia representative of IC	[19]
C57BL/6J background	Moderate ischemia representative of IC	[48, 52]
Aged (6 month old)	Reduced rate of spontaneous recovery of blood flow	[54]
ApoE$^{-/-}$ knockout	Coexisting dyslipidemia and atherosclerosis (risk factors for lower limb PAD)	[46]

1.3 AAA

1.3.1 Formation and pathophysiology of AAA

AAA are characterised by weakening and dilation of a segment of the aorta. The initial triggers for AAA are largely unknown [66]. Dilation of the aorta is largely a result of the degradation of medial elastin tissue within the vessel wall promoted by a disproportionate increase in proteases compared with tissue protease inhibitors [67, 68]. Smooth muscle cells also support wall strength and integrity in the healthy abdominal aorta. In AAA, smooth muscle cells undergo apoptosis [69] and exhibit a reduced proliferative capacity [70]. Therefore in addition to elastase breakdown, most AAA also lack structural support due to smooth muscle cell apoptosis and senescence which further compromises vessel wall structure and aortic integrity [71, 72]. AAA grow larger over time and many AAA

are accompanied by an intraluminal thrombus (ILT) during later stages of development which are typically host to high amounts of neutrophils and macrophages [73]. ILT size has been reported to positively correlate with reduced elastin content, increased collagen stiffness and reduced tissue strength within the aortic wall [74]. ILT have been associated with aneurysm rupture at smaller diameters and lower stress [75]. Thick intramural thrombi cause hypoxia in aortic tissue [76, 77]. Decreased nutrient diffusion into the aortic tissue and infiltration of inflammatory cells may in part explain the correlation between ILT size and aneurysm severity. The aforementioned features can be seen in Figure 1.4.

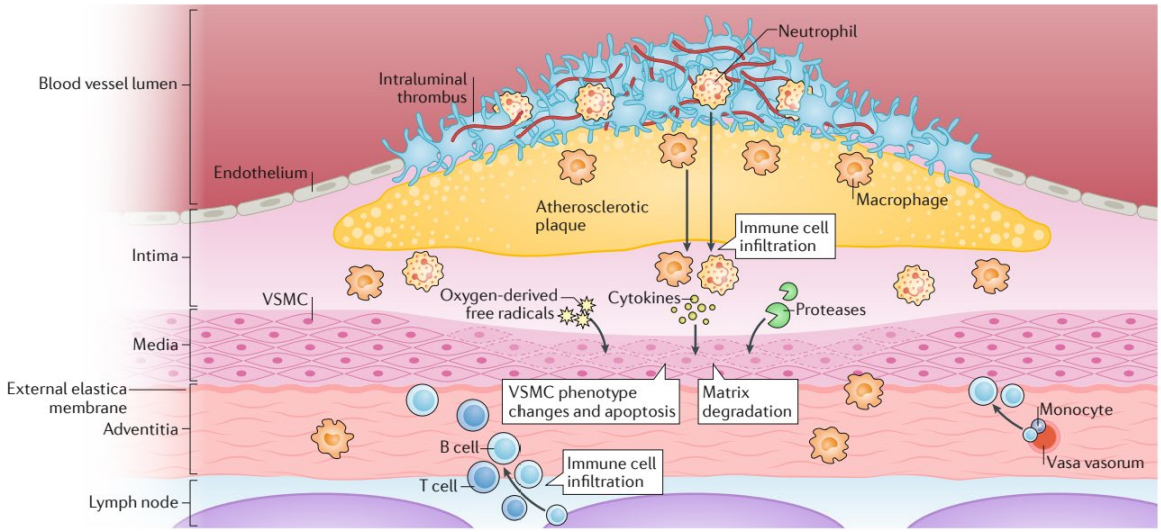

Figure 1.4. Diagram depicting the major pathophysiological features of AAA. Pathophysiology of AAA typically include matrix degradation, smooth muscle senescence and apoptosis, and intraluminal thrombus with infiltrating neutrophils and macrophages. Adapted from Golledge [78].

1.3.2 Current management strategies for AAA

1.3.3 Currently, there are no non-surgical pharmacological treatments available specifically to reduce the growth of AAA other than management of risk factors. No treatments are available for small AAA which are simply monitored over time, a process referred to as watchful waiting. For large AAA (>5.5cm), surgery is often necessary as the risk of rupture is high [18]. Aneurysms are currently treated surgically with endovascular aneurysm repair (EVAR) or open surgery. EVAR involves the insertion of a stent into the aorta, guided through a catheter inserted in to the femoral artery [79]. In open surgery, an incision is made in the abdomen and the aorta is repaired using grafts. EVAR is associated with lower early and midterm perioperative mortality and complications than open surgery but not all patients are suitable

for the procedure [79]. Furthermore, repeat surgery is required in up to 20% of patients [79-81]. Current animal models of AAA

A number of mouse models of AAA are currently in use. The Ang II model, elastase infusion model, topical application models including elastase, calcium chloride and calcium phosphate models, and the recently published elastase and 3-aminopropionitrile fumarate salt **(**BAPN) model are the most recognised.

The Ang II infusion model is currently the most utilized and validated animal model of AAA [82]. Ang II (1000ng/kg/min) is administered subcutaneously through implanted mini-osmotic pumps in male *ApoE-/-* mice [83]. Dissecting aneurysms (growth of the vessel caused by blood entering the intima-media space after an intimal tear) begin to develop in the suprarenal aorta (SRA) within the first week of Ang II administration and the duration of Ang II administration is typically 28 days [84, 85]. Aneurysm diameter in Ang II-infused *ApoE-/-* mice can vary between no aneurysm formation (approximately 1mm or less in SRA) to 2-4mm aneurysms [15, 86]. Aneurysms commonly contain thrombi [73, 82], and ruptures occur up to a rate of 40% within 28 days [15, 85]. Aneurysms develop in approximately 70% of mice receiving Ang II [15]. There are minimal variations in methods between studies and surgeries are technically easy to perform, which allows for the creation of reproducible aneurysms and more reliable comparisons between separate animal studies (Table 1.3).

Perfusion of the infrarenal aorta (IRA) with type 1 porcine pancreatic elastase is another commonly used AAA model. In this model an abdominal incision is made and the IRA is separated from the inferior vena cava [87]. The superior and inferior IRA is then ligated and perfused with elastase for 5-15 minutes [88, 89]. The elastase breaks down elastin tissue within the aorta in order to reduce structural integrity and induce inflammation and aneurysm . This model forms true infrarenal aneurysms that can grow as large as 1.2mm (compared to IRA with no AAA which range between 0.6-0.9mm) in C57BL/6J mice over 14 days before stabilising and regressing [88, 89] (Table 1.3).

Topical applicants, including elastase, calcium chloride or calcium phosphate, can be applied to the IRA as an alternative to intraluminal perfusion [90, 91]. The IRA is separated from the inferior vena cava as occurs in the elastase perfusion model, however in this case the topical agent is applied directly to the outside of the aorta. Elastase breaks down elastin as in the previously described model, while calcium chloride and calcium phosphate appear to cause elastin calcification, vascular smooth muscle cell apoptosis and

endothelial cell fragmentation [92]. Aneurysms developed by topical elastase, calcium chloride or calcium phosphate application have been reported to be between 1-1.6mm by day 14 and these diameters have been reported to be maintained for up to 86 days without growth or regression [90, 92, 93] (Table 1.3).

Recently, a novel model has been developed which improves upon the topical elastase model to produce large non-resolving aneurysms [82, 93]. In this model, topical elastase application is accompanied by oral administration of 0.2% w/v BAPN in drinking water. In this model true aneurysms (ballooning or dilation of the entire aortic wall) similar to those of other topical application models are formed after 14 days, however they continue to grow much larger up to (and potentially longer than) 100 days [82, 93]. Aneurysms diameter of the E-BAPN mice 100 days after surgery was reported to be 801±160% (up to 6mm) [93]. Additionally, aneurysms are reported to form ILT and undergo rupture at rates of up to 46% [93, 94]. Surgeries are of the same complexity as other topical application models. Photographs of aneurysms from the most common AAA models are shown in Figure 1.5 and important model features are summarised in table 1.3.

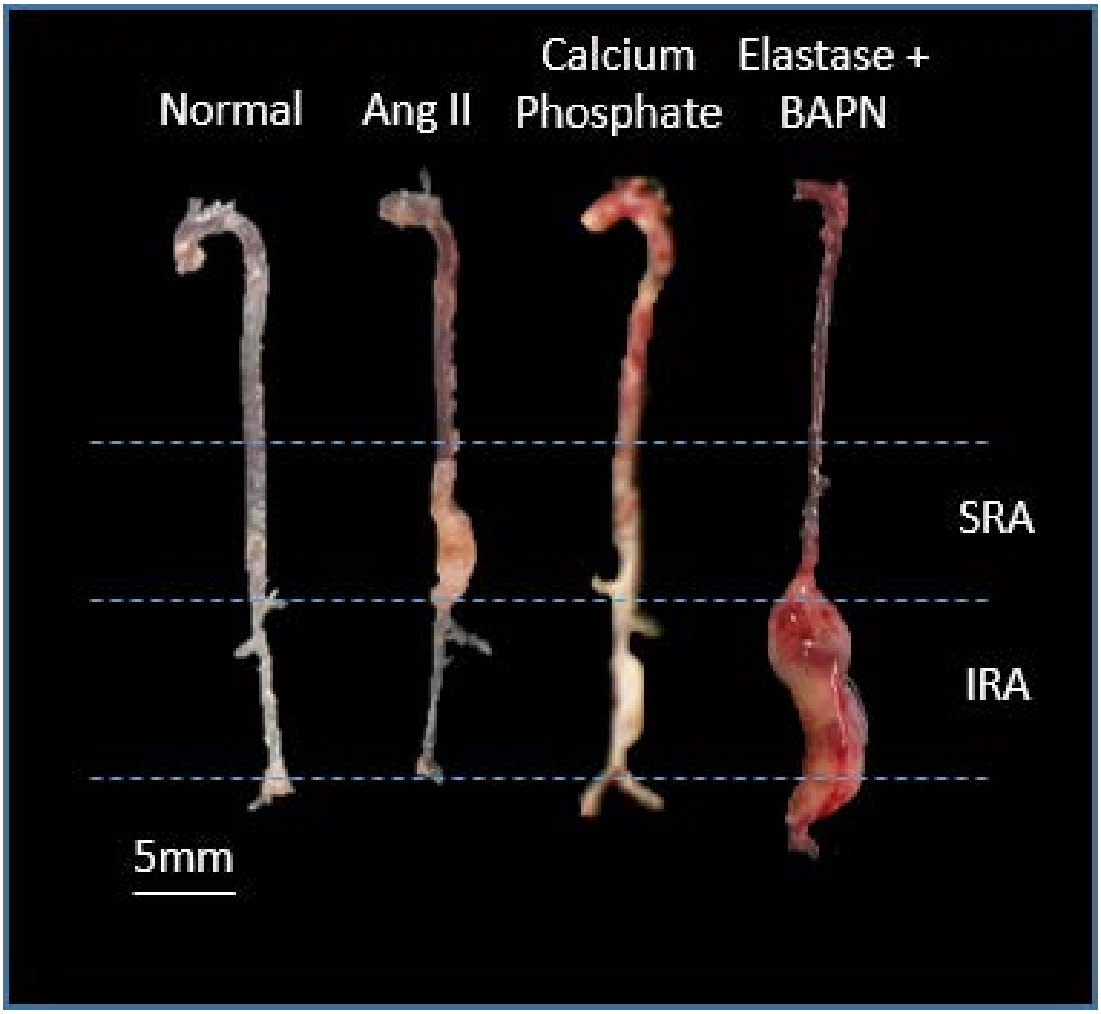

Figure 1.5. Representative images of *ex vivo* aortas from the most commonly used mouse models of AAA.

Table 1.3. Characteristics of the most commonly used mouse models of AAA.

Model (Strain)	**Aneurysm diameter** (mm)	**Aneurysm type**	**Location**	**Common duration** (days)	**Ruptures**	**Thrombus**	**Other concurrent disease**	**% forming aneurysm**	**Surgical difficulty**	**Refs**
Ang II ($ApoE^{-/-}$)	2-4	Dissecting	SRA	28-84	Yes (40%)	Yes	Hypertension Dyslipidemia Atherosclerosis	60-70%	Easy	[15, 73, 82-85]
Elastase perfusion (C57BL/6J)	1.2	True	IRA	14-28	No	Yes	No	63-100%	Hard	[87-89, 95-97]
Topical elastase, Calcium phosphate, calcium chloride (C57BL/6J)	1-1.6	True	IRA	40	No	No	No	50-93%	Medium	[92, 93, 98-102]
E-BAPN* (C57BL/6J)	3-8	True	IRA (can expand)	100	Yes (46%)	Yes	No	93%	Medium	[93]

*Data based on one study. Refs, references.

1.3.4 Selection of suitable mouse models of AAA

As discussed above, there are four main model categories of mouse AAA available that are currently in use. Each model has strengths and limitations and different models may be suitable depending on the outcome being assessed and the intervention being used.

The Ang II model has a number of strengths. It includes risk factors which correlate and are comorbid with human AAA incidence, including dyslipidemia and atherosclerosis [83]. Ang II is believed to be one of the chemical effectors of the harmful effects of cigarette smoking, and is a potent pressor hormone [103, 104]. Additionally, a retrospective cohort study reported that angiotensin converting enzyme inhibitors reduce the risk of death and requirement of surgery in AAA patients [105], suggesting Ang II is clinically relevant. Importantly, aneurysms in this model include thrombi [73, 82] and are prone to rupture [15, 85], which are important features of human AAA. This model does however have a number of limitations. Firstly, the aneurysms produced by Ang II infusion appear to be dissecting in character, as opposed to true dilated aneurysms observed in most patients [84]. Secondly, Ang II-induced AAA forms in the SRA, while most human AAAs form in the IRA and juxtarenal aorta [82]. While the Ang II model has been extended to 84 days, early rupture and death makes chronic use of this model difficult [15, 85]. Furthermore, up to 30% of surviving mice do not develop aneurysm [15]. This reduces sample size and statistical power for evaluating the effects of intervention on endpoint *ex vivo* aneurysm diameter substantially. The acute nature of this model also makes the assessment of chronic interventions difficult, and as such potential therapeutic agents are usually evaluated in this model as a prevention rather than a treatment.

The elastin infusion model produces AAA with very different characteristics to Ang II-induced AAA. Elastin infusion causes destruction and fragmentation of elastin tissue within the IRA which is a crucial feature of clinical AAA [96]. Furthermore, similar to human patients, this model forms true dilated aneurysms which form from the inside out due to the location of elastase application [87]. There are however limitations associated with this model. The elastase perfusion surgery is technically difficult to perform and can lead to high operator variability between studies, and high avoidable deaths in experimental mice. Although there is presence of more chronic inflammation and endothelial destruction, these aneurysms typically do not continue to grow after 14 days

post surgery, therefore studies utilize this model for only 14-28 days prior to sacrifice [88, 89]. This limits the value of this model in assessing interventions in pre-existing disease.

Aneurysms developed by topical elastase, calcium chloride or calcium phosphate also reach their maximum diameter in the first 14 days after surgery suggesting these models have similar limitations [92]. Aneurysms induced by elastase perfusion do not form ILT, which are a characteristic feature of human AAA [73, 90, 91]. Elastase perfusion, topical elastase, calcium chloride and calcium phosphate induced aortic aneurysms do not cause aortic rupture in mice [93, 102]. Aortic rupture is the primary cause of AAA-related death in patients and the lack of ruptures in these models calls in to question the relevance of these surgically induced aneurysms.

The topical elastase and oral BAPN (E-BAPN) model of aneurysm does not have many of the limitations associated with the elastase perfusion, and topical elastase, calcium chloride and calcium phosphate models. Aneurysms in the E-BAPN model have been reported to continually expand for up to 100 days [93]. All layers of the aortic wall are uniformly dilated and aneurysms contain ILT similar to human patients, and rupture rates similar to those seen in the Ang II model [93, 94]. BAPN has also been reported to induce dissecting aneurysm formation in both the thoracic and abdominal aorta of mice without the presence of topical elastase, although at doses three times higher than that used in the topical elastase model [106, 107]. The challenge with creating long term models of AAA is that effective aneurysm induction and continued growth (as opposed to spontaneously resolving aneurysms) is often accompanied by high rupture rates and deteriorating health. Animal welfare is also a consideration for long term animal models when wellbeing is compromised by illness. Currently only one study has been published using this model which makes it difficult to thoroughly assess its strengths and limitations [93].

Each of aforementioned models have features that are and are not clinically relevant for the study of AAA (Table 1.4). For this thesis, the Ang II infusion model will be used for studies assessing prevention of AAA, and the E-BAPN model will be used for assessment of longer term treatments in established aneurysms. These models were selected primarily due to a combination of the presence of aortic rupture, feasibility for assessing longer treatment duration and presence of thrombus.

Table 1.4. Presence of clinically relevant features in AAA models.

Model (Strain)	**Rupture**	**>28 days aneurysm growth**	**Thrombus**	**Infrarenal aneurysm**	**Additional risk factors**	**True aneurysm**
Ang II ($ApoE^{-/-}$)	Y	Y	Y	N	Y	N
Elastase perfusion (C57BL/6J)	N	N	Y	Y	N	Y
Topical elastase, Calcium phosphate, calcium chloride (C57BL/6J)	N	N	N	Y	N	Y
E-BAPN* (C57BL/6J)	Y	Y	Y	Y	N	Y

*Data based on one study. Y, yes. N, no. Dissecting aneurysms; tear in the intimal layer of the vessel leading to a bleed between the intimal and medial layers. True aneurysms; all layers of the blood vessel are dilated.

1.4 Pre-clinical study design features and impact on translatability of results

Some study limitations are intrinsic to the animal models used. However, rigorous attention to suitable experimental design is also important to improve power and reduce the chance of false positive results. Currently, many drugs have had positive effects in animal studies of AAA and IC, but almost none of these effects have been translated to human studies [46, 108].

Anti-inflammatory and antioxidant agents [109-111], pro-angiogenic agents [112, 113], anti-hypertensives [114], and stem cell and exosome therapies [115-117] have been investigated in animal models of HLI. Increases in blood flow as a result of treatment have been reported in each major drug category [110, 111, 113, 114, 116, 117]. Despite this, there is minimal success or progress in the management strategies for IC, and cilostazol remains the only treatment specifically approved for the treatment of IC. No current animal studies have measured the effect of these interventions on exercise performance, which is the main contributor to decreases in quality of life in patients.

Similarly, in AAA, anti-inflammatory agents [118-123], antiplatelet, antithrombotic and anticoagulants [124-127], ACE inhibitors, beta-blockers and anti-hypertensives [128-130], weight loss interventions [131], matrix metalloproteinase inhibitors [132-134], and stem cell therapies [135-138] have been investigated. The effects of these treatments in AAA have been reviewed in-depth previously [139]. Treatments from each of these categories have had success in reducing aneurysm diameter in AAA mouse models [120, 121, 126, 128, 131, 133, 138]. However, clinical trials of therapeutic agents have yielded insignificant and disappointing results thus far. Despite this, animal studies are an important avenue to bridge the gap between *in vitro* and clinical research. Pre-clinical studies require closer attention to detail for study design in order to increase the likelihood of findings that have clinical relevance.

In a specific example, five out of six animal studies that investigated the effects of doxycycline in AAA administered the drug prior to or at the same time as the model was induced [134, 140-144]. Interestingly, the study that administered the drug after establishment of the AAA model was the only study that found that doxycycline had no positive effects, which was also the case in clinical trials [108, 134]. The clinical relevance of administering drugs prior to model induction in animal models is questionable, unless interventions will also be used prophylactically in the clinical setting.

Rationale for the widespread use of drugs prior to induction of animal disease models may include the short time frame of these models and their rapid induction, as well as lower chances of getting a false negative result. Of course, prophylactic administration of drugs also increases the chance of a false positive finding, which can cost significant time and research funding. Additionally, many current animal studies do not include statistical sample size calculations, drug dose rationale and translation calculations, and blinding of outcome measures [145]. The Animal Research: Reporting of *In vivo* Experiments (ARRIVE) guidelines are a set of criteria to improve the design and reporting of animal studies [146]. The ARRIVE guidelines are supported by many journals however some evidence suggests that this support has not led to improvement in study quality or adherence of published studies to these guidelines [147].

1.5 Potential therapeutic interventions for IC and small AAA

As the population is living for longer, the prevalence of both IC and AAA are increasing, and there is a need for pharmacological interventions which effectively treat these diseases. Some success has been had in preventing PADs, however most patients seek intervention after disease is already present and after quality of life is impacted. Research must be conducted into finding both preventions, which can be encouraged from an early age, and treatments for pre-existing disease. Interventions must be tolerable and feasible for long term use in potentially vulnerable elderly patients, readily available and easily accessible. The interventions proposed below for IC and AAA have been identified as particularly promising based on results from current *in vitro, in vivo* and human studies.

1.5.1 The flavonoid quercetin as a potential treatment for IC

Quercetin, one of the most studied flavonoids, has been reported to influence a number of processes that are implicated not only in the development but also the downstream pathology of PAD [60, 148-151]. Quercetin is found in tomatoes, onions, lettuce, celery, tea, olive oil and nuts [152]. Deficiencies of these foods have been linked to increased primary and secondary occurrences of major adverse cardiovascular events, and use of quercetin has been linked to improvements in exercise performance in healthy humans [153, 154]. Prophylactic administration of quercetin can reduce atherosclerotic plaque formation [145, 148], improve blood flow in ischemic muscle [60], reduce inflammatory cytokines in skeletal muscle [149], and can reduce oxidative stress in the spinal cord leading to reduced limb pain [151]. Importantly, quercetin has been reported to improve

endurance capacity in healthy human subjects [150] and reduce pain due to decreased pH in skeletal muscle in mice [149]. These findings are of particular relevance as the major symptoms of IC and CLI are reduced exercise capacity and increased pain on exertion due to ischemia and lactic acid build-up in the limbs. Based on these data, supplementation with Quercetin may alleviate symptoms of pre-existing IC. The following sections discuss the effects of quercetin on the aforementioned aspects of lower limb PAD in depth.

1.5.1.1 Quercetin can reduce the development of atherosclerosis

Multiple studies have reported antiatherogenic effects following quercetin administration in animal studies [145]. Specifically, in *ApoE-/-* mice, dietary administration of purified quercetin significantly reduced atherosclerotic lesion area development in as little as six weeks [155, 156]. This reduction in lesion area appears to be primarily due to the antioxidant properties of quercetin reducing LDL-oxidation, a key step in atherogenesis [155, 157]. Quercetin administration had an additive effect when combined with exercise to further prevent increases in lesion area [148]. Although beneficial in prevention, quercetin has minimal effects on reducing the size of established plaque lesions [158]. Although quercetin may not reduce the size of established plaques, studies have reported quercetin administration can increase collagen content in atherosclerotic plaque lesions [159-161]. Current research suggests quercetin can reduce the development of atherosclerotic plaques as well as increase the stability of existing plaques, which may serve to reduce the chance of plaque rupture [145].

1.5.1.2 Quercetin can improve blood flow and angiogenesis

Multiple studies have tested the effects of quercetin on blood flow and angiogenesis *in vivo* and *in vitro* [60, 162-169]. Quercetin glucosides increased blood flow recovery and capillary density in limbs of mice over four weeks in a model of unilateral HLI [60]. These effects were not observed in eNOS deficient mouse models [60], suggesting that eNOS, which has endogenous antioxidant functions [170], is crucial for the observed increases in blood flow. *In vitro* studies have also reported that quercetin can upregulate eNOS in aortic endothelial cells [168]. Additionally, quercetin was reported to increase hypoxia-inducible factor-1 (HIF-1) in normal oxygen conditions [169]. HIF-1 is normally activated under hypoxic conditions and increases blood flow and angiogenesis (Figure 1.6) [169, 171]. Conversely, *in vitro* studies on human umbilical vein endothelial cells

have reported that quercetin suppresses vascular endothelial growth factor (VEGF) and has anti-angiogenic effects [164-167, 172]. Quercetin decreased VEGF in coronary venular endothelial cells *in vitro*, while the quercetin metabolite, quercetin-3'-sulphate, increased VEGF in the same experiment [162], and therefore *in vivo* effects of quercetin on VEGF may depend on its pharmacokinetic profile. The effects of quercetin on blood flow and angiogenesis may also depend on whether the endothelium has increased VEGF expression or eNOS expression at baseline.

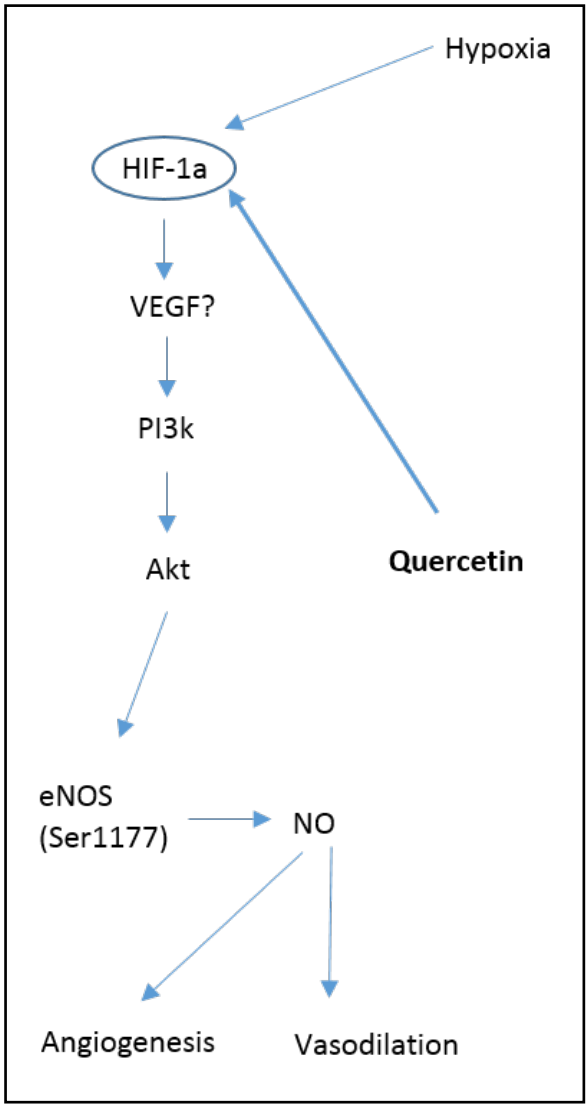

Figure 1.6. Summary of the potential involvement of quercetin in pathways relating to blood flow and angiogenesis. Circles indicate mediators that have been directly measured following quercetin administration. Blue arrows indicate stimulation.

1.5.1.3 Quercetin can improve mitochondrial biogenesis and function

Growth and replication of mitochondria, known as mitochondrial biogenesis, is important in increasing the aerobic efficiency and functional capacity of cells [173]. This is particularly important in cells under high demand or hypoxic conditions, as with more mitochondria, a larger fraction of the oxygen present in the blood can be utilized. Quercetin was reported to increase mitochondrial biogenesis in skeletal muscle [174, 175], hippocampal neurons [176], and hepatocytes [177, 178] of healthy rats and mice. This increase in mitochondrial biogenesis following oral quercetin administration was blocked by the inhibition of heme oxygenase 1 (HO-1) [177, 178], which suggests quercetin mediated mitochondrial biogenesis is due to HO-1 upregulation. HO-1 is a nicotinamide adenine dinucleotide phosphate (NADPH) oxidase inhibitor, therefore this HO-1 mediated increase in mitochondrial biogenesis may be due to a reduction in oxidative stress due to HO-1 mediated NADPH oxidase inhibition (Figure 1.7) [179, 180]. Oxidative stress caused by NADPH oxidase causes mitochondrial damage, as well as inflammation which causes endothelial dysfunction and therefore exacerbates lower limb PAD [181, 182].

Some evidence also suggests that quercetin increases AMP-activated protein kinase (AMPK) activity, which can improve mitochondrial biogenesis and glucose uptake into muscle [163, 168]. Increases in mitochondrial biogenesis were also linked to an increase in Sirtuin 1 and peroxisome proliferator-activated receptor-gamma coactivator 1 alpha (PGC1α) expression (Figure 1.7) [174, 176, 183, 184]. Sirtuin 1 and PGC1α are activated downstream of AMPK activation, which further supports a role of quercetin in activating this pathway.

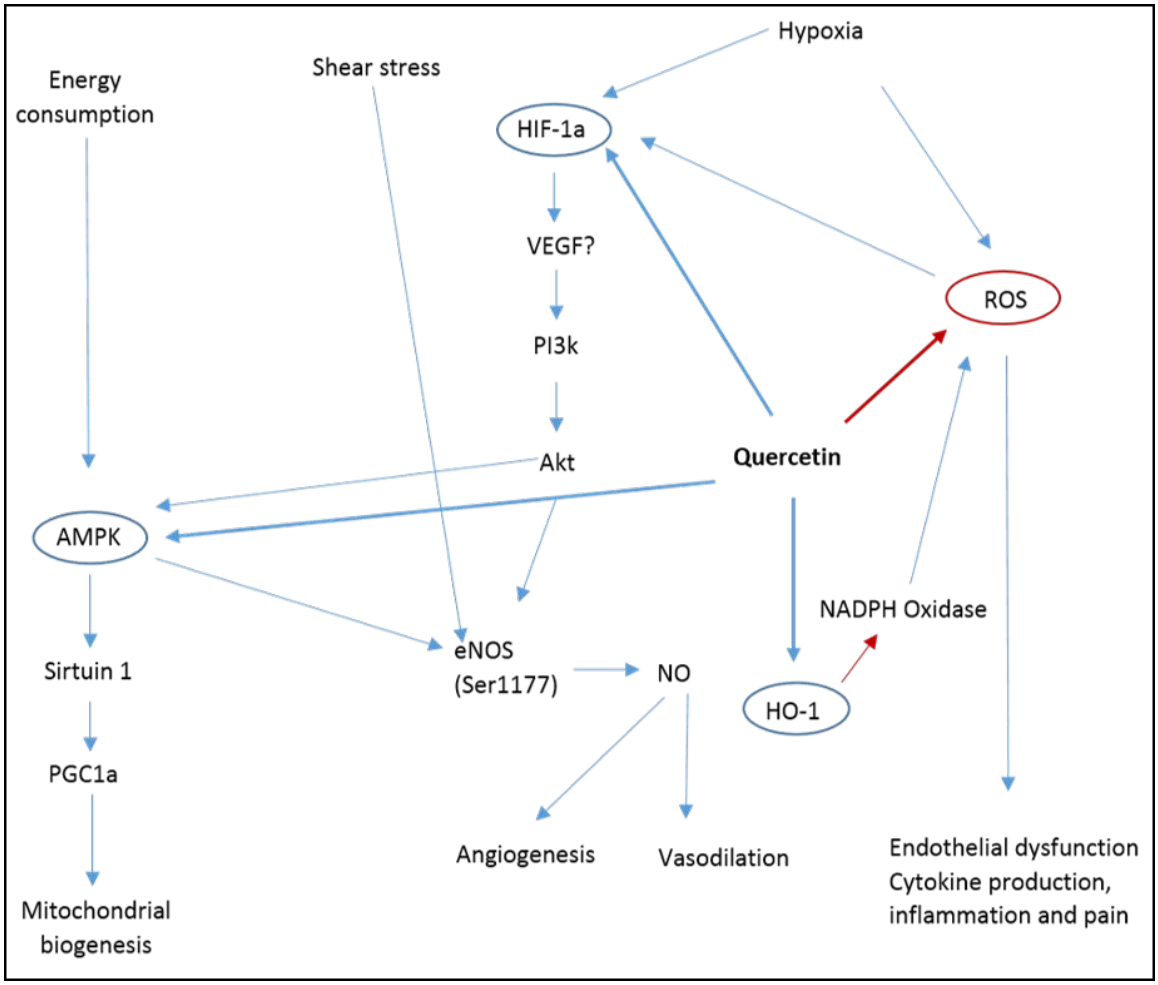

Figure 1.7. Summary of the potential involvement of quercetin in pathways relating to blood flow and angiogenesis, mitochondrial biogenesis, inflammation, pain and muscle damage. Circles indicate mediators that have been directly measured following quercetin administration. Red arrows indicate inhibition, blue arrows indicate stimulation.

Conversely, decreases in mitochondrial biogenesis in skeletal muscle and cardiac muscle have also been reported following administration of quercetin [185, 186]. The studies showing beneficial effects on mitochondrial biogenesis administered quercetin orally at doses between 10-100mg/kg/d [174, 176, 177]. The study reporting reduced mitochondrial biogenesis administered quercetin intravenously at a dose of 50mg/kg/d. This evidence suggests that higher doses may not be favourable for the treatment of lower limb PAD [186].

1.5.1.4 Quercetin can improve exercise performance

Quercetin was reported to significantly increase voluntary wheel running and chronic endurance capacity in sedentary mice [174, 187]. In mice with a cut sciatic nerve (lacking mobilisation in the hind-limb) quercetin reduced disuse atrophy in the gastrocnemius

muscle [175]. In obese sedentary mice, quercetin was reported to reduce muscle inflammation and protect against muscle atrophy [188]. While quercetin has been reported to increase performance and decrease atrophy in sedentary animals, decreased superoxide dismutase and sirtuin 1 have been reported in exercised rats that were administered quercetin compared with exercised controls [187-189]. Furthermore, an increase in oxidative damage in both sedentary and exercised rats has been reported following quercetin administration, as evidenced by an increase in protein carbonyl content [187]. However, these studies which showed possible negative metabolic effects did not measure functional changes in exercise output [187, 188].

Human studies report conflicting results on the effects of quercetin on exercise performance in young healthy subjects. Quercetin was reported to reduce body fat percentage, muscle damage, and increase total body water, basal metabolic rate, and total energy expenditure [190, 191]. These changes were not associated with an increase in exercise capacity, as measured by time to exhaustion and maximal oxygen uptake [190, 191]. In other studies, quercetin supplementation has been reported to increase ride time to fatigue [150], increase distance achieved in a 12 minute time trial at 60% maximal oxygen uptake [192], and increase time to exhaustion [193]. In other trials looking at healthy male subjects, no improvements in 10 minute maximal effort cycling trials [194], and 5km time trials [195] were reported. This inconsistency between studies suggests that the perceived benefits of quercetin on exercise capacity in young healthy male subjects may be marginal. Duration of intervention ranged from one week [150] to eight weeks [193], at doses between 500mg/d [190, 191] and 1000mg/d [150, 192-195]. Effects do not appear to correlate with duration of intervention or dose of quercetin used.

The effects of quercetin supplementation may be masked when combined with exercise due to the significant impact exercise can have on mitochondrial biogenesis and function [196]. This is supported by animal studies as it appears that sedentary animals, including denervation [175] and obesity models [188], benefit more strongly from quercetin supplementation compared with exercised animals [187-189]. Current human studies have assessed the effects of quercetin supplementation on young and healthy male subjects [150, 190-195]. The effects of quercetin on exercise performance may be more noticeable in sedentary subjects, or patients with underlying pathophysiology which affects muscle function and exercise capacity such as IC.

1.5.1.5 Quercetin can reduce pain in mouse models

Pain during ischemia can arise due to a decrease in extracellular pH as a result of a build-up of lactate and other metabolic by-products [33]. Quercetin has been reported to significantly reduce writhing in mice due to acetic acid injection when administered orally [149] and intraperitoneally [197]. Furthermore, quercetin was reported to alleviate mechanical hypersensitivity in rats with chronic constriction injury, a model of peripheral neurological pain, when administered one hour prior to pain tests [198]. In normal and diabetic mice, quercetin administered orally significantly reduced thermal hyperalgesia [199]. Some evidence suggests quercetin may alleviate mechanical hypersensitivity through an opioid dependent analgesic pathway, as evidenced by inhibition of quercetin induced analgesia with the use of opioid receptor antagonist naloxone [200]. Pain can also be activated by inflammation due to the presence of key cytokines including IL-1β, IL-6 and TNF-α, which are present in muscle in PAD patients [20, 38, 201]. Quercetin may therefore also reduce pain through its inhibition of these cytokines [20, 38, 201]. There is however no direct experimental evidence to support quercetin reducing pain through an anti-inflammatory mechanism. The potential effects of quercetin on lower limb PAD leading to IC are summarised in table 1.5 below.

Table 1.5. The potential beneficial effects of quercetin on the pathophysiology of lower limb PAD

Pathophysiology	Symptoms	Quercetin
Reduced blood flow	Reduced exercise performance [25-28]	Improves blood flow [60]
Reduced mitochondrial function	Reduced exercise performance [29-32]	Increases mitochondrial biogenesis, reduces muscle atrophy [174, 175]
Build-up of lactic acid and other metabolites	Pain [33, 34]	Reduces acid induced pain [33] and reduces mechanical hypersensitivity through an opioid dependent pathway [200]
Oxidative stress and Inflammation	Pain [20, 36-38]	Reduces inflammatory cytokines including IL-1β, IL-6 and TNF-α [20, 38, 201]

Based on current research, quercetin appears to have some beneficial effects that may treat the multiple pathologies that impact PAD. There is evidence to suggest that quercetin can reduce the chance of plaque rupture, improve blood flow and mitochondrial efficiency, improve exercise performance and reduce muscle pain. Evidence suggests increased blood flow is a result of elevated eNOS and HIF-1 activity. Increased mitochondrial efficiency may be due to activation of the AMPK pathway and downstream sirtuin 1 and PGC1α activation. Decreased pain signalling may be due to reduced inflammatory mediators, including IL-1β, IL-6 and TNF-α, as a result of HO-1 mediated antioxidant and anti-inflammatory pathways. Increased exercise performance may result from a combination of increased blood flow, increased mitochondrial efficiency and decreased muscle pain.

1.5.2 Nut supplementation as a potential preventative for AAA

There is evidence to suggest that multiple different tree nuts may be beneficial in reducing the risk of many cardiovascular diseases [153, 202-204]. A recent randomized controlled trial, PREDIMED, reported that supplementation with a mixture of almonds, hazelnuts and walnuts reduced the risk of developing lower limb PAD by 50%, compared with control patients consuming a similar diet without nuts when consumed over a median of 4.8 years [153]. In addition to findings of primary prevention from PREDIMED, a higher consumption of nuts has also been associated with beneficial effects in patients with pre-existing CVDs. Supplementation with pistachio nuts has been associated with reduced total peripheral resistance, increased cardiac output and decreased systolic blood pressure in patients with type 2 diabetes compared with controls [202]. Walnuts have been reported to reduce peripheral vascular resistance and diastolic blood pressure at rest and during stress in hypercholesterolemic patients [203]. Mixed tree nut consumption has been shown to reduce concentrations of c-reactive protein (CRP) and IL-6 [204], and walnuts have been shown to reduce non-HDL cholesterol and apolipoprotein B in healthy subjects in randomized crossover trials [205].

The major constituents of almonds, hazelnuts, walnuts, macadamias and pecans are fatty acids, a large proportion of which are monounsaturated fatty acids (MUFA), omega-3 (n-3) and omega-6 (n-6) polyunsaturated fatty acids (PUFA) [206-209]. MUFA have been reported to improve dyslipidemia, decrease inflammation, decrease pro-inflammatory cytokines and reduce reactive oxygen species [210-213]. Importantly, it has been reported that n-3 PUFA supplementation reduces Ang II-induced AAA formation in mice [214]. Despite evidence for beneficial effects of PUFA consumption, recent evidence suggests only 20% of the Australian population consumes the recommended amount of n-3 PUFA [215].

In addition to MUFA and PUFA, some types of nuts, including pecans, almonds, hazelnuts and walnuts also have a high flavonoid content [206, 207]. The flavonoids have been reported to suppress AAA development in an Ang II model of AAA [216]. Deficiencies of these foods have been linked to increased primary and secondary occurrences of major adverse cardiovascular events [153, 154]. Based on these data, nut supplementation may be a useful and readily available dietary supplement to help prevent the development of AAA.

1.5.3 Colchicine as a potential treatment for AAA

The development of new drugs and safety testing of new drugs is costly and takes a lot of time [217]. Colchicine is a drug already clinically available for gout treatment, however recent evidence suggests it may be beneficial in reducing cardiovascular mortality. A cohort study recently reported patients with gout had lower all-cause cardiovascular mortality when receiving colchicine compared with controls [218]. Further evidence suggests it may be beneficial in treating metabolic disorders, improving insulin sensitivity [219] and myocardial infarction [220], potentially due to its inhibition of microtubule polymerization and therefore macrophage NACHT domain, leucine-rich repeat, and pyrin domain-containing protein 3 (NLRP3) inflammasome assembly [219].

Macrophage inflammasome activation by NLRP3 and caspase 1 appear to be key in the development of AAA in commonly used animal models including calcium phosphate and Ang II-induced AAA [221]. Activation of the inflammasome allows caspase-1 mediated cleavage of pro-interleukin-1-beta (proIL-1β) and pro-interleukin-18 (proIL-18) into active IL-1β and IL-18 and is a key step in the initiation of the adaptive immune response [222, 223]. The NLRP3 inflammasome can be activated by pathogens as well as other inflammatory cytokines such as tumour necrosis factor alpha (TNF-α) [224-226]. Inhibition of NLRP3 has been associated with decreased aneurysm incidence, decreased aneurysm diameter, decreased elastic lamina degradation and decreased metalloproteinase activation in Ang II-infused mice [227]. Inflammasome activation increases macrophage IL-1β release, mitochondria derived oxygen species, and leukocyte recruitment [221, 227]. Aortic NLRP3 gene expression has been reported to be elevated in human subjects suffering from AAA compared with controls [228]. Additionally, activation of the NLRP3/caspase-1 inflammasome has been associated with smooth muscle cell degradation in human aortas [229]. This suggests targeting of the NLRP3 inflammasome may reduce inflammation and smooth muscle cell apoptosis associated with developed AAA.

As previously mentioned, NLRP3 gene expression is elevated in human subjects suffering from AAA [228]. Activation of the NLRP3 inflammasome has been reported to increase elastic lamina degradation and MMP activation [227], increase smooth muscle cell apoptosis [229], directly increase IL-1β and leukocyte migration [221, 227], and

accelerate arterial thrombosis [230] in mouse studies. Each of these factors are individually involved in the pathogenesis of AAA. Inhibition of the NLRP3 inflammasome by colchicine may reduce the progression of AAA by reducing each of the factors mentioned above.

Colchicine may have potentially beneficial effects in AAA due to its inhibition of the NLRP3 inflammasome. Currently, however, there is minimal research available on the direct effects of colchicine on AAA related pathology, and the effects of colchicine are inferred due to its effects on the NLRP3 inflammasome. Older studies suggest that colchicine reduces alveolar neutrophil elastase in chronic obstructive pulmonary disease patients [231], and reduces the surface expression of adhesion molecules, destroys microtubules and destroys surface microvilli in neutrophils and T cells [232-234]. However, no studies have directly measured the effects of colchicine on aortic IL-1β or intraluminal thrombus formation.

1.6 Summary of thesis focus and aims

There are currently minimal pharmaceutical interventions that have been successful in clinical trials for the treatment of PADs. Doxycycline has reduced AAA development in many preclinical studies including multiple animal models but has amassed no clinical evidence [108]. Cilostazol, the one agent that is approved for PAD patients has severe side effects and is not currently recommended by the European guidelines [16]. Many interventions have had promising effects in animal studies however there is a lack of translatability of positive effects from animal models to patients. The positive effects seen in many animal studies are largely due to specific intrinsic limitations of the animal models used as well as experimental design that favours a positive effect. For example, study designs where the drug is administered for weeks or months prior to model induction are much more likely to produce a positive effect than studies that assess the effects of drugs on pre-existing disease. Positive effects from these animal models are of little relevance to patients unless the agent is also intended to be used long term as a prevention in the clinical setting, as may be the case with dietary interventions.

Creating suitable disease models for interventions of pre-existing disease is difficult, however. As discussed above, current PAD models do not allow for an experimental duration long enough to assess the effects of interventions as opposed to preventions. Animal models are of importance as there are no other alternatives to bridge the gap

between *in vitro* and clinical work. Different available models have different strengths and limitations and it is important to design experiments accordingly.

Further research must be conducted into dietary and pharmacological preventions and interventions to reduce the need for surgery in vulnerable patients. Suitable animal models and experimental design are imperative in order to avoid false positive results which lead to failed clinical trials and wasted time and money.

The aims of this thesis are to utilise novel and clinically relevant animal models to evaluate promising drug interventions for potential trial in patients with PADs.

CHAPTER 2
GENERAL MATERIALS AND METHODS

This chapter describes general methods used for multiple chapters and methods for key outcomes requiring reproducibility testing which are reported in chapter 3.

2.1 Animals

Animals were obtained from the Animal Resources Centre, Canning Vale, Western Australia and housed in the small animal house in building 86, James Cook University, Townsville and building 47, James Cook University, Townsville. In both buildings, mice were housed in individually ventilated cages in the Techniplast digital ready green line mouse rack system with 501cm^2 floor area on corn starch bedding. Temperature was maintained at 22°C, with a relative humidity of 55% and a 14/10h light dark cycle with daylight hours of 6am to 8pm. Food and water was provided ad libitum during acclimatization, aging and experiments except for two-hour fasting periods prior to tail vein blood sampling, sacrifice, and situations mentioned in specific chapters. Cages were cleaned weekly and mice were monitored twice daily during experimental periods. Ethics approval was obtained for all experiments from the James Cook University Animal Ethics Committee (A2352, A2353, A2574; Table 2.1).

Table 2.1. Details of all experimental mice used within the chapters of this thesis

Ethics Number	Mouse strain	Total mice	Age (weeks)	Study intervention	Route of administration
A2352	*ApoE-/-*	48	22-24	Quercetin	Oral (diet)
A2353	*ApoE-/-*	34	10-12	Tree nuts	Oral (diet)
A2574	C57BL/6J	73	8	Colchicine	Oral gavage

2.2 Isoflurane anaesthesia

Isoflurane (ISOTHESIA, Henry Schein, Ohio) was used for all procedures requiring general anaesthesia. Isoflurane was administered at 4% in oxygen at a flow rate of 1L/min for a two-minute induction period or until mice were unconscious, as confirmed with a toe pinch reflex test. Isoflurane was then administered at 3% to maintain anaesthesia for the remainder of the procedures. Following all procedures using isoflurane, mice were

allowed to recover individually in a recovery chamber with heat mat before being returned to their cages.

2.3 Ultrasound assessment of aortic diameter

Mice were anaesthetised using isoflurane (Chapter 2.2) and depilatory cream (Veet, France) was applied to the chest and abdominal regions. After one minute all cream was removed using a cotton pad with phosphate buffered saline (PBS) followed by the application of 70% ethanol. Mice were then scruffed to expose the chest and abdominal regions for ultrasound measurements. Maximum diameters of SRA and IRA were measured using a linear ultrasound transducer (Esaote, Italy) at 12 MHz with ultrasound transmission gel (Aquasonic, Parker, USA) attached to a Mylab 30 ultrasound machine (Esaote, Italy). The largest part of the SRA and IRA were located by imaging the aorta longitudinally. Once the largest region was located, a cross section of the aorta was captured. Measurements were always taken during late systole or early diastole when lumen diameters were widest. Following measurements, mice were cleaned of excess gel using cotton pads and returned to cages for recovery.

2.4 Tail cuff plethysmography for measurement of blood pressure

Blood pressure was measured using a non-invasive tail cuff blood pressure monitor (Kent Scientific, USA) with an interval of 10 seconds and a deflation time of 15 seconds. The blood pressure monitor consists of a medium occlusion cuff (OCC-M) and a medium volume pressure sensor (VPR-M). Mice were restrained using a Perspex mouse restraint (Kent Scientific, USA). The occlusion cuff was placed around the base of the tail, and the volume pressure sensor was placed 1mm below the occlusion cuff. A heat pad (Kent Scientific, USA) and heat lamp was used to provide adequate tail blood flow for blood pressure measurements. Systolic, diastolic and mean arterial blood pressure were measured 10 times for each mouse, and the three closest consecutive values were averaged to provide the final blood pressure values for each mouse. Mouse restraints were washed thoroughly between uses to reduce stress due to mouse scent. Measurements were performed between 6am and 11am to minimize the effects of diurnal variation, as previous mouse studies suggest blood pressures are most stable between 1am and 11am [235].

2.5 Laser Doppler perfusion imaging

Blood flow was measured in both hind limbs of mice using laser Doppler perfusion imaging (LDPI; Moor Instruments, UK). Isoflurane was administered as described in chapter 2.2. Hind feet were taped with the plantar surface of the foot facing downward on a black background. The laser was located 26cm directly above the mouse hind limbs when LDPI imaging was performed. The colour flux image produced by LDPI was analysed to produce perfusion units using computer software (Laser Doppler Perfusion Measure, *V3.08*, Moor Instruments, UK). These perfusion units were then normalised as left/right hind limb ratios to allow comparison between groups.

2.6 *Ex vivo* morphometric assessment of aortic diameter

Entire aortas for each mouse were flushed with PBS, harvested from the aortic arch to the iliac bifurcation and placed on a black background with a ruler. Photographs were taken using a digital camera and analysed with ImageJ software (National Institutes of Health) [18]. Diameters of the largest portion of the aortic arch, thoracic aorta, SRA and IRA were measured.

2.7 Tail vein blood sampling

Blood samples were taken at different time points throughout the animal experiments using tail vein blood sampling. Mice were fasted for two hours prior to blood sampling in order to reduce the risk of postprandial effects interfering with chronic changes in content of the plasma [236, 237]. Topical anaesthetic EMLA cream (AztraZeneca, Australia), which contains 25mg/g Lignocaine and 25mg/g Prilocaine, was applied to the tail of mice five minutes before blood samples were taken. Mice were placed in a cage supplied with a heat lamp to allow sufficient warming and blood flow to the tail prior to sampling. Mice were then transferred to a Perspex box with a cut-out which allowed access to the tail. Tails were held firmly and a scalpel blade was used to make a small cut midway down the tail vein. Six drops of blood (200µl) were added to a lithium-heparin lined tube (BD Microtainer, USA), mixed, and placed on ice awaiting centrifugation. Light pressure was applied to the tail vein to stop bleeding and riodine (Orion, Australia) was applied to prevent infection. Mice were monitored after sampling to ensure no adverse events had occurred.

2.8 Cardiac puncture

Endpoint blood samples were taken using cardiac puncture to maximise the volume of blood collected for analysis. Following euthanasia, the thoracic cavity was quickly opened, and a 27 Gauge needle attached to 1mL syringe was inserted directly into the right ventricle. Blood was withdrawn slowly to prevent closing of the ventricles. Blood was added to a lithium-heparin lined tube and stored on ice awaiting centrifugation.

2.9 Blood centrifugation for plasma

Blood samples were stored on ice for no longer than 1 hour prior to being centrifuged at 4ºC, 2000 x g for 10 minutes. Supernatant was transferred to microcentrifuge tubes for further centrifugation at 15000 x g for 10 minutes. Supernatant plasma was aliquoted into microfuge tubes, snap frozen in liquid nitrogen and stored in -80ºC freezers. Cardiac puncture end point blood samples were aliquoted to two microfuge tubes to allow easier access to samples with minimal freeze thaw cycles.

2.10 Sacrifice/Dissection

Mice were sacrificed using carbon dioxide asphyxiation (5L/min, 2 minutes) and death was confirmed by toe pinch prior to dissection. Following retrieval of blood and tissues, mouse carcasses were disposed of in biohazard bins.

2.11 *En face* staining of aortic arch

2.11.1 Preparation of *en face* staining

Silicone elastomer base (Sylgard 184, Dow Corning) and curing agent (Sylgard 184, Dow Corning) were mixed in a 9:1 ratio to prepare a silicone elastomer gel for the pinning of aortic arches. The mixture was transferred to petri dishes which were filled to half capacity and transferred to a 50ºC incubator for 24 hours to allow the elastomer to set. Sudan IV staining solution was prepared by mixing a 50% mixture of 70% ethanol and acetone with five grams of sudan IV (Sigma-aldrich). Aortic arches, stored in optimal cutting temperature compound (OCT, Tissue-plus), were thawed and transferred to PBS to remove OCT and peri-aortic fat tissue. Once cleaned, aortic arches were stored in 10% neutral buffered formalin (Sigma-aldrich, HT501128-4L) at 4ºC for 24 hours. Arches were then drained of formalin and submerged in PBS solution on an elastomer coated petri dish for cutting and pinning. The first cut was made along the interior side of the entire aortic arch. The base of the arch was then pinned and a second cut was made on the

external side of the aortic arch, from the origin of the brachiocephalic artery to the aortic root. This allowed aortic arches to be pinned open in the shape of a Y.

2.11.2 Sudan IV staining procedure

Pinned aortic arches were flushed with PBS twice to remove debris. Aortas were stained for 15 minutes in Sudan IV (0.1%, dissolved in 1:1 acetone: 70% ethanol) staining solution and decolourised with 80% ethanol solution until clear differentiation of atherosclerotic and non-atherosclerotic tissue could be observed. Aortas were then washed in PBS and photographed using a digital camera.

2.11.3 Sudan IV data analysis

Sudan IV stained aortic arch images were analysed in Adobe Photoshop CC 2015. The aortic arch was traced using the lasso tool, and its total area was measured. The inverse of the selected arch was deleted to leave the arch alone with a black background. A small area of representative Sudan IV stained tissue was selected, and the select similar tool was used to allow for automatic selection of all Sudan IV stained regions.

2.12 Histology

2.12.1 Fixing, processing and paraffin embedding

Following dissection from recently euthanized animals, tissues were fixed in 10% formalin (Sigma-aldrich, HT501128-4L) and stored at 4ºC for 24 hours. Small samples, such as brachiocephalic arteries, were fixed for the final four hours in 10% formalin with eosin to help visualisation during processing and embedding. Tissues were then processed in an automated Shandon excelsior ES processing machine (Thermo Electron Corporation) through graded ethanol and xylene washes prior to embedding with paraffin wax. Tissues embedded in paraffin wax were cooled on ice prior to sectioning to reduce folding of paraffin sections. Tissues were first faced on a microtome at 20µm until a clear cross sections of tissues could be observed. Tissues were then sectioned at 5µm. Prior to staining tissues, slides containing paraffin embedded sections were deparaffinized by washes in 2x 100% xylene for three minutes each, followed by 1:1 xylene:100% ethanol for three minutes, followed by 100%, 95%, 70%, and 50% ethanol for three minutes each.

2.12.2 Storing and preparation of frozen sections

Following dissection from recently euthanized animals, tissues were placed in cryomolds containing OCT, oriented, and allowed to acclimate for five minutes prior to freezing in

2-methylbutane submerged in liquid nitrogen. Frozen tissues were faced in a cryostat at -25°C, and 5µm sections were added to slides. Slides were stored at -80°C until staining. Prior to staining, frozen sections were allowed to reach room temperature for five minutes, fixed in a 1:1 methanol:acetone solution for 15 minutes, and rinsed in tris-buffered saline (TBS).

2.12.3 Haematoxylin and Eosin staining

Mayer's haematoxylin was filtered prior to use for tissue staining. Slides were submerged in Mayer's haematoxylin for four minutes. Following staining with haematoxylin, tissues were submerged in tap water for four minutes with three changes, until all colour was removed from the water. Slides were then washed in Scott's tap water substitute for 30 seconds, followed by tap water for an additional two minutes. Slides were then submerged in eosin for eight dips before again being washed in tap water for four minutes with three changes. Slides were then dehydrated through 50%, 70%, 80%, 90% and 100% ethanol washes, and xylene for four minutes with three changes. Slides were then mounted with coverslips using vectamount permanent mounting medium (Vector Laboratories, H-5000) and incubated for 24 hours at 37ºC.

2.12.4 Verhoeff Van Gieson's elastin staining

Slides were incubated at 37ºC for 30 minutes prior to staining with Verhoeff Van Gieson's stain (ProSciTech, Australia). Paraffin embedded tissues were deparaffinised in xylene for 20 dips with 2 changes, followed by distilled water for 20 dips with 2 changes. Verhoeff solution was prepared by mixing 20mL 5% alcoholic haematoxylin, 8mL 10% aqueous Ferric Chloride, and 8mL Ioidine solution (PolySciences, 25089A-C). Slides were then stained with Verhoeff solution for one hour. Following staining, slides were washed in tap water with 3 changes to remove excess Verhoeff solution. Slides were differentiated using 2% aqueous Ferric Chloride. Each slide was examined individually under a microscope to determine sufficient differentiation of tissue layers had occurred to allow for differentiation of elastin and surrounding tissue. Slides were then washed in tap water for 30 dips with 3 changes, treated with 5% Sodium Thiosulphate for 1 minute, and washed in tap water for a further 5 minutes with 2 changes. Slides were then dehydrated through 50%, 70%, 80%, 90% and 100% ethanol washes, and xylene for four minutes with three changes. Slides were then mounted with coverslips using vectamount permanent mounting medium and incubated for 24 hours at 37ºC.

2.12.5 Picrosirius red staining

Prior to staining, slides were rinsed in tap water for two minutes. Slides were placed in phosphomolybdic acid for two minutes and rinsed in distilled water for 30 seconds. Slides were then placed in picrosirius red staining solution (Polysciences) for 60 minutes. Slides were then transferred to 0.1M hydrochloric acid for two minutes. Slides were then dehydrated through 50%, 70%, 80%, 90% and 100% ethanol washes, and xylene for four minutes with three changes. Stained slides were mounted with coverslips using vectamount permanent mounting medium and incubated for 24 hours at 37ºC.

2.13 Brachiocephalic artery atherosclerosis lesion area determination

Cross sections of brachiocephalic arteries were paraffin embedded (Chapter 2.12.1) and stained with Verhoeff Van Gieson's Elastin stain (Chapter 2.12.4) as described. Slides were examined under a microscope (Nikon Eclipse 50*i*) and photographed under 100x magnification using a CCD camera (DS-F*i*1). Plaque lesion area was assessed in brachiocephalic arteries by measuring the intima:media area ratio using a previously reported protocol [238]. The tunica media area was calculated by subtracting the area within the internal elastic lamina from the area within the external elastic lamina. The tunica intima area was calculated by subtracting the luminal area from the area within the internal elastic lamina. The ratio of intima:media area was calculated to normalise and compare the degree of atherosclerosis between mice. Measurements were performed using Adobe Photoshop CC 2015.

2.14 Protein extraction and quantification of aortic total protein concentration

IRA tissue was lysed in radio immunoprecipitation assay buffer (Thermo Fisher Scientific, Australia) containing protease inhibitor (Sigma, Australia) and metal beads and placed in a tissue homogeniser (Next Advance, USA) for 15 minutes. Samples were then centrifuged at 14000xg for 20 minutes at 4ºC. Supernatants containing soluble protein were transferred to new tubes and protein concentration of samples was determined using a pierce bicinchoninic acid (BCA) assay kit (Thermo Fisher Scientific, Australia, Cat. No. 23225). BCA assay buffer (100µl) and 5µl of soluble protein from standards or samples was added to each well. Plates were covered and incubated at 37ºC for 30 minutes. Plates were then allowed to cool to room temperature and absorbance was measured at 562nm on a plate reader (POLARstar Omega, Bmg Labtech, Australia). Sample total protein

concentrations were determined using a standard curve modelled by linear regression using 1000, 500, 400, 300, 200, 100, 50 and 0µg/mL total protein standards.

2.15 Statistical analyses

Data were tested for gaussian distribution using the D'Agostino and Pearson test. Normally distributed data were expressed as mean ± standard error of mean (SEM), and non-normally distributed data were expressed as median with interquartile range (IQR) including all individual data points. End point measurements limited to two experimental groups and one time point were compared using unpaired two-sample t-tests. Mann-Whitney U tests were used to compare data from two groups at one time point when data were not normally distributed. Incidence of adverse outcomes was compared between groups using Fisher's exact test and deaths between groups were compared using Mantel-Cox (Log-rank) test. Data measured at multiple time points throughout the studies were compared using linear mixed effects (LME) models. LME models have some advantages over the two-factor ANOVA. LME models allow for unequal sample sizes at different time points, which is common in the current studies due to deaths from experimental parameters. LME models also allow for relaxing of the assumption of equal variance between experimental groups and different time points. Due to surgical and therapeutic interventions occurring at different time points, variance in groups can change significantly over time. The interaction of time and treatment was assessed in order to determine statistical significance. The degree to which data met the assumptions of the LME models was assessed by analysing qq-normal and residual versus fits plots as previously described [15](see appendix B). In cases where qq-norm plots showed evident shift from normal distribution, data were log transformed. Where potentially influential outliers were identified, sensitivity analyses were conducted excluding these outliers. For all statistical analyses, differences were considered statistically significant when *p*-values were less than 0.05. Statistical analyses for all chapters were performed using graphpad prism (version 6, GraphPad Software Inc), R Studio (R studio, PBC) and RevMan5 (Cochrane library).

Described in this chapter are general methods used for multiple chapters and methods for key outcomes requiring reproducibility testing. Intra-observer and inter-observer reproducibility measures of key outcomes, the methods of which are described above, are presented in the following section.

CHAPTER 3
REPRODUCBILITY OF OUTCOME MEASURES

3.1 Outline

Intra-observer and inter-observer reproducibility measurements were calculated for key outcome measures where results are highly dependent on user input and technique. For intra-observer analysis, outcomes were measured two times seven days apart. For inter-observer analysis, the average of these results were compared with results of a second person who is experienced in the technique. The coefficient of variation was calculated for intra-observer and inter-observer variance by dividing the sum of all standard deviations (SD) of duplicate measurements by the sum of all means of duplicate measurements divided by total number of samples measured (depicted in the equation below).

$$\frac{(SD(X1+X2)+\cdots+SD(Y1+Y2)/n)}{(M(X1+X2)+\cdots+M(Y1+Y2)/n)}$$

Where SD is standard deviation, M is mean, n is number of samples, and X and Y are different samples each measured in duplicate. The coefficient of variation was expressed as mean percentage plus or minus SEM. All intra-observer and inter-observer coefficients of variation that are below 10% are considered ideal, while all coefficients of variation below 20% are considered acceptable.

3.2 Ultrasound measurements of cross-sectional aortic diameter

Maximum diameters of the SRA and IRA were measured *in vivo* (Chapter 2.3). Intra-observer and inter-observer reproducibility measurements are reported based on measurements from n=10 mice (Figure 3.1). Intra-observer and inter-observer measurements were below 10% for both SRA and IRA measurements which are considered ideal.

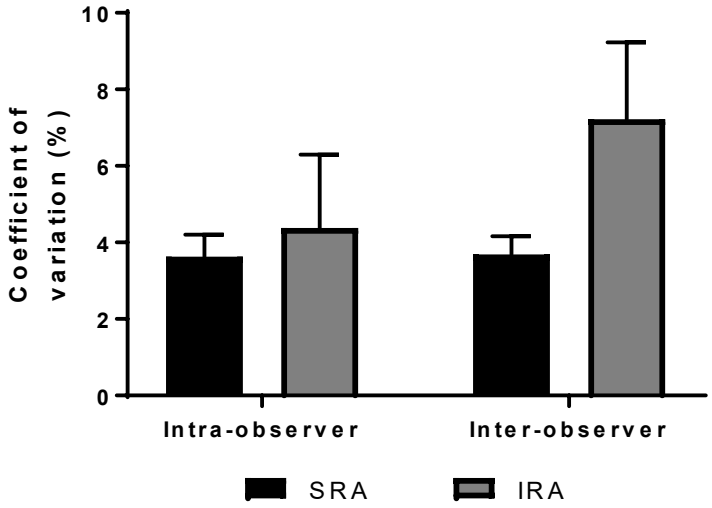

Figure 3.1. Intra-observer and inter-observer reproducibility of maximum aortic diameter measured by ultrasound.

3.3 Blood pressure

Blood pressure was measured using tail-cuff plethysmography (Chapter 2.4). Intra-observer reproducibility was calculated by measuring systolic, diastolic and mean arterial blood pressure in the same mice one week apart (n=15, Figure 3.2). Intra-observer variation is high in blood pressure measurements due to acclimatization and uncontrollable physiological changes. Measurements were taken in the same environment, using the same standard operating procedures, between 6am and 11am on both days. All blood pressure measurements were taken by one observer. The reproducibility of these results are higher than ideal however they are expected based on previously reported variation for tail cuff plethysmography measurements [239].

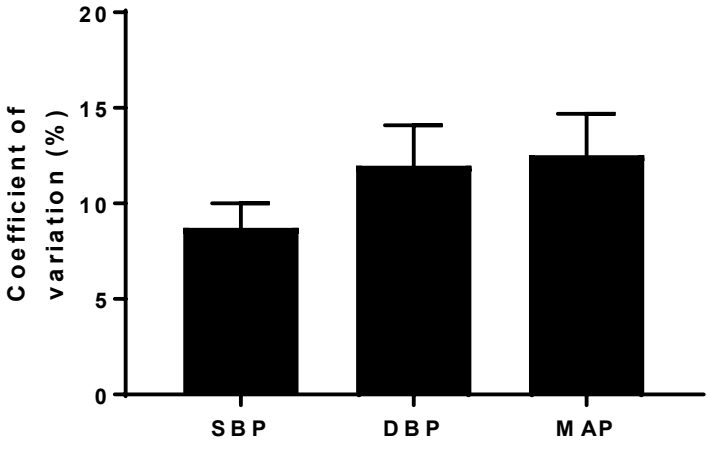

Figure 3.2. Intra-observer reproducibility of systolic, diastolic and mean arterial blood pressure measured by tail-cuff plethysmography. SBP, systolic blood pressure; DBP, diastolic blood pressure; MAP, mean arterial pressure.

3.4 Blood flow measurements using laser Doppler perfusion imaging

Blood flow was measured in both limbs of mice using laser Doppler perfusion imaging and values of ischemic limbs were normalised to non-ischemic limbs in the same mouse (Chapter 2.5). Intra-observer and inter-observer reproducibility coefficients of variation are reported based on measurements from n=20 mice (Figure 3.3). Intra-observer and inter-observer measurements were below 10% for both SRA and IRA measurements which are considered ideal.

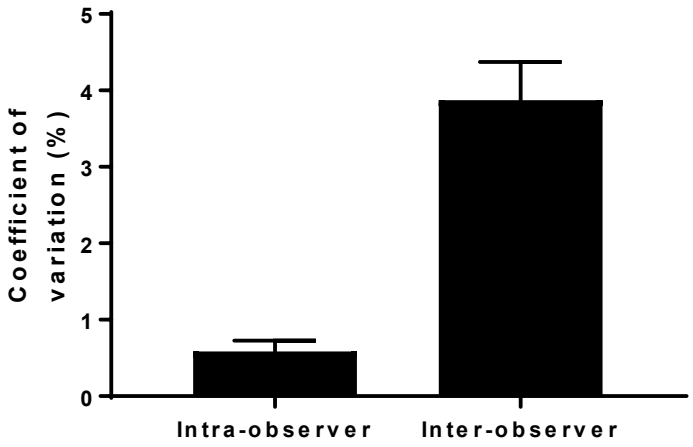

Figure 3.3. Intra-observer and inter-observer reproducibility of blood flow measurements using laser Doppler perfusion imaging.

3.5 *Ex vivo* measurements of aortic diameter

Maximum diameters of the aortic arch, thoracic aorta, SRA and IRA were measured *ex vivo* according to the methods outlined in general materials and methods (Chapter 2.6). Intra-observer and inter-observer reproducibility measurements are reported based on measurements from n=22 mice (Figure 3.4). The intra-observer reproducibility of aortic diameter measurements are considered ideal, which the inter-observer reproducibility measurements are acceptable but not ideal. Due to this, all aortic measurements were performed by one person, to minimise variation between results.

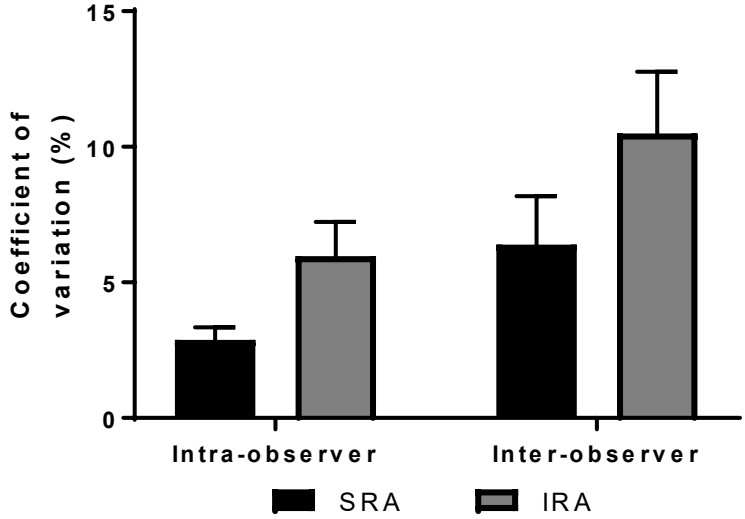

Figure 3.4. Intra-observer and inter-observer reproducibility of *ex vivo* maximum aortic diameter measurements. TA, thoracic aorta.

3.6 Atherosclerosis lesion area in the brachiocephalic artery

Atherosclerosis lesion area was quantified from histological elastin van-gieson stained images of brachiocephalic artery cross sections (Chapter 2.12.4 and 2.13). Intra-observer and inter-observer reproducibility coefficients of variation are reported based on measurements from n=19 mice (Figure 3.5). Intra-observer and inter-observer measurements were below 10% for both SRA and IRA measurements which are considered ideal.

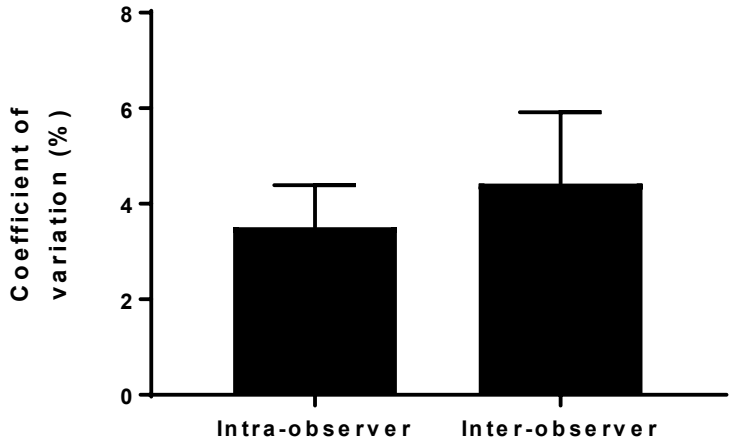

Figure 3.5. Intra-observer and inter-observer reproducibility of atherosclerosis lesion area measurements in the brachiocephalic artery.

CHAPTER 4
FLAVONOLS REDUCE AORTIC ATHEROSCLEROSIS LESION AREA IN MICE: A SYSTEMATIC REVIEW AND META-ANALYSIS

4.1 Introduction

Atherosclerosis and associated thrombosis are the main underlying cause of stroke, myocardial infarction and peripheral artery disease which, collectively, are the leading cause of death globally [240]. Much of the focus on the primary and secondary prevention of CVD over the last few decades has been on drugs to manage cardiovascular risk factors such as statins to lower cholesterol, blood pressure lowering medications and anti-platelet agents [241-243]. Diet has been linked to the development and complications of CVD for centuries [244]. However, it is only more recently that trials demonstrating the benefits of dietary interventions in humans have been completed [245-247]. A recent multicentre randomized controlled trial, which included 7447 participants, reported that the Mediterranean diet with either extra virgin olive oil or nut supplementation reduced the incidence of cardiovascular end points by 30%, compared to control subjects educated on a low fat diet [248]. The beneficial effects of extra virgin olive oil and nuts have been linked to their high phenolic content [249, 250], and reductions in blood pressure and LDL oxidation have been reported for other foods high in phenols including dark chocolate, green tea, apples, tomatoes, kale, lettuce and onions [251-253].

A subclass of phenols, known as the flavonoids, have been of particular interest in recent research for their potent anti-oxidant and anti-atherosclerosis effects [254]. The most studied flavonoids are the flavan-3-ols, the flavonols, and the flavonol glycosides (e.g. enzymatically modified isoquercitrin; EMIQ) (Figure 4.1) [255, 256]. However, the impact of consuming purified flavonoids on cardiovascular events have not been examined in human clinical trials.

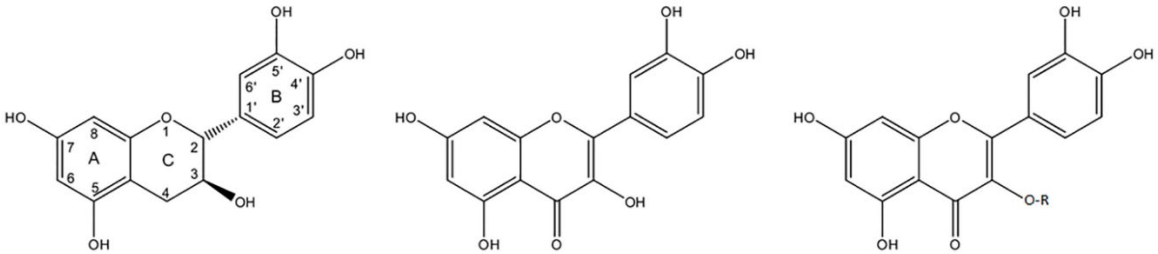

Figure 4.1. Structural properties of the major flavonoid classes (examples in brackets) used in atherosclerosis research in *ApoE-/-* mice. Catechin and epicatechin are flavan-3-ols; Quercetin, Kaempferol and Isorhamnetin are flavonols; and EMIQ and myricitrin are flavonol glycosides. R, glucose chain (n=3-9). Adapted from de Pascual-Teresa, Moreno [257].

ApoE-/- mice have been used to assess the effect of flavonoids on atherosclerosis, however the overall effect of the flavonoids, and the effect of individual classes of flavonoids on the severity of atherosclerosis remain unclear. The *ApoE*$^{-/-}$ mouse model is particularly useful for studying atherosclerosis due to its quick and predictable development of atherosclerosis [258, 259]. Furthermore, the model responds to lipid lowering interventions which have been shown to reduce complications of atherosclerosis in humans [258, 260, 261].The aim of this systematic review and meta-analysis was to examine the effect of purified flavonoids on the severity of aortic atherosclerosis in *ApoE*$^{-/-}$ mice.

4.2 Materials and methods

4.2.1 Search strategy, inclusion and exclusion criteria

This review was prepared according to the 2009 Preferred Reporting Items of Systematic Reviews and Meta-Analyses (PRISMA) statement. Literature searches were conducted to identify pre-clinical studies testing the effects of flavonoids on atherosclerosis lesion area in *ApoE*$^{-/-}$ mice. Medline, Pubmed, Science direct and Web of Science were searched between 16th March 2016 and 27th May 2017. Studies published from all years were included. Science direct searches were filtered to include only journal articles. The full search strategy included the terms ("Apolipoprotein* E" OR ApoE) AND (Mice OR Mouse) AND (Phenol* OR Flavonoid* OR Quercetin OR Catechin OR Glabridin OR Kaempferol OR Epicatechin OR Baicalin OR Isorhamnetin) utilising both medical subject headings and keyword searches. Resulting titles and abstracts from all years were screened for relevance and all potentially eligible abstracts were assessed in full text.

Reference lists of included studies were also screened for relevant articles. Controlled studies which used purified flavonoids, or flavonoids with glucoside moieties such as isoquercitrin, in an *ApoE*$^{-/-}$ mouse model were included. Of these, only studies which included atherosclerosis lesion area as an outcome measure were included. Studies which did not report atherosclerosis lesion area as a percentage or as lesion area out of total area measured were excluded. Included studies were restricted to those published in English. Reviews, editorials, books, letters, case reports, and clinical trials were excluded. Studies where sample size could not be determined were excluded.

4.2.2 Data extraction and quality assessment tool

Full text articles eligible for data extraction were independently assessed by three authors, JP, SMK and SMO, and results were later discussed in a consensus meeting. The data extracted included mouse age, sex and diet, flavonoid purity and dose, duration of treatment, control and treatment group sample sizes, location of atherosclerosis area assessed, stain used for lesion assessment, lesion area as a percentage of total area, plasma triglyceride (TG), LDL cholesterol (LDL-C), HDL cholesterol (HDL-C), total cholesterol (TC) and measures of LDL-oxidation and reactive oxygen species. Data were extrapolated from figures in 10 of the studies using Adobe Photoshop CS6. In cases of missing data, corresponding authors were contacted. Authors of seven papers were contacted [159, 262-267], and two responded [265, 266]. Study quality was assessed using a quality assessment tool adapted from a previous preclinical systematic review [268]. Questions focused on the reporting of study design, mouse age and sex, diet, housing conditions, method of group allocation, ethics approval, justification of sample sizes, justification of flavonoid dose, flavonoid purification processes, methods of lesion area analysis and blinding procedures for outcome assessments. Each question was assessed as a yes or no answer and the number of yes answers reported as a percentage out of 17 questions, or out of 15 questions for studies that did not measure plasma lipids. These percentage scores were used as an indication of overall study quality. Studies were rated as poor (<50%), moderate (51-75%), good (76-90%), or excellent quality (91-100%).

4.2.3 Statistical analysis

A meta-analysis was used to assess the overall effects of the administration of purified flavonoids on atherosclerosis lesion area in *ApoE*$^{-/-}$ mice. In four studies [155, 156, 160, 269], the same control group was used to compare multiple flavonoids or flavonoid doses. In these instances, the number of control animals was divided by the number of comparator groups to prevent an artificial increase in sample size in the meta-analysis. Sub-analyses were performed to test the overall effect of the flavonols and flavan-3-ols on atherosclerosis lesion area.

Heterogeneity in the data was expected due to the use of multiple flavonoids, at different doses with different durations of treatment, and therefore random effects models were used. Data were expressed as standardised mean difference with 95% confidence intervals (CI). Sensitivity analyses were performed using the leave one out approach to test the effect of each study on the standard mean difference (SMD). I^2 values were used to assess heterogeneity between studies. Heterogeneity above 30% was considered moderate, and heterogeneity above 50% was considered substantial. Funnel plots were used to test for publication bias. Statistical analyses were performed using RevMan 5.3, and tests were considered significant when P values were <0.05.

4.3 Results

4.3.1 Study selection

Database searches identified a total of 1192 studies, of which 224 articles were duplicates (Figure 4.2). The titles and abstracts of the remaining 968 articles were screened and 942 were excluded. The full text was assessed for the remaining 26 articles. Eight of these studies were excluded because atherosclerosis lesion area was not reported and one study was excluded because a crude extract rather than a purified flavonoid was administered. After contacting corresponding authors, a further three studies were excluded because sample sizes for lesion area measurements could not be obtained [262, 263, 266], and three studies were excluded after no reply from authors because total area of the aorta measured was not reported [264, 267, 270]. In total, eleven studies were included in the current systematic review and meta-analysis.

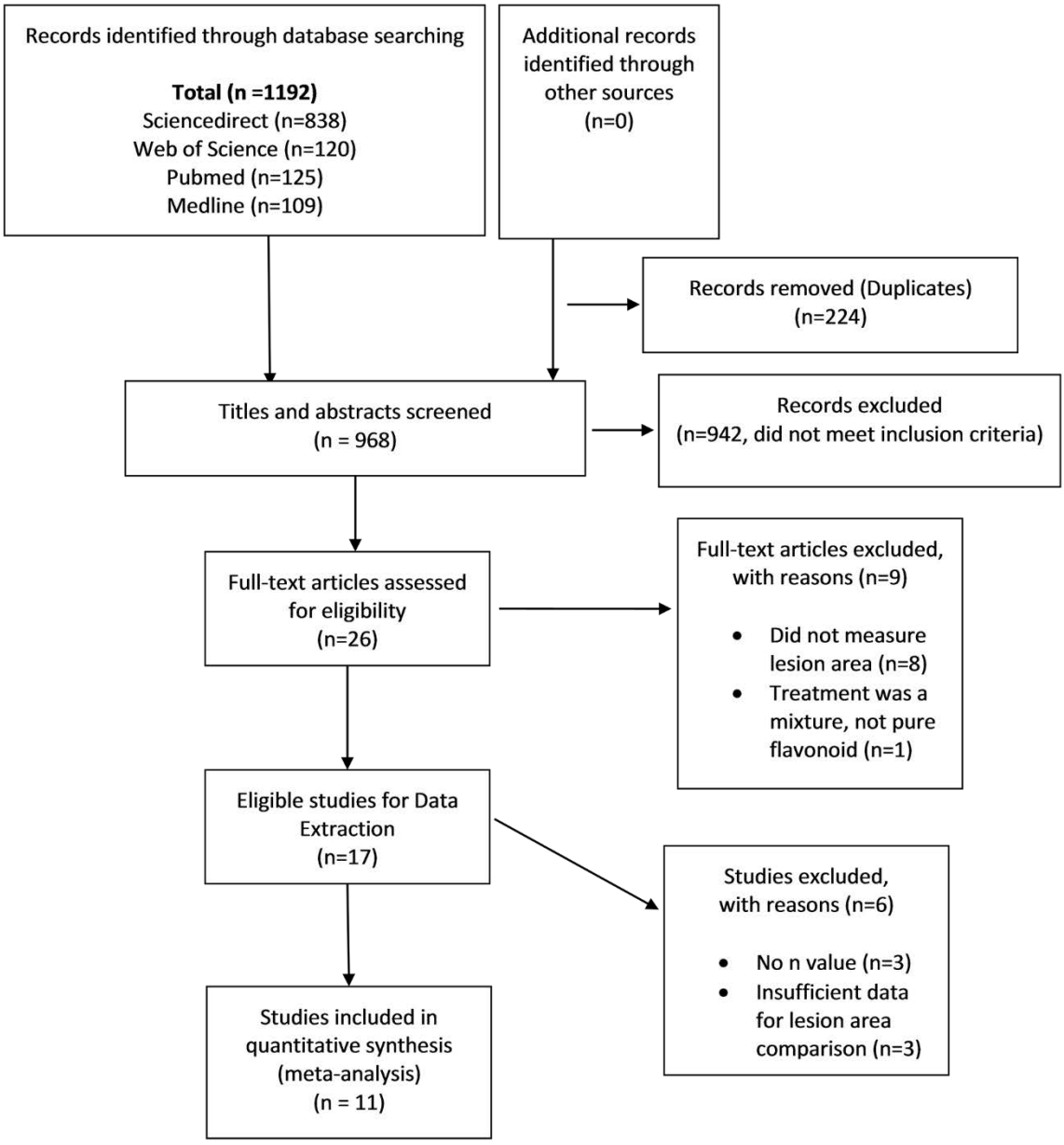

Figure 4.2. Preferred Reporting items of Systematic Review and Meta-analyses flow diagram. A total of 1192 articles were identified from Science direct, Web of Science, Pubmed and Medline. Of these, 26 full-text articles were assessed for eligibility and 11 articles were included in the review. Eight studies were excluded as they did not measure atherosclerosis lesion area. One study was excluded as it administered a crude extract. Three studies were excluded because sample sizes could not be retrieved, and three studies were excluded because of insufficient data for lesion area comparison.

4.3.2 Study characteristics

The characteristics of the eleven included studies are shown in table 4.1. Mice from all included studies were male, except for one study in which the sex was not reported [155]. Mice received a standard chow diet in three studies [155, 160, 265]; a high fat diet in seven studies containing either 20% fat and 0.3% cholesterol [271-273], 21% fat and 1.25% cholesterol [269], 47% carbohydrates, 21% fat and 20% protein [159], or 1.25% cholesterol and 10% coconut oil [274, 275]; and the American Institute of Nutrition (AIN) 93 diet, containing 4% fat, 73% carbohydrates, and 14% protein, in one study [156]. The age of the mice when flavonoid administration was initiated was four weeks in one study [155], six weeks in seven studies [156, 159, 265, 269, 271-273], eight weeks in one study [275], nine weeks in one study [274], and 15 weeks in one study [160]. Six studies administered the flavonoids via the intragastric route [160, 271-275], two studies administered the flavonoids by adding it to the drinking water [155, 265], and three studies administered the flavonoids by adding to the chow [156, 159, 269].

Table 4.1. Characteristics of studies included in this meta-analysis.

Study	Flavonoid	Purity	Mouse Age (weeks)	Mouse Sex	Diet	Study length (weeks)	Dose (mg/kg/d)	Route	Lesion area measured	Staining	Analysis
[274]	Baicalin	98%	9	Male	HCD	12	100	IG	Aortic root	Oil red O	CS
[275]	Baicalin	98%	8	Male	HFD	12	100	IG	Aortic root	Oil red O	CS
[155]	Catechin	?	4	?	SCD	6	~1.6	Water	Aortic arch	Osmium	CS
[156]	Epicatechin	98%	6	Male	AIN-93M	26	64	Chow	Aortic Sinus, Thoracic aorta	Sudan IV	CS
[265]	Glabridin	98%	6	Male	SCD	6	~0.6	Water	Aortic valves	Osmium	CS
[159]	EMIQ	?	6	Male	HFD	14	~30	Chow	Aortic sinus	Oil red O	CS
[271]	Isorhamnetin	98%	6	Male	HFD	8	20	IG	Aortic valves	Oil red O	CS

~ indicates dose was calculated based on average body weights and food consumption reported in previous *ApoE*$^{-/-}$ mouse studies. AIN, American institute of Nutrition; HCD, high-cholesterol diet; HFD, high-fat diet; IG, Intragastric; M, maintenance; SCD, standard chow diet; ?, unknown; H&E, hematoxylin and eosin; CS, cross sectional.

Table 4.1 (continued). Characteristics of studies included in this meta-analysis.

Study	Flavonoid	Purity	Mouse Age (weeks)	Mouse Sex	Diet	Study length (weeks)	Dose (mg/kg/d)	Route	Lesion area measured	Staining	Analysis
[160]	Kaempferol	98%	15	Male	SCD	4	50 or 100	IG	Aortic root to Iliac branches	Sudan IV	En face
[273]	Myricitrin	98%	6	Male	HFD	8	50	IG	Aortic root	Oil red O	CS
[272]	Myricitrin	98%	6	Male	HFD	6	50	IG	Aortic root	Oil red O	CS
[155]	Quercetin	?	4	?	SCD	6	~1.6	Water	Aortic arch	Osmium	CS
[156]	Quercetin	98%	6	Male	AIN-93M	26	64	Chow	Aortic Sinus, Thoracic aorta	Sudan IV	CS
[269]	Quercetin	98%	6	Male	HFD	24	25-100	Chow	Aortic Sinus	H&E	CS

~ indicates dose was calculated based on average body weights and food consumption reported in previous *ApoE*$^{-/-}$ mouse studies. AIN, American institute of Nutrition; EMIQ, enzymatically modified isoquercitrin; HCD, high-cholesterol diet; HFD, high-fat diet; IG, Intragastric; M, maintenance; SCD, standard chow diet; ?, unknown; H&E, hematoxylin and eosin; CS, cross sectional.

The eleven included studies collectively measured the effects of nine unique flavonoids, at multiple doses in a total of 18 comparisons, based on the outcome of atherosclerosis lesion area. Quercetin was administered at 25, 50 and 100mg/kg/d for 24 weeks [269], 64mg/kg/d for 26 weeks [156] and 1.6mg/kg/d for six weeks [155]. Myricitrin was used in two studies at 50mg/kg/d for six weeks [273] and eight weeks [272]. Baicalin was administered at 100mg/kg/d for 12 weeks in two studies [274, 275]. Catechin was administered at 1.6mg/kg/d for six weeks [155]. Epicatechin was administered at 64mg/kg/d for 26 weeks [156]. Glabridin was given at 0.6mg/kg/d for six weeks [265]. Isorhamnetin was administered at 20mg/kg/d for 8 weeks [271]. Kaempferol was given at 50 and 100mg/kg/d for 4 weeks [160]. EMIQ was administered at 30mg/kg/d for 14 weeks [159]. Three studies did not report dose per kilogram and gave no body weight measurements [155, 159, 265], therefore an estimated dose assuming an average mouse weight of 30g per mouse [276] and an average food intake of 3.45g/d [277] was calculated. The purity of individual flavonoids was >98% in nine studies, as measured through high performance liquid chromatography [156, 160, 265, 269, 271-275]. The purification procedure was described but purity was not stated in one study [159], and no flavonoid source or purification procedure was given for one study [155].

4.3.3 Atherosclerosis lesion area

Ten studies measured cross sectional aortic lesion area in mice receiving flavonoids and controls [155, 156, 159, 265, 269, 271-275]. Of these, nine of the studies measured aortic lesion area at the level of the aortic root, sinus or valves [156, 159, 265, 269, 271-275], and one study also measured lesion area within the thoracic aorta [156]. One study measured aortic lesion area only within the aortic arch [155]. One study measured longitudinal aortic lesion area from the aortic root to the iliac branches (Table 4.2) [160]. All studies reported that the administered flavonoid significantly reduced atherosclerosis lesion area compared with control mice, except one study testing epicatechin where no significant difference was reported (Table 4.2) [156].

Table 4.2. Effect of different flavonoids on atherosclerosis lesion area in *ApoE*$^{-/-}$ mice and key aspects of the methods of the included studies.

[#]	Flavonoid (Dose, mg/kg/d)	Lesion area decrease (%)	P<	Sample Size		Blind	RM	SS	DJ
				C	E				
[274]	Baicalin (100)	9.4 ± 5.7	0.05	10	10	N	N	N	N
[275]	Baicalin (100)	19.4 ± 3.3	0.01	5	5	N	N	N	N
[155]	Catechin (1.6)	2.1 ± 1.5	0.01	20	19	Y	N	N	N
[156]	Epicatechin (64)	5.3 ± 6.3	NS	20	19	N	N	Y	Y
[156]	Epicatechin (64)	5.4 ± 8.2	NS	20	19	N	N	Y	Y
[265]	Glabridin (0.6)	30.6 ± 7.7	0.01	14	14	N	N	N	N
[159]	EMIQ (30)	7.5 ± 4.3	0.01	8	7	N	N	N	N
[271]	Isorhamnetin (20)	19.2 ± 4.8	0.01	10	10	N	N	N	N
[160]	Kaempferol (50)	4.9 ± 1.1	0.05	10	10	N	N	N	N
[160]	Kaempferol (100)	8.8 ± 1.0	0.01	10	10	N	N	N	N
[273]	Myricitrin (50)	4.0 ± 5.0	0.05	10	10	N	N	N	N
[272]	Myricitrin (50)	8.1 ± 6.1	0.01	10	10	N	N	N	N
[155]	Quercetin (1.6)	2.4 ± 1.5	0.01	20	20	Y	N	N	N
[156]	Quercetin (64)	28.5 ± 4.6	0.05	20	18	N	N	Y	Y
[156]	Quercetin (64)	18.6 ± 8.3	0.05	20	18	N	N	Y	Y
[269]	Quercetin (25)	2.1 ± 1.9	NS	3	3	N	N	N	Y
[269]	Quercetin (50)	5.8 ± 1.9	NS	3	3	N	N	N	Y
[269]	Quercetin (100)	12.2 ± 2.0	0.05	3	3	N	N	N	Y

[#], study number; NS, not significant; C, control; E, experimental group receiving flavonoid; Y, yes; N, no; RM, repeated measures; SS, sample size justification; DJ, dose justification.

4.3.4 Plasma lipids

Eight studies measured plasma [156, 159, 265, 271, 274] or serum [272, 273, 275] TC, six studies measured plasma [159, 271, 273] or serum TG [272, 273, 275], six studies measured plasma [155, 271, 274] or serum [272, 273, 275] LDL-C, and seven studies measured plasma [155, 159, 271, 274] or serum [272, 273, 275] HDL-C. In all studies, flavonoids were reported to have no significant effect on plasma or serum TC, TG, LDL-C or HDL-C.

4.3.5 Oxidative stress

Three of the included studies measured the effects of flavonoids on indicators of oxidative stress in mouse aortic tissue, including reactive oxygen species [160], oxysterols [265], and F2 isoprostanes [156]. One study measured the effect of flavonoids on serum oxidised LDL [273]. One study investigated the effects of flavonoids on susceptibility of mouse LDL to oxidation *ex vivo* [155], and two studies measured oxidation in cultured cells [269, 272], with one also testing NADPH oxidase activity [269]. One study investigated human LDL oxidation in the presence of flavonoids *ex vivo* [265]. Quercetin [155] and glabridin [265] were reported to reduce LDL-oxidation *ex vivo*, while catechin was not [155]. Myricitrin was reported to significantly reduce serum LDL-oxidation in *ApoE*$^{-/-}$ mice [273]. Kaempferol was reported to reduce aortic reactive oxygen species [160], and epicatechin and quercetin were reported to reduce plasma superoxide concentrations [156].

4.3.6 Quality assessment of included studies

The mean quality assessment score for all eleven studies was 59% (moderate quality), with the highest score being 76% (good quality) (Table 4.3) [156] and the lowest scoring being 20% (poor quality) [265] (Table 4.1). All studies failed to report intra- and inter-observer repeatability testing and blinding of the outcome assessor during lesion area analyses. All studies failed to justify the sample size and dose of flavonoids used, with the exception of one study [156]. Only one study measured the concentration of the ingested flavonoid in the plasma of mice [155]. Body weights were measured at the start and finish of the experiments in five studies [156, 159, 269, 272, 273]. Of the eleven studies, three did not confirm that study conditions were identical between the control and treatment groups [155, 265, 273]. Ethics approval statements were missing from three studies [265, 275, 278]. Two studies neglected to report the sex of the mice [155, 265], however email

correspondence confirmed the sex, starting age and diet in one of these studies [265]. One study failed to report that animals were randomly allocated to control or intervention groups [265]. One study did not report the purity of the flavonoid or the process of extraction [155]. All eight studies which measured plasma lipids reported the source of assay reagents and equipment used, however reproducibility testing for plasma lipid analyses was reported for only one study [271].

Table 4.3. Study quality assessment tool.

	Study reference										
Quality assessment questions (Part 1 – Study design and Atherosclerotic lesion area)	[274]	[155]	[156]	[265]	[159]	[271]	[160]	[273]	[272]	[275]	[269]
Was there an ethics approval statement?	Y	N	Y	N	Y	Y	Y	Y	Y	N	Y
Was there random group allocation?	Y	Y	Y	N	Y	Y	Y	Y	Y	Y	Y
Was the gender of mice reported?	Y	N	Y	N	Y	Y	Y	Y	Y	Y	Y
Was the age of mice when flavonoid administration began reported?	Y	Y	Y	N	Y	Y	Y	Y	Y	Y	Y
Was the diet during treatment reported?	Y	Y	Y	N	Y	Y	Y	Y	Y	Y	Y
Was the body weight of mice measured before and after treatment?	N	N	Y	N	Y	N	N	Y	Y	N	Y
Was the sample size justified?	N	N	Y	N	N	N	N	N	N	N	N
Were study conditions identical between control and treatment groups with the exception of Flavonoid intervention?	Y	N	Y	N	Y	Y	Y	N	Y	Y	Y
Was the purification of the flavonoid clearly reported or purity stated?	Y	N	Y	Y	Y	Y	Y	Y	Y	Y	Y
Was the dose of the Flavonoid justified?	N	N	Y	N	N	N	N	N	N	N	Y

Questions were answered with either yes, no or not applicable. Scores were expressed as a percentage of yes answers out of the total questions for each study. NA, not applicable; Y, yes; N, no, P, poor quality; M, moderate quality; G, good quality.

Table 4.3 (Continued). Study quality assessment tool.

	Study reference										
Quality assessment questions (Part 1 – Study design and Atherosclerotic lesion area)	[274]	[155]	[156]	[265]	[159]	[271]	[160]	[273]	[272]	[275]	[269]
Was the concentration of the flavonoid measured in the plasma?	N	Y	N	N	N	N	N	N	N	N	N
Was intra- and inter-observer repeatability testing reported for atherosclerotic lesion area analysis?	N	N	N	N	N	N	N	N	N	N	N
Was the method for location of section and slide preparation described in detail?	Y	Y	Y	Y	Y	Y	Y	Y	Y	Y	Y
Did the authors report the stain used?	Y	Y	Y	Y	Y	Y	Y	Y	Y	Y	Y
Were the investigators blinded to treatment groups during analysis?	N	Y	N	N	N	N	N	N	N	N	N
Quality assessment questions (Part 2 – Plasma lipid analysis)	1	2	3	4	5	6	7	8	9	10	11
Was the source of assay reagents and equipment included in the methods?	Y	Y	Y	NA	Y	Y	NA	Y	Y	Y	NA
Was repeatability testing reported for plasma lipid analysis?	N	N	N	NA	N	Y	NA	N	N	N	NA
Score (%)	59	53	76	20	65	65	60	59	65	53	73
Study Quality	M	M	G	P	M	M	M	M	M	M	M

Questions were answered with either yes, no or not applicable. Scores were expressed as a percentage of yes answers out of the total questions for each study. NA, not applicable; Y, yes; N, no, P, poor quality; M, moderate quality; G, good quality.

4.3.7 Meta-analysis, sensitivity analyses and funnel plots

Eleven studies, including a total of 18 comparisons, tested the effects of flavonoids on aortic atherosclerosis lesion area. A total of 208 flavonoid administered and 126 vehicle control *ApoE*$^{-/-}$ mice were included in the overall meta-analysis (Figure 4.3). The overall effect of the flavonoids was to significantly lower atherosclerosis lesion area compared with controls (SMD 1.10, 95% CI 0.69, 1.51), however there was substantial heterogeneity between the studies (I^2=56%). Sub-group analyses were performed to compare the effects of the flavonols and flavan-3-ols on atherosclerosis lesion area. Administration of flavonols, including flavonol glycosides, led to a significant decrease in atherosclerosis lesion area (SMD 1.31, 95% CI 0.74, 1.87) in a total of 122 experimental mice (77 control were included). The flavan-3-ols did not significantly reduce atherosclerotic lesion area (SMD 0.33, 95% CI -0.19, 0.85), based on data from a total of 57 experimental and 20 control mice.

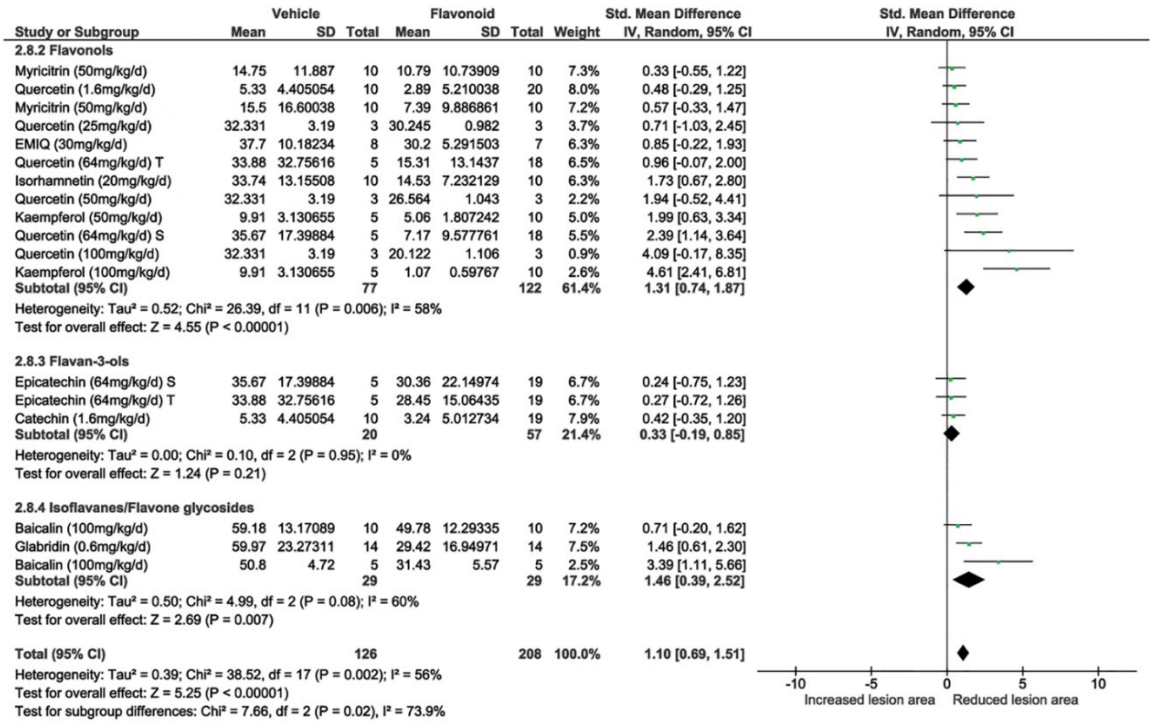

Figure 4.3. Forest plot showing the effects of flavonoids on atherosclerosis lesion area. Sub-analyses were performed to test the effect of flavonols, flavan-3-ols, isoflavones and flavone glycosides on atherosclerosis lesion area. The meta-analysis included 11 studies and a total of 18 flavonoid comparisons. Comparisons were made using standard mean differences and a random effects model. Std, standard; S, Aortic Sinus; T, Thoracic Aorta.

Sensitivity analyses using the leave one out approach showed that all studies contributed to the findings of the meta-analysis and the removal of individual studies did not change the overall findings (Table 4.4). Funnel plots suggested evidence of publication bias (Figure 4.4).

Table 4.4. Leave one study out sensitivity analyses for the effects of flavonoids on atherosclerosis lesion area.

Study removed	SMD (95% CI)	P value	I^2 value (%)
None	1.10 (0.69, 1.51)	0.00001	56
Liu, Liao et al. 2014 [274]	1.14 (0.70, 1.58)	0.00001	58
Hayek, Fuhrman et al. 1997 [155]	1.24 (0.77, 1.71)	0.00001	57
Loke, Proudfoot et al. 2010) [156]	1.17 (0.69, 1.65)	0.00001	56
Rosenblat, Belinky et al. 1999 [265]	1.08 (0.64, 1.51)	0.00001	57
Motoyama, Koyama et al. 2009 [159]	1.13 (0.69, 1.56)	0.00001	58
Luo, Sun et al. 2015 [271]	1.05 (0.63, 1.48)	0.00001	56
Xiao, Lu et al. 2011 [160]	0.91 (0.55, 1.26)	0.00001	40
Qin, Luo et al. 2015 [273]	1.16 (0.73, 1.60)	0.00001	56
Sun, Qin et al. 2013[272]	1.15 (0.71, 1.59)	0.00001	58
Wang, Liao et al. 2016 [275]	1.02 (0.63, 1.42)	0.00001	53
Xiao, Liu et al. 2017 [269]	1.07 (0.64, 1.50)	0.00001	61

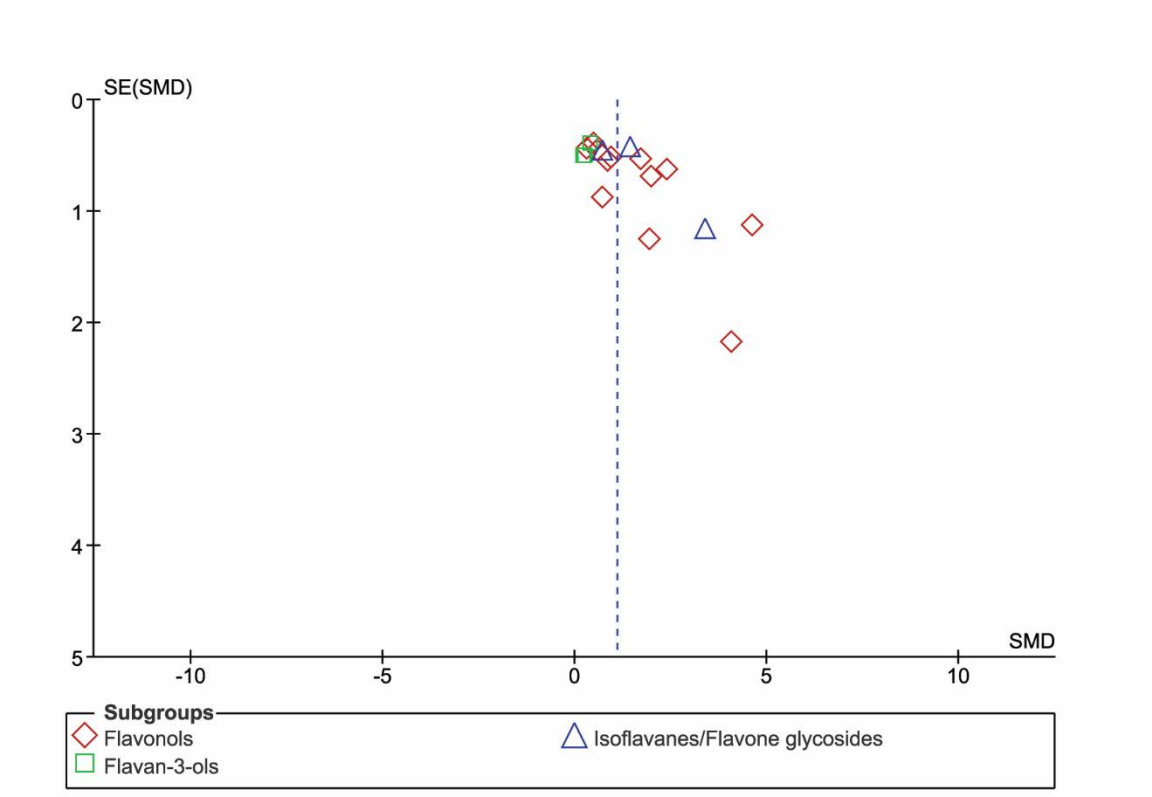

Figure 4.4. Funnel plot for assessment of publication bias of included studies assessing the effects of flavonoids, flavonols and flavan-3-ols on atherosclerosis lesion area.

4.4 Discussion

The main finding of this meta-analysis was that aortic atherosclerosis lesion area was significantly lower after administration of flavonoids compared with controls in *ApoE*$^{-/-}$ mice. Findings were generally consistent between studies however differences were seen in studies using flavonols compared with the flavan-3-ols. There was a high degree of heterogeneity between studies in terms of the flavonoid examined, starting age, the dose and diet administered, the duration of treatment and area of the aorta which lesion area was measured. Mice in two studies were administered standard mouse chow with experimental end points occurring at 10 [155] and 12 [265] weeks old. Previous studies suggest there is minimal plaque development by 12 weeks of age [279]. Study duration ranged from 4 weeks [160] to 26 weeks [156], and flavonoid doses ranged from 0.6mg/kg/d [265] to 100mg/kg/d [269, 274, 275]. Quality assessment revealed only two studies justified the dosage of flavonoid used [156, 269]. Heterogeneity in study methodology makes quantitative comparisons difficult for individual flavonoids and flavonoid classes. Future studies involving nutraceuticals would benefit from a stronger rationale for dose, mouse age and study duration, which are poorly justified in many current studies.

All studies failed to report reproducibility testing for lesion area measurement, and only one study reported blinding of the outcome assessor [155]. Furthermore, only one study provided sample size calculations [156]. Multiple studies did not report body weight or food consumption to allow for accurate conversion to per kilogram dosage. The funnel plot suggested the possibility of publication bias which may suggest that a number of negative studies have not been published.

Flavonoids have previously been proposed to influence atherosclerosis development through multiple mechanisms including improved lipid profile, reduction in LDL-oxidation, and reductions in a number of inflammatory cells and mediators [280]. At the doses used in the included studies, purified flavonoids were reported to have no significant effect on plasma TC, TG, LDL-C or HDL-C in *ApoE*$^{-/-}$ mice. However, flavonoids were reported to have a significant effect on the oxidative stress parameters measured in all individual studies, with the exception of one study which reported that quercetin, but not catechin, reduced LDL-oxidation *ex vivo* [155]. Heterogeneity of methods prevented quantitative comparison of the effects of flavonoids on oxidative

stress, however. Direct *in vitro* antioxidant effects have been shown for multiple flavonoids [281], however there is also evidence for an indirect antioxidant effect through upregulation of HO-1 [271, 282]. Despite the integral role of LDL-oxidation in the pathogenesis of atherosclerosis, only one of the nine included studies have measured the effects of a flavonoid on LDL-oxidation *in vivo* [273].

In addition to antioxidant effects, flavonoids have been reported to reduce endothelial cell apoptosis, increase aortic eNOS activity [156, 273] and decrease dendritic cell number [274]. Flavonoids have also been reported to increase the collagen content of plaque lesions [159], and decrease expression of CD44 [160], suggesting an ability to promote atherosclerosis plaque stability [161].

The major classes of flavonoids which have been studied for their anti-atherosclerosis effects are the flavonols and the flavan-3-ols. Both of these flavonoid classes contain hydroxyl groups on carbon three of the heterocyclic ring, and are differentiated by whether or not they contain a ketone functional group on carbon 4 (Figure 4.1). Flavonoid glycosides were classed as flavonols due to evidence of metabolism to flavonols within the body [255, 256]. The flavonols were the most studied flavonoid, included in seven of the nine studies, while flavan-3-ols were included in two, and isoflavanes and flavone glycosides were included in only one study each. In sub-analyses limited to the flavonoid class, flavonols but not flavan-3-ols significantly reduced atherosclerosis lesion area. The small sample size of the flavan-3-ol analysis (57 experimental mice compared with 113 in the flavonol group) may possibly explain this finding. This finding may also be related to key structural differences between the flavonols and flavan-3-ols, such as the presence of a ketone functional group in the flavonols but not the flavan-3-ols. The latter may be important in reducing LDL-oxidation, which was shown to occur after administering all the flavonols tested [155, 265, 273] but not the flavan-3-ol catechin [155].

Reported beneficial effects of flavonoids on atherosclerosis severity and plaque stability suggest they may be useful for prevention and treatment of atherosclerosis in humans. A randomized crossover trial reported that quercetin, administered as quercetin-3-glycoside, significantly decreased the inflammatory biomarkers soluble endothelial selectin and IL-1β compared with placebo after four weeks supplementation [283]. However, no other clinical trials have assessed the effects of quercetin and other flavonoids on markers of atherosclerosis in humans. The antioxidant effects of the flavonoids are likely to have

more impact on the formation of atherosclerosis as opposed to a decrease in size of pre-existing plaques, which is a limitation of many newly discovered pharmacotherapies [284]. Based on these results however, supplementation of flavonoids may be beneficial for healthy patients to prevent or reduce the likelihood and severety of atherosclerotic plaques forming. Modifications of markers of plaque stability may be a better indication of clinically relevant benefits of flavonoids in terms of likelihood of reducing cardiovascular events [285]. Currently, there is some animal research (as discussed above) but no clinical research to support a role of flavonoids in increasing plaque stability [159, 160]. Future animal studies should aim to measure the effects of flavonoids in models of plaque stability, such as tandem stenosis models in order to better evaluate possible clinical outcomes [286].

Quercetin is currently the most studied flavonoid in animal and human studies. In the included studies, the highest dose of quercetin administered was 100mg/kg/d [269]. Previous clinical studies have administered quercetin orally at 15mg/kg/d, for up to eight weeks, without observable side effects [195]. Based on body surface area calculations, this dose translates to 185mg/kg/d in mice [287]. Therefore the doses used in these preclinical models, which were found to have beneficial effects on lesion area and atherosclerosis biomarkers, are the equivalent of relatively low doses in humans. Furthermore, quercetin is inexpensive and readily available as a dietary supplement. Based on the preclinical findings, dose tolerance, cost and availability of quercetin, future clinical studies should aim to test the benefit of quercetin supplementation in combination with currently used therapies on cardiovascular end points.

The current meta-analysis is limited by a number of factors. Firstly, none of the specific flavonoids have been tested for their effects on lesion area in more than three separate studies. Therefore statistical comparisons were performed between the most commonly studied flavonoid classes, the flavonols and flavan-3-ols, and individual flavonoids were not compared. Secondly, only one of the included studies measured plaque stability, and only one measured LDL oxidation *in vivo*, both of which are important in atherosclerosis pathology. Future animal studies should aim to assess the effects of flavonols on plaque collagen content, as preliminary evidence suggests they may improve plaque stability, which is a clinically relevant finding.

In conclusion, this meta-analysis suggests that flavonoids reduced the severity of atherosclerosis in *ApoE*$^{-/-}$ mice. The flavonoid subclass, the flavonols, appear to be the most effective at reducing lesion area based on the studies available.

CHAPTER 5
QUERCETIN DOES NOT IMPROVE EXERCISE PERFORMANCE OR BLOOD FLOW IN A NOVEL MODEL OF SUSTAINED HIND LIMB ISCHEMIA

5.1 Introduction

Peripheral artery disease (PAD) is a common cause of leg pain, walking impairment, low physical activity and poor health-related quality of life [19, 288, 289]. Cilostazol is the only currently available drug therapy for lower limb PAD but because of low efficacy is not currently recommended by the European guidelines [16].

The flavonoids are a group of polyphenols found in some foods [152]. Prior reports suggest that the flavonoid quercetin can improve limb blood flow recovery and capillary density [60], reduce muscle atrophy [175, 188], and reduce oxidative stress and pro-inflammatory cytokines in skeletal muscle [149, 151] in animal models. Cytokines, including IL-6 and TNF-α have been detected at high levels in skeletal muscle of PAD patients [36]. High concentrations of these cytokines and low availability of NO have been correlated with the most common and debilitating symptoms of PAD, i.e. poor ambulatory performance [38] and muscle pain due to lactic acid build-up [36]. Quercetin has been reported to improve exercise performance in healthy mice [174], and reduce acid-induced pain stimulation [149]. This is potentially achieved through a reduction of TNF-α and through increases in endothelial NO production [60]. These research findings suggest that quercetin may be an effective treatment for PAD, however the relevance of these prior studies to people with PAD is unclear.

Previous animal studies on PAD have a range of limitations, including the use of an acute ischemia model in which blood supply rapidly recovers, investigating young rodent strains with excellent angiogenesis ability, poor study design and employing outcome measures unrepresentative of the clinical situation, as previously reviewed in detail [46]. A novel two-stage surgical HLI mouse model was previously developed in order to better simulate human PAD [59]. This two-stage model has sustained HLI without spontaneous recovery and impaired exercise performance [59]. The aim of this study was to test the effect of quercetin supplementation on exercise performance, physical activity and blood

supply within this novel rodent model through a well-designed randomised controlled trial.

5.2 Materials and Methods

5.2.1 Mice

Mouse husbandry is described in detail in chapter 2.1. Briefly, male *ApoE*$^{-/-}$ mice aged 18-22 weeks were acclimatized for four weeks. Mice were housed one per cage in individually ventilated techniplast cages. All conditions were kept constant between experimental groups with the exception of quercetin being incorporated into the diet of the intervention group. All procedures were approved by the James Cook University Animal Ethics Committee (A2352).

5.2.2 Study design and outcome assessment

At 22-24 weeks old, mice were allocated to two experimental groups with equal exercise performance and blood flow (Figure 5.1). The two groups were then randomly allocated to receive a diet which contained quercetin (n=24) or an otherwise identical control diet that did not contain quercetin (n=24). HLI was induced over 14 days through two sequential operations as previously described [59]. Mice were allowed to recover from surgery and 5 days later, they were fed either the diet containing quercetin or the control diet until the end of the experiment (37 days after ischemia establishment). Research was conducted in accordance with the ARRIVE guidelines [146]. Exercise performance was tested on a treadmill at baseline (day 0), and on days 24, 34 and 44 (10, 20 and 30 days after second HLI surgery). Physical activity was monitored through open field tests on day 44, and limb pressure sensitivity was estimated on day 48. Hind limb blood flow was measured at baseline (day 0), prior to the second surgery (day 13), the day after the second surgery (day 15), and on days 28, 35 and 49 (Figure 5.2). Blood samples were taken from the tail vein on day 0 (baseline), day 30 and cardiac puncture on day 51 (endpoint). Body weight was measured weekly. At the end of the experiments mice were euthanized by carbon dioxide asphyxiation.

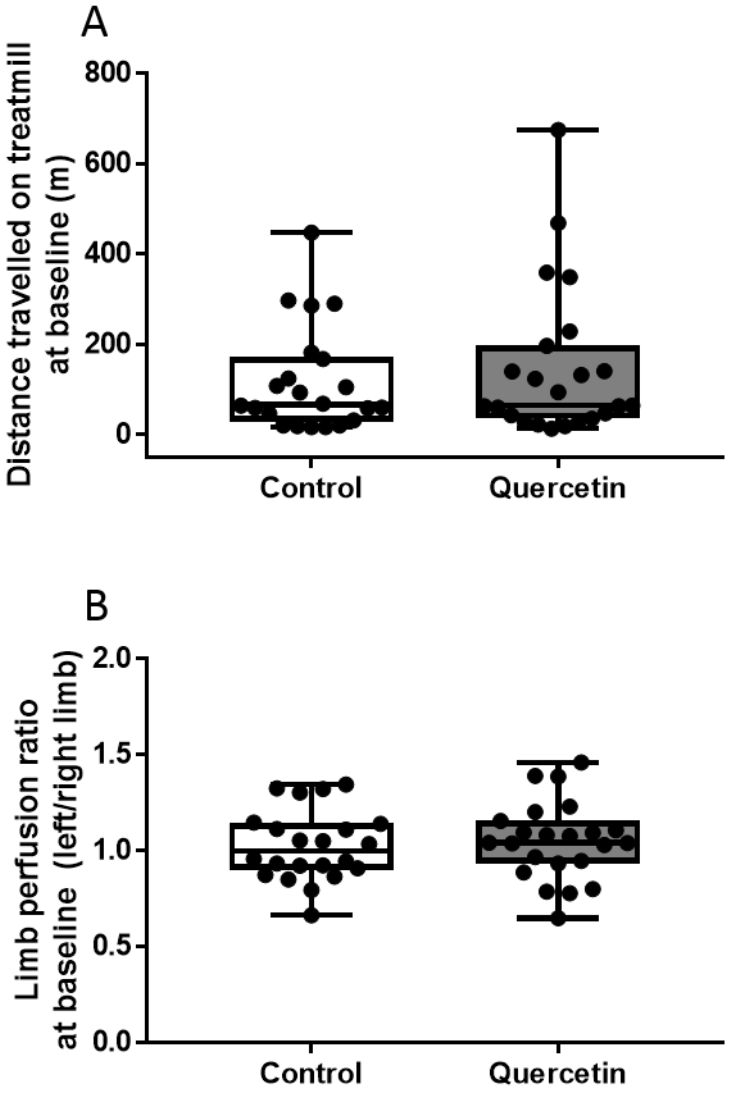

Figure 5.1. Baseline limb perfusion and distance travelled on a treadmill for intervention groups prior to randomised assignment of intervention.

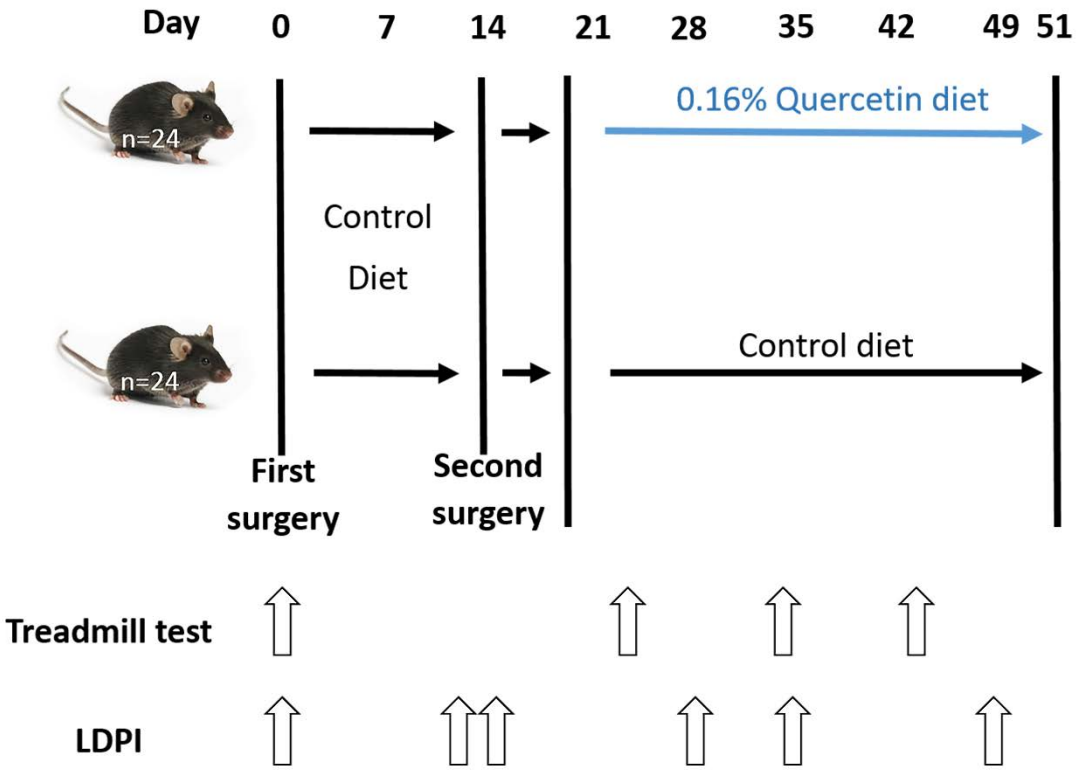

Figure 5.2. Study design and timing of quercetin dietary intervention and outcome assessments.

5.2.3 Two-stage induction of HLI

Mice were anaesthetised (section 2.2) and depilatory cream was applied to the left hind limb next to the left inguinal ligament to allow for clean surgical incision. The cream was removed after one minute with cotton pads and PBS, the surface of the skin was lightly cleaned with 70% ethanol, and riodine was applied. A 10mm vertical incision was made to expose the inguinal ligament and allow access to the femoral neurovascular bundle. Care was taken not to remove adipose and other tissue during the surgery. The femoral artery was carefully separated from the femoral vein and femoral nerve using a stereotactic microscope (Leica), and care was taken to maintain the integrity of the nerve and vessels. Two hygroscopic ameroid constrictors with an internal diameter of 0.25mm (Research instruments SW, Escondido) were placed on the femoral artery, one inferior to the internal iliac artery branch, and one superior to the deep femoral artery branch. The femoral vein and femoral nerve were repositioned next to the femoral artery and the displaced adipose was placed over the vessels and stitched using dissolvable internal sutures. The incision was closed using 6-0 silk sutures, riodine was applied, and the mice were monitored until they had recovered from anaesthesia.

Fourteen days later, following hair removal and application of riodine, a horizontal incision was made at the same location as the first surgery and the femoral artery with hygroscopic ameroid constrictors was exposed and separated from the femoral nerve and femoral vein. The femoral artery was ligated using 6-0 silk sutures at two sites, one distal to the distal ameroid constrictor, and one proximal to the proximal ameroid constrictor, so that the vessel could be resected along with both ameroid constrictors. The displaced adipose was placed over the vessels and stitched using dissolvable internal sutures. The incision was closed using 6-0 silk sutures, riodine was applied and mice were monitored until they had recovered from anaesthesia.

5.2.4 Experimental groups

Control mice received a diet containing 20% protein, 4.8% fat, 4.8% crude fibre, 0.80% calcium, 0.70% phosphorous, 0.36% salt and 14MJ/kg digestible energy (Specialty feeds, Glen Forrest, WA Australia). The intervention group received quercetin (Sigma Q4951, Castle Hill, NSW Australia, 0.16% w/w) incorporated into a diet otherwise identical to the control diet. This dose of quercetin equates to approximately 185mg/kg/d, based on an average food consumption of 3.45g/d [277]. This dose was estimated to be equivalent to the most commonly used dose in human patients (1000mg/d) based on body surface area calculations [195, 290].

5.2.5 Assessment of exercise performance with a treadmill test

This was the primary outcome for the study. A treadmill test (TMT) was performed using a six-lane treadmill (Columbus Instruments Excer3/6, Port Macquarie, NSW Australia) as described previously [59]. Mice were acclimatised to the treadmill over a three day period for 15 minutes each day before experiments took place. Over the first two days of the acclimation period mice were allowed to get used to the treadmill with gentle encouragement and shock grids turned off. On the third day mice were allowed to run with shock grids turned on (0.75mA, 163V, 1Hz). Prior to each TMT, mice were fasted for two hours to avoid postprandial effects. Over the first minute, speed was increased to 15m/min, and shock grids were turned on. Total distance travelled was recorded from the start of running at 10m/min, and mice were considered fatigued once they had 10 separate visits to the shock grid.

5.2.6 Assessment of physical activity with an open field test

Mice were acclimatized in the building where open field experiments occurred three days prior to recording. Mice were placed in an open field cube (40×40×40 cm, divided into an outer field and a central field of 20×20 cm), and their movement was recorded for 20 minutes with a Logitech quick capture webcam. Analyses of open field recordings were performed using TopScan Lite 2.0 software. Total distance travelled and total velocity were recorded for each mouse, to allow for comparison between groups.

5.2.7 Assessment of pressure sensitivity from pressure application

Limb pressure sensitivity was measured using a pressure application measurement device (PAM, Ugo Basile, VA Italy) as previously reported [59]. Mice were restrained in a supine position and pressure was applied to the hind limb with a force transducer at a rate of 20g/s. The point at which mice withdrew the limb, vocalised, or had twitching of whiskers in response to the device was considered the endpoint. The peak force applied immediately prior to the endpoint was considered the limb withdrawal threshold. The data was normalised as the limb withdrawal threshold ratio of the left (ischemic) and right (contralateral) hind limb, to allow comparison between groups.

5.2.8 Assessment of blood flow with laser Doppler perfusion imaging

Blood flow was measured in both hind limbs of mice using laser Doppler perfusion imaging (Chapter 2.5).

5.2.9 Preparation of plasma samples

Blood samples were prepared according to the procedure detailed in the general materials and methods (Chapter 2.9).

5.2.10 Total plasma nitrate and nitrite concentration

Total nitrate and nitrite concentrations were quantified in the plasma as a measure of NO concentration. Analysis was performed on plasma samples from control and quercetin treated mice at baseline and day 30 (16 days after HLI induction). The experimental procedure was performed using a NO fluorometric assay kit (Abcam ab65327, Melbourne VIC, Australia) according to the instructions for use. Fluorescence was measured at Ex/Em 360/450nm and converted to mM concentrations using a standard curve.

5.2.11 Quantification of plasma cytokines

Plasma IL-6, IL-10, IL-12 and TNF-α were measured at baseline (day 0) and endpoint (day 51) using a mouse cytokine magnetic bead panel (milliplex, MCYTOMAG-70K)

according to instructions for use. Plasma samples (25µl) were incubated over night with bead-antibody complexes at 4ºC to allow for binding of cytokines. Samples were incubated with detection antibodies and streptavidin-phycoerythrin. The plate was washed twice and 150µl of drive fluid (Millipore, Australia) was added to each well. The MAGPIX machine (Luminex, Australia) was then run utilising 50µl drive fluid per run to quantify cytokines. Median fluorescent intensity was converted into concentration measurements using a 5-parameter logistic plot using MAGPIX xPONENT 4.2 software (Luminex, Australia).

5.2.12 Sample size calculation

Sample size was estimated based on the effect size reported for quercetin improving exercise performance in a TMT in healthy mice [174]. In that study, 16 mice were given quercetin (25mg/kg/d) for seven days and achieved 37% ± 9.5% (mean ± SEM) longer distance during the test than controls [174]. The sample size calculation was two-tailed, power was set to 0.80 and the alpha value was set at 0.05. Based on these values, a minimum required sample size of 20 mice per group was estimated. Sample size was increased by 20% to account for potential drop-outs due to surgical complications or mice welfare concerns.

5.2.13 Statistical analyses

Data were analysed as described in chapter 2.15. Specifically, open field distance and velocity were compared between groups using unpaired two-tailed t-tests as data were normally distributed. Limb withdrawal forces, total nitrate concentrations and cytokine concentrations were compared between groups using Mann-Whitney U tests as these data were not normally distributed. Plasma cytokine values that did not fall within the assay detection range were excluded. Blood flow, distance travelled and body weight were measured at multiple time points throughout the study and were compared between groups using LME models. Blood flow, distance travelled, or body weight and time were set as fixed effects, and variation between individual mice was set as a random effect. Differences were considered statistically significant when p-values were <0.05.

5.3 Results

5.3.1 Mice welfare

A total of 48 mice commenced the experiment (24 mice per group). Three mice (1 from the intervention group and 2 controls) did not wake up from anaesthesia following HLI induction. These mice were excluded from the data analysis as the intervention had not commenced. At the experimental endpoint, 23 mice from the intervention group and 22 mice from the control group were sacrificed. Body weight of all mice did not change significantly over the duration of the experiment (p=0.590) and were similar in both groups (p=0.625, Figure 5.3). The exclusion of outliers identified in body weight data did not change the statistical interpretations.

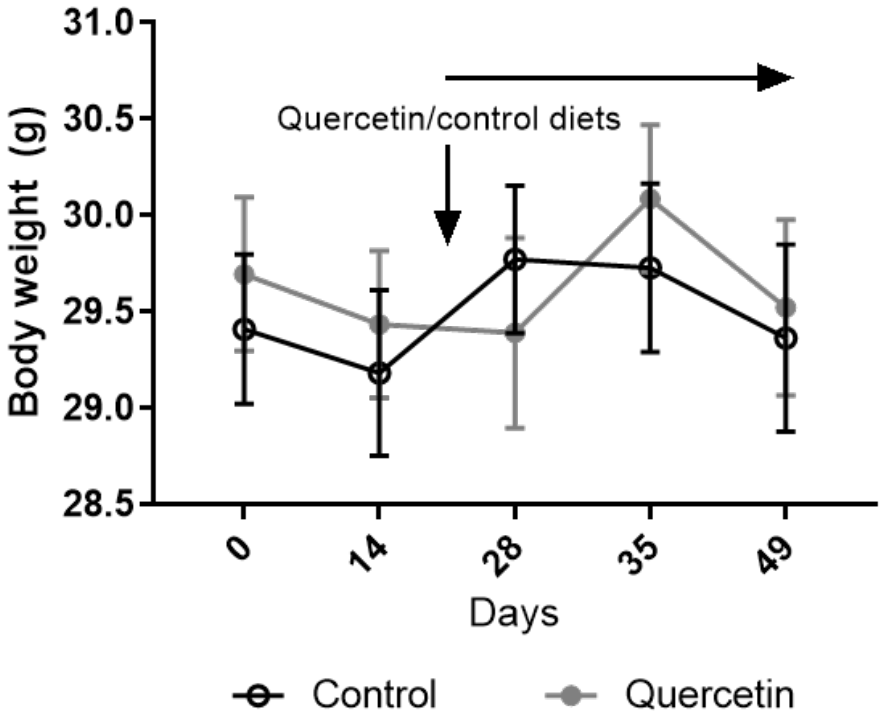

Figure 5.3. Body weight in mice receiving quercetin and controls throughout the experimental period. Data are presented as means ± SEM. Data were analyzed using a LME model.

5.3.2 Quercetin did not improve exercise performance, reduce pressure sensitivity or improve physical activity

The distance travelled during the TMT increased significantly over time in both groups (Figure 5.4A, p<0.001), but did not differ between interventional and control animals

(p=0.785). There was no significant difference in the ratio of withdrawal force after pressure application between groups (Figure 5.4B, p=0.866). Mean velocity (p=0.412) and mean distance travelled (p=0.151) in an open field test were also not significantly different between groups (Figure 5.4C, D).

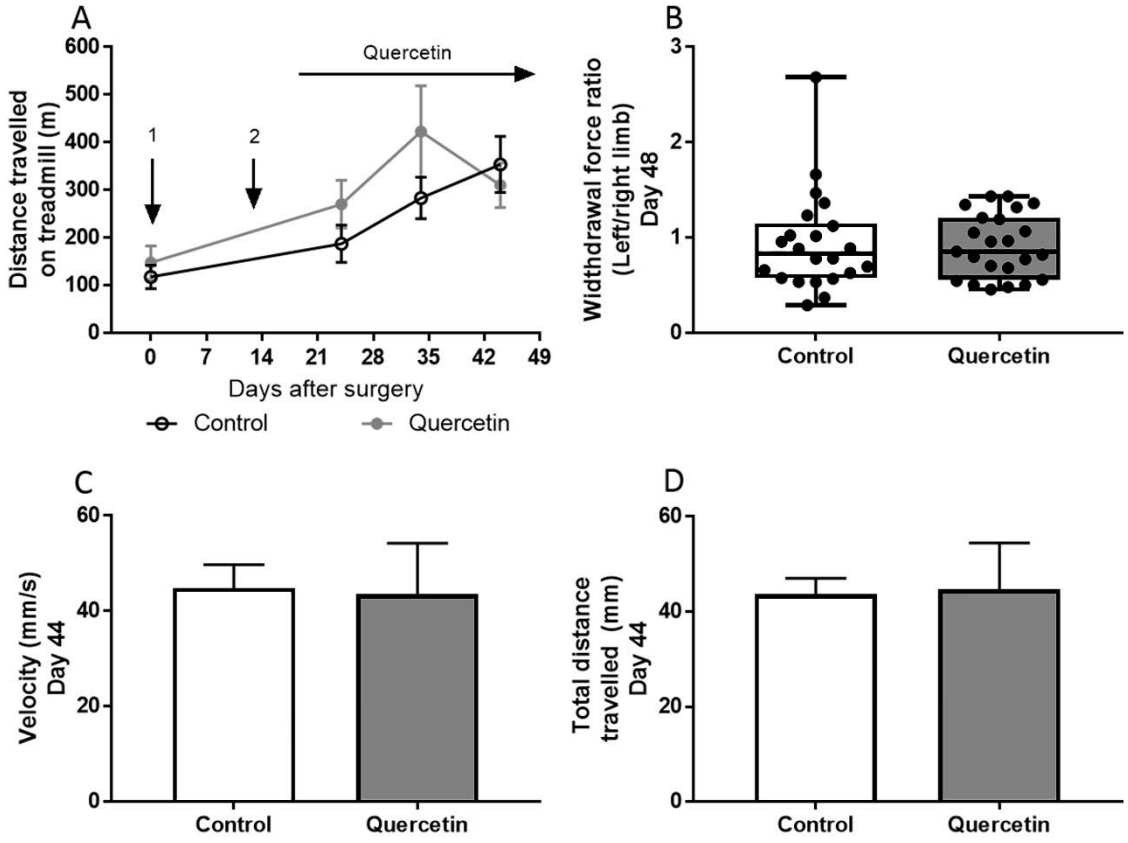

Figure 5.4. The effect of quercetin on ambulatory performance, pressure sensitivity and voluntary activity. (A) Distance travelled in a TMT. Data were analyzed using a LME model. Data were log transformed during statistical analysis to conform to model assumptions however raw values are shown. (B) Force applied to hind limb paw immediately prior to limb withdrawal or signs of distress, expressed as a ratio of left (ischemic) to right (contralateral) limb. Data are presented as medians with IQR. Data were analyzed using a Mann-Whitney U test. (C) The average velocity at which mice moved during an open field test in the whole area, and specifically within the exterior and centre zones. (D) Distance travelled during an open field test in the whole area, and specifically within exterior and centre zones. Open field data were compared using unpaired two-tailed t-tests. Quercetin, n=23; controls, n=22. Data in A, C and D are presented as means ± SEM. 1, surgical procedure to implant ameroid constrictors; 2, surgical procedure to ligate femoral artery and establish HLI.

5.3.3 Quercetin did not improve hind limb blood supply despite increase in plasma total nitrates

In both groups, hind limb perfusion ratios decreased following the two-stage HLI model ($p<0.001$), however quercetin administration did not influence severity of HLI (Figure 5.5A,B, $p=0.954$). There was no significant difference in total plasma nitrate and nitrite concentration between groups at baseline (prior to quercetin consumption, $p=0.272$, Figure 5.5C). Mice that consumed quercetin had significantly greater total plasma nitrate and nitrite concentrations than controls 30 days after surgery (11 days after quercetin consumption began, $p=0.021$, Figure 5.5D).

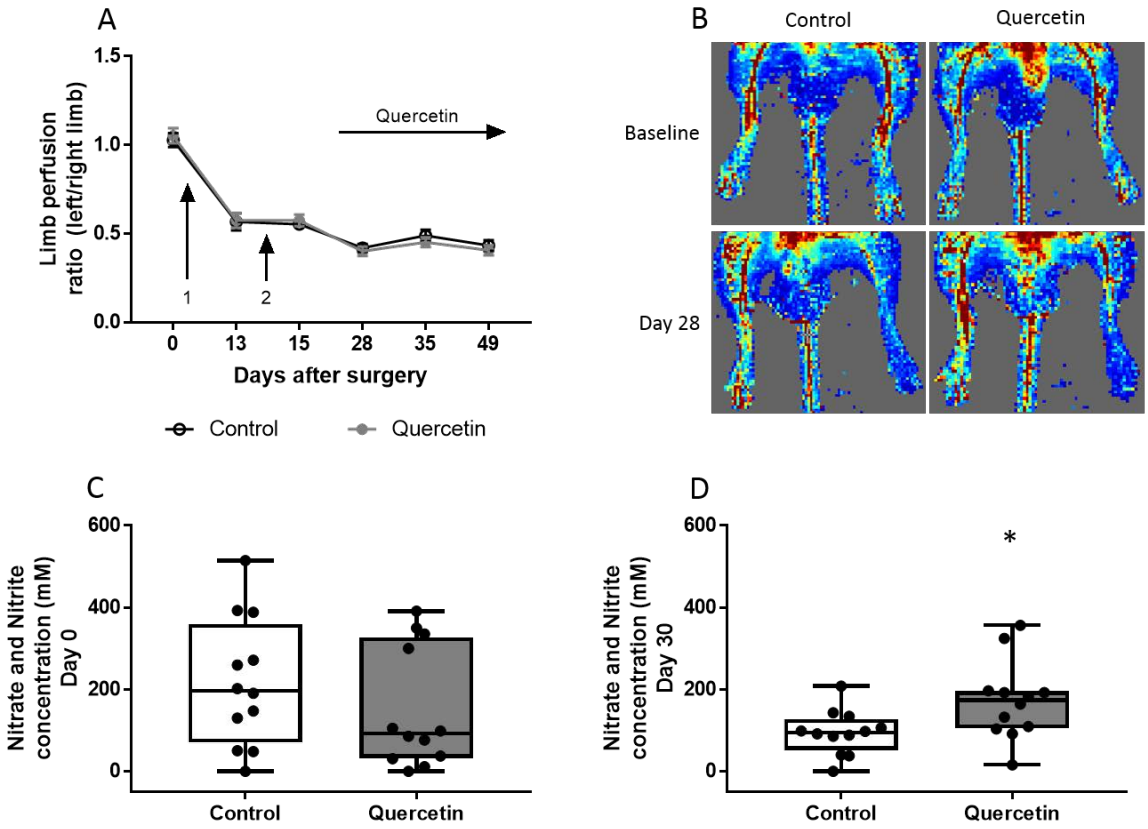

Figure 5.5. The effect of quercetin on hind limb perfusion measured by LDPI and plasma nitrate and nitrite concentrations. (A) Hind limb perfusion decreased following surgery in both groups but did not differ between groups, quercetin, n=23; controls, n=22. Data were presented as means ± SEM and analyzed using a LME model. (B) Representative LDPI images of hind limb perfusion at baseline and day 28. (C) Total plasma nitrate and nitrite concentration did not differ between groups at baseline, quercetin, n=12; controls, n=12. Data are presented as median with IQR and analysed using a Mann-Whitney test. (D) Total plasma nitrate and nitrite concentrations were significantly higher in mice consuming quercetin on day 30; quercetin, n=12, controls, n=12. * Significantly different from control (p<0.05). Data were presented as median with IQR and analysed using a Mann-Whitney test. 1, surgical procedure to implant ameroid constrictors; 2, surgical procedure to ligate femoral artery and establish HLI.

5.3.4 Quercetin did not influence plasma cytokine concentrations

There was no significant difference in plasma TNF-α (p=0.619), IL-6 (p=0.565), IL-10 (p=0.704) or IL-12 (p=0.724) between experimental groups (Figure 5.6).

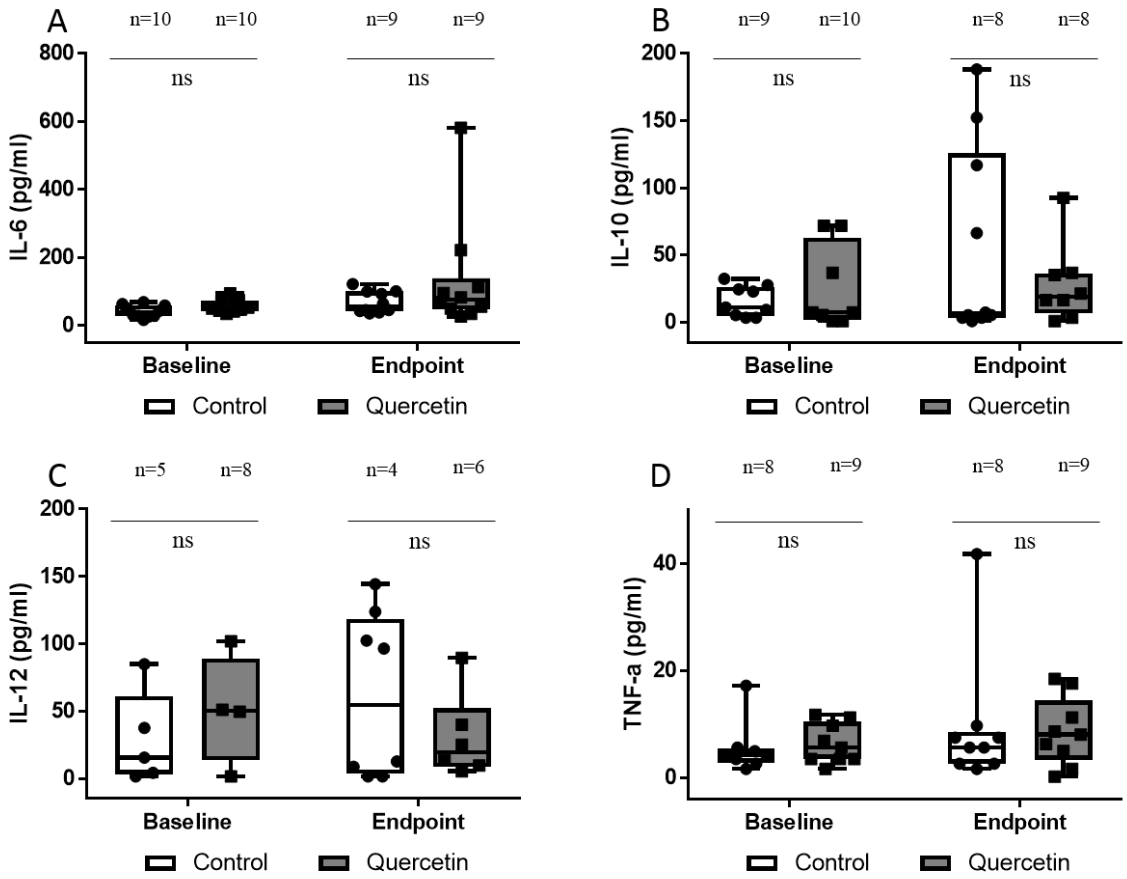

Figure 5.6. Plasma cytokine concentration at baseline before HLI or quercetin administration, and at the endpoint following four weeks quercetin administration. Plasma IL-6 (A), IL-10 (B), IL-12 (C) and TNF-α (D) were measured. All data are presented as medians with IQR. Data were analyzed using Mann-Whitney U tests. IL-6, interleukin 6; IL-10, interleukin 10; IL-12, interleukin 12; TNF-α, tumor necrosis factor alpha; ns, not significant.

5.4 Discussion

The current study found that administration of quercetin after HLI induction did not improve exercise performance or increase physical activity in a novel model of lower limb PAD with many patient relevant features.

It was previously reported that administration of isoquercitrin conjugated to glucose moieties (a form of bioavailable quercetin) to mice improved hind limb blood supply when started two weeks prior to induction of acute HLI [60]. Conversely, the current study found that administration of quercetin after HLI induction did not improve limb perfusion. Previous mouse studies reported that a dose of 185mg/kg/d of quercetin, which was used in the current mouse study, was effective at improving exercise performance, reducing muscle atrophy, and reducing inflammation [174-177, 185, 291]. This dose was also estimated to equate to 1000mg/d in human subjects based on body surface area calculations [287]. A dose of 1000mg/d has been tolerated in human subjects for up to eight weeks with no reported side effects, and beneficial effects on exercise performance in healthy subjects have been reported at this dose [195, 290]. In the current study, quercetin administration increased total plasma nitrates (an indicator of NO) suggesting that quercetin had a biological effect. NO has been critically implicated in improving blood flow and increasing angiogenesis and is the suggested mechanism by which quercetin has improved hind limb blood supply in previous studies [60, 292]. This study suggests that the observed increase in NO was insufficient to improve perfusion in the two-stage HLI model used.

The current study used old mice prone to atherosclerosis with sustained HLI in order to model human PAD. Old mice are less responsive to interventions which stimulate arteriogenesis, angiogenesis and mitochondrial biogenesis [293]. The two-stage surgical model used in this study also limits changes in shear stress due to gradual occlusion and abolishes collateral circulation that usually forms quickly after acute HLI [46, 58]. This may explain why quercetin did not improve exercise performance and blood flow in the current study, in contrast to the previously reported studies utilising other mouse models [174].

Limb pain is a common symptom in patients with PAD but difficult to assess in animal models. Quercetin has been previously reported to reduce pain from acetic acid injection [149], however the effects of quercetin on pain has not been previously evaluated in HLI

models. The current study assessed the effects of quercetin on hind limb hypersensitivity to mechanical pressure and found no benefit. Furthermore, quercetin administered in the diet did not appear to alter plasma IL-6, IL-10, IL-12 or TNF-α concentrations. The findings suggest quercetin is unlikely to be beneficial for pain secondary to ischemia.

This study had a number of strengths and limitations. Strengths were the inclusion of key design features, such as randomisation, adequate sample sizes and use of a clinically relevant model. Quercetin was added to the diet to mimic human consumption through the diet as opposed to direct administration through gavage. Body weight data suggest mice in both groups were consuming diet equally. Supplementation may be modelled through gavage in mice, and this route of administration may have shown better efficacy. Quercetin was administered after sustained HLI was established, in order to reflect what occurs clinically as patients seek treatment once symptoms are present. Quercetin was tested over a 30 day-period and it is possible that a longer duration of administration may have had a different effect. Male mice were used in the current study as the newly developed model of sustained HLI has not yet been tested in female mice. It is of vital importance that future studies utilise male and female mice as PAD is of equal or potentially higher burden in women [294].

In conclusion this study suggests that quercetin does not improve exercise performance, physical activity, blood supply or reduce pressure sensitivity when administered in a model of sustained HLI described in the current study.

CHAPTER 6
TREE NUT SUPPLEMENTATION REDUCES THE SEVERITY OF ATHEROSCLEROSIS BUT NOT AAA IN MICE

6.1 Introduction

CVD is the leading cause of mortality and a major cause of morbidity worldwide, mainly as a result of atherosclerosis and its associated complications [240]. Western diets high in saturated fats and sugarsare widely believed to stimulate development and progression of atherosclerosis. Studies within the last decade have strongly supported the benefit of a diet enriched with tree nuts in limiting the development of atherosclerosis within experimental models and also reducing the incidence of atherosclerosis-associated cardiovascular events in patients [248, 296, 297].

AAA is an important cause of death in older adults due to aortic rupture [298]. The pathological mechanisms implicated in AAA include marked transmural inflammation, severe extracellular matrix remodeling leading to medial weakening and eventual aortic rupture [299]. While atherosclerosis has been traditionally implicated in AAA pathogenesis, has also been widely discussed that AAA is a distinct disease with different pathological mechanisms and some distinct risk factors [300, 301]. Hypertension, obesity, older age and cigarette smoking are important risk factors for both atherosclerosis and AAA [300, 302]. Diabetes is an important risk factor for athero-occlusive disease but negatively associated with AAA [300]. Due to these distinctions, interventions which are effective against atherosclerosis-associated CVDs cannot be automatically assumed to limit AAA development, growth and rupture.

Tree nuts consist mainly of unsaturated fatty acids, including n-3 PUFA, and polyphenols [206-208]. Previous studies have reported that administrating n-3 PUFAs or polyphenols can limit AAA development and severity within experimental animal models [214, 216]. Based on this previous experimental evidence it is possible that a diet enriched with tree nuts may limit the development and severity of AAA (Chapter 1.5.2), however no previously published experimental or clinical studies have investigated this hypothesis. The aim of this study was to test the effect of a diet enriched with tree nuts on the

development of AAA within a mouse model. It was hypothesised that a diet enriched with tree nuts would limit the development and severity of AAA.

6.2 Materials and Methods

6.2.1 Mice

Mouse husbandry is described in detail in chapter 2.1. Briefly, male *ApoE*$^{-/-}$ mice aged 6-8 weeks sourced from the animal resources centre were acclimatized for four weeks. Mice were housed 3-5 per cage in individually ventilated techniplast cages. Baseline measurements and dietary interventions were initiated when mice were 10-12 weeks old. All procedures were approved by the James Cook University Animal Ethics Committee (A2353).

6.2.2 Study design

At 10-12 weeks old, mice were randomized to control or intervention diets. Allocated diets were continued from the beginning (day 1) until the end of the experiment (day 56) or mouse fatality. Subcutaneous micro-osmotic pumps were implanted (Model 1004, Alzet, Australia) on day 28, which continuously infused Ang II (1.44mg/kg/d; Sigma) for 28 days to induce AAA formation [303]. The maximum diameter of the SRA was measured on days 0, 23, 34, 41, 48 and 54 (Figure 6.1). Systolic and diastolic blood pressures were measured on days 0, 24, 35 and 49. Body weight and food weight were measured every two days. Outcome assessors were blinded to treatment groups at the time of measurement for all end point analyses. At the end of the experiments mice were euthanized with carbon dioxide asphyxiation.

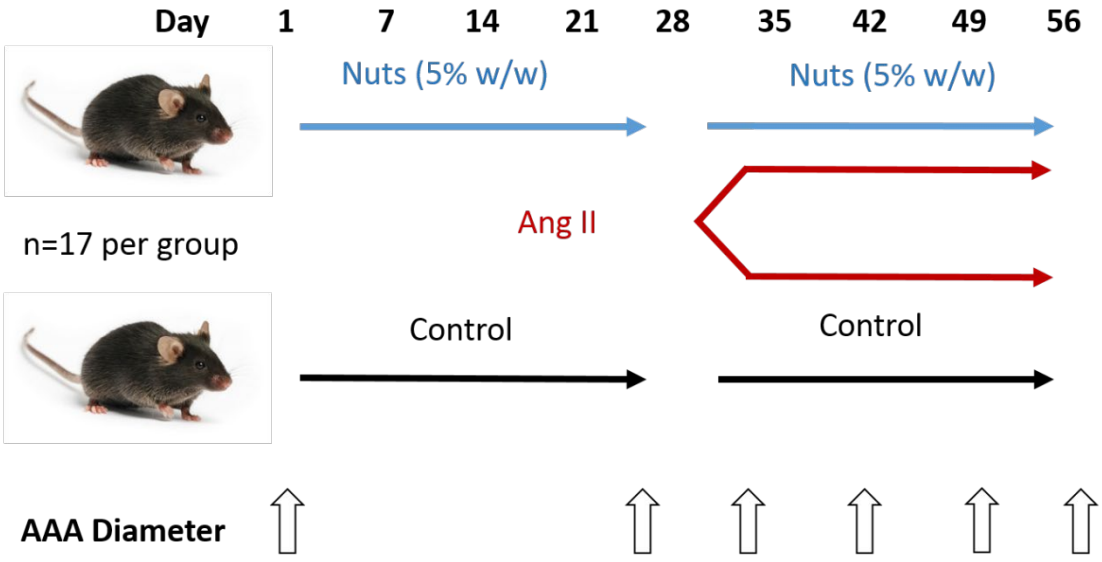

Figure 6.1. Animal study design from the beginning of the intervention with a diet enriched with macadamia and pecan nuts through until sacrifice.

6.2.3 Micro-osmotic pump implantation

Hair was removed, riodine was applied and a small incision, approximately 5mm, was made between the scapulae. Skin was blunt dissected from the subcutaneous tissue to create a pocket using long-nosed haemostats, and pumps were inserted to the left at the level of the rib cage. The skin was closed using 3/0 non-absorbable monofilament sutures, and riodine was applied to the site.

6.2.4 Dietary interventions

The control mice (n=17) received standard mouse chow containing 20% protein, 4.8% fat, 4.8% crude fibre, 0.80% calcium, 0.70% phosphorous, 0.36% salt and 14MJ/kg digestible energy (Specialty feeds, Glen Forrest WA). The experimental mice (intervention group, n=17) received the same standard mouse chow diet enriched with 2.5% macadamia nuts and 2.5% pecan nuts (Specialty feeds, Glen Forrest WA). The diets were formulated to achieve a nut content of 5.75g/kg/d, which is estimated to translate to an amount of 0.5g/kg/d body weight in humans based on body surface area calculations [287]. This nut content equates to approximately 30g/d in humans; an amount which has previously been reported to reduce cardiovascular endpoints [248]

6.2.5 Assessment of AAA severity

AAA severity was assessed by measuring the maximum diameter of the SRA from ultrasound images (Chapter 2.3) and *ex vivo* morphometry (Chapter 2.6). Observers were blinded to treatment groups at the time of analysis. Mice that died during the experimental period were autopsied to confirm whether aortic rupture was the cause of death. It has previously been reported that saline infused *ApoE*$^{-/-}$ mice do not have external SRA diameters exceeding 1.5mm [20]. Therefore the diagnosis of AAA was defined by a maximum SRA diameter of >1.5mm.

6.2.6 Assessment of blood pressure

Systolic and diastolic blood pressures were measured using a non-invasive tail cuff blood pressure monitor (Chapter 2.4).

6.2.7 Quantification of atherosclerosis severity

Atherosclerosis lesion areas were quantified in the aortic arches of mice using *en face* Sudan IV staining and in cross sections of the brachiocephalic arteries using elastic Van Gieson's staining. *En face* staining was performed in aortic arches harvested following the 56-day experimental period (Chapter 2.11). Brachiocephalic arteries were paraffin embedded (Chapter 2.12.1), stained with Van Gieson's stain (Chapter 2.12.4), and atherosclerotic lesion area was quantified using Adobe Photoshop CC 2015 (Chapter 2.13).

6.2.8 Sample size calculation

The required sample size was calculated based on results from a previous study in which the effect of n-3 PUFA administration on Ang II-induced AAA was reported [214]. This study reported a mean (± SD) SRA diameter normalized to adjacent aortas of 0.92±0.14 in mice receiving n-3 PUFA compared with 1.91±0.71 in controls [214]. From these values, an effect size of 1.93 was calculated. The estimated effect size was reduced by 30% to account for relative lower amount of fatty acids present in the nuts administered in the current study compared to the n-3 PUFA administered in the previous study. The sample size was increased by an additional 30% to account for anticipated deaths due to aortic rupture during Ang II infusion. The desired power was set to 0.9 and the alpha value was set at 0.05. Based on these calculations a sample size of 17 mice per group was required for this study. Calculations were performed using G Power 3.1.

6.2.9 Statistical analyses

Data were analysed as described in chapter 2.15. Specifically, *ex vivo* aortic diameters were compared using unpaired two-tailed t-tests as data were normally distributed. Incidence of AAA development and AAA rupture were compared between groups using Fisher's exact test and Mantel-Cox (Log-rank) test, respectively. Aneurysm diameter Data measured at multiple time points throughout the study were compared between groups using LME models. Aortic diameter, blood pressure, body weight or food consumption, and time were set as fixed effects, and variation between individual mice was set as a random effect. Levene's test was applied to test for unequal variance between time points due to Ang II increasing the variance of many physiological parameters. Due to the significant difference in variance between time points for systolic and diastolic blood pressure ($p<0.001$), different SDs were allowed in the LME model before versus after Ang II administration. Differences were considered statistically significant when *p*-values were <0.05.

6.3 Results

Thirty-four mice commenced the experiment of which 17 were allocated to the nut-enriched diet and 17 to the control diet. Thirteen (38%) mice died during the Ang II infusion secondary to aortic rupture, and one (2.9%) mouse from the control group was euthanised due to ethical considerations. Mice which died or were euthanised prior to the experimental end point were included in continuous data up until the point of death. At the experimental end point, 12 mice from the control group and 8 mice from the intervention group were sacrificed. Body weight gain throughout the experimental period was not significantly different between groups ($p=0.064$, Figure 6.2). Food consumption over the 56-day period was not significantly different between the groups ($p=0.972$, Figure 6.2).

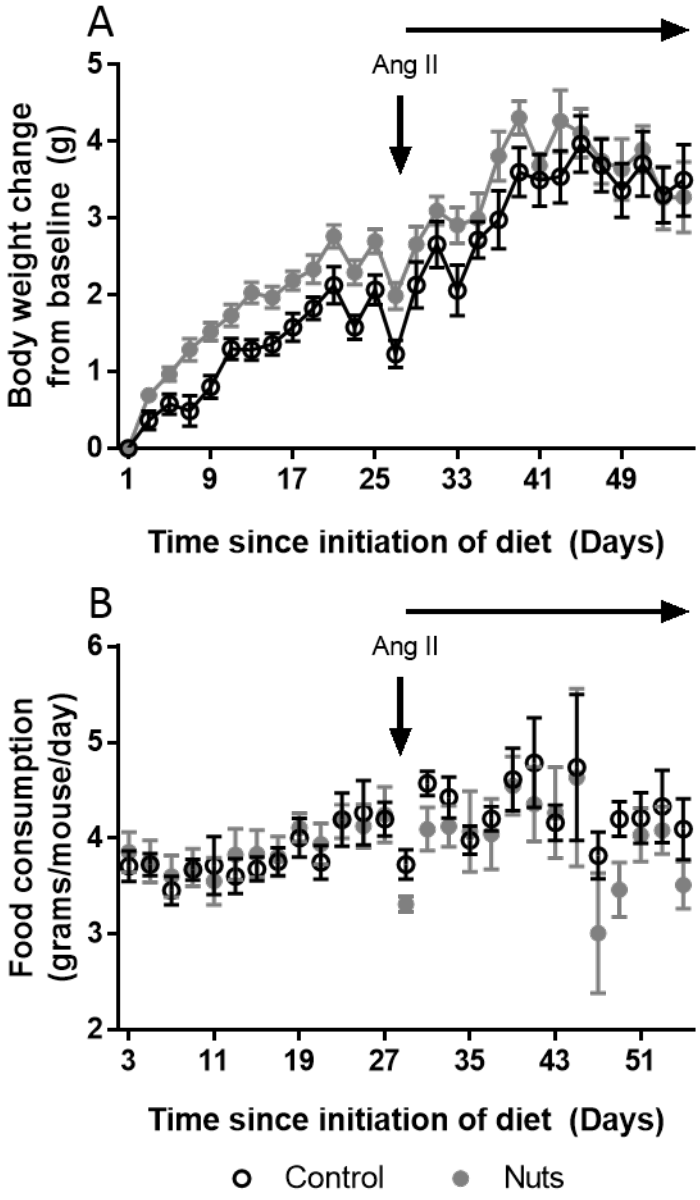

Figure 6.2. Body weight and food consumption from the beginning of the intervention with a diet enriched with macadamia and pecan nuts through to sacrifice. (A) Body weight, (B) Food consumption.

6.3.1 A diet enriched with nuts did not influence Ang II-induced AAA incidence or severity

The SRA diameters as measured by ultrasound changed similarly over time in the mice receiving the nut enriched diet and controls (p=0.313, Figure 6.3A). At the end of the experiment, *ex vivo* SRA diameters were similar in both groups (p=0.576, Figure 6.3B, Figure 6.4). Additionally, there were no significant differences in the maximum diameters of the IRA, aortic arch, or thoracic aorta between mice receiving a diet enriched with nuts and controls (Figure 6.3B). At the end of the experiment AAAs were present in 7 (58%) controls and 4 (50%) mice receiving the diet enriched with tree nuts (p=0.999, Figure 6.3C). Deaths due to aortic rupture occurred in 4 (25%) controls and 9 (53%) mice allocated a diet enriched with nuts (p=0.509, Figure 6.3D). AAAs (>1.5mm) were present in all mice that died from aortic rupture prior to the experimental endpoint.

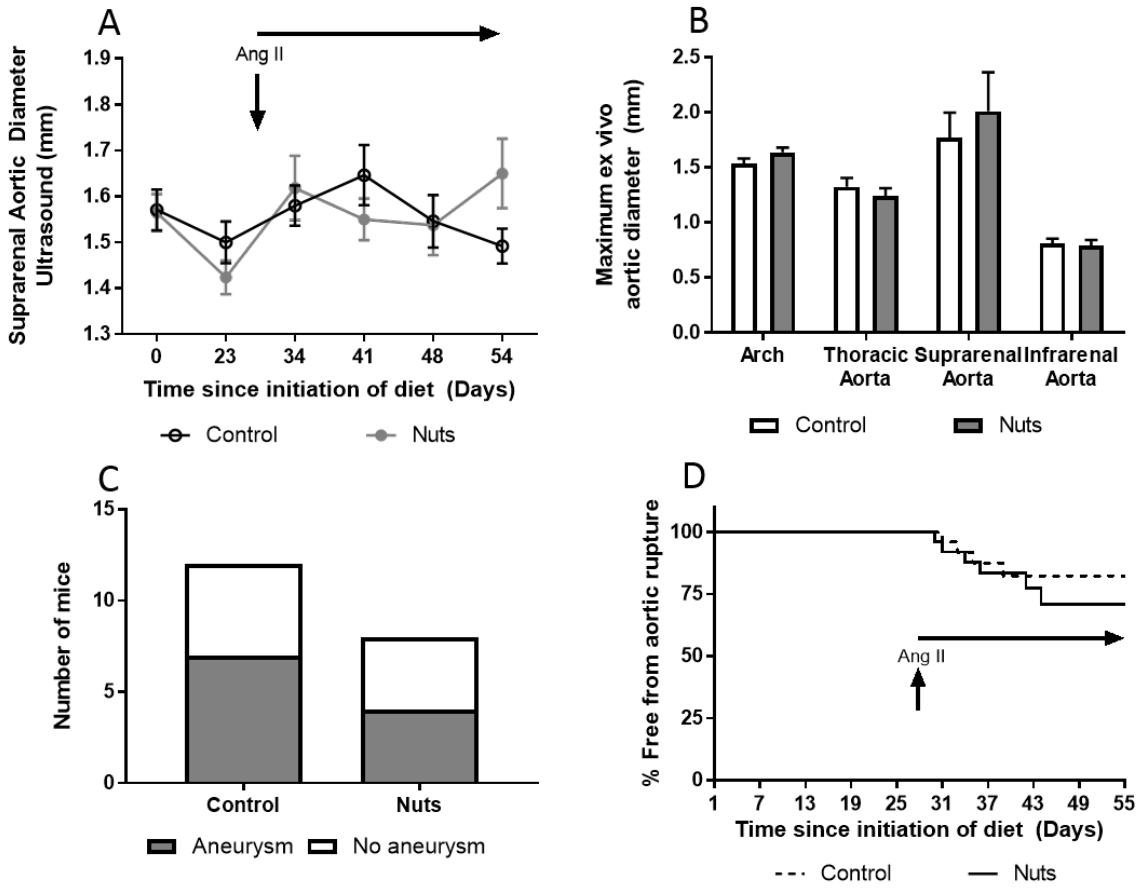

Figure 6.3. The effect of a diet enriched with tree nuts on Ang II-induced AAA incidence and severity. (A) Maximum diameter of the SRA measured by ultrasound throughout the experiment. Data are presented as means ± SEM and were analyzed using a LME model of log transformed data. (B) Maximum diameter of the aortic arch, thoracic aorta, SRA and IRA measured from images of harvested aortas of mice at the experiment end point. Data are presented as means ± SEM, and data were analyzed using unpaired two-sample t-tests. (C) AAA incidence in relation to dietary allocation. Data were presented as number of mice and compared using a Fisher's exact test. (D) Survival free from aortic rupture in mice within the intervention and control group. Data were analyzed using Mantel-Cox (Log-rank) test.

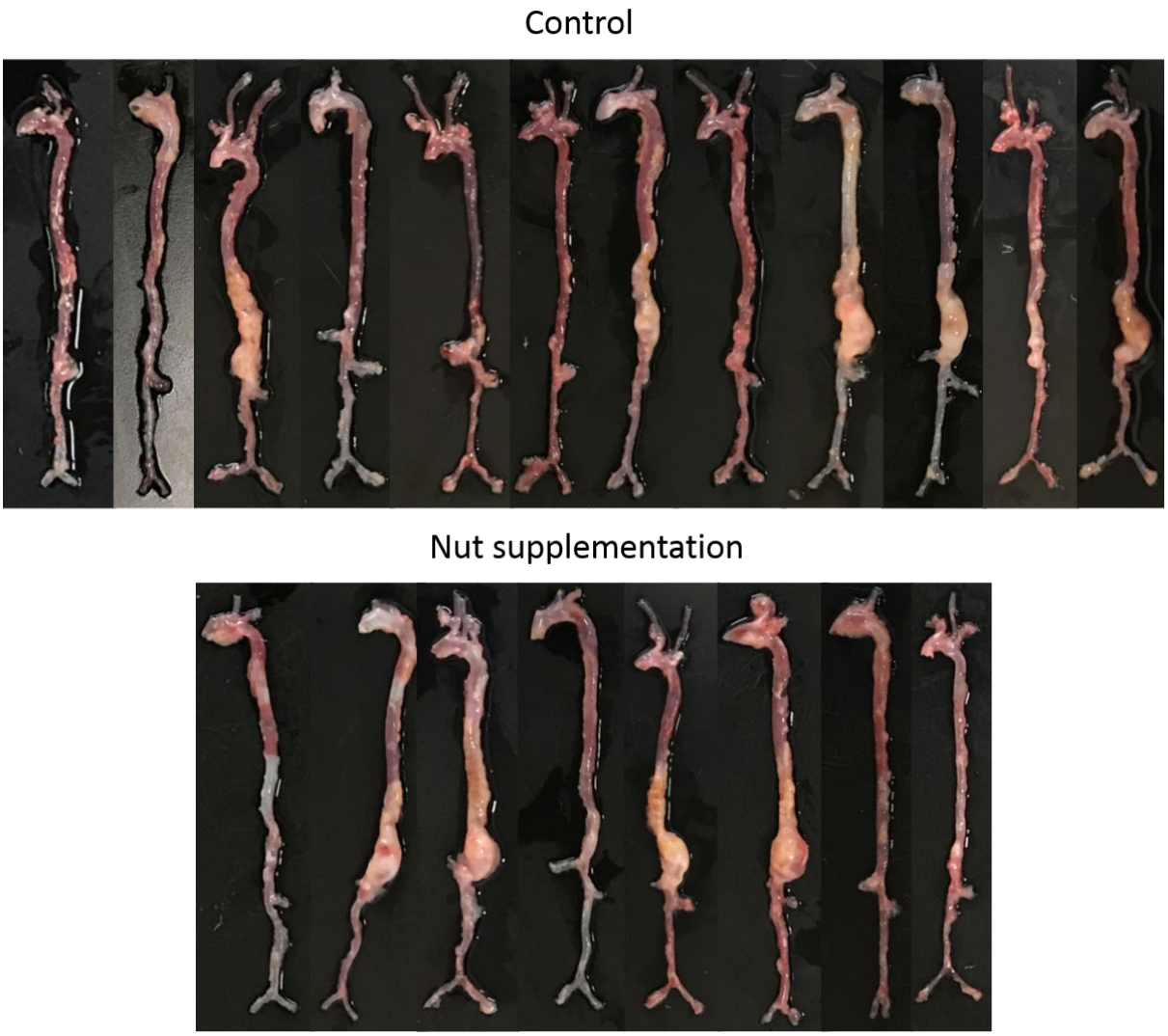

Figure 6.4. All aortas from mice receiving a diet enriched with tree nuts and control mice at experimental endpoint (day 56).

Ex vivo diameters of the SRA from mice that died from aortic rupture were not significantly different between groups (p=0.148; Figure 6.5).

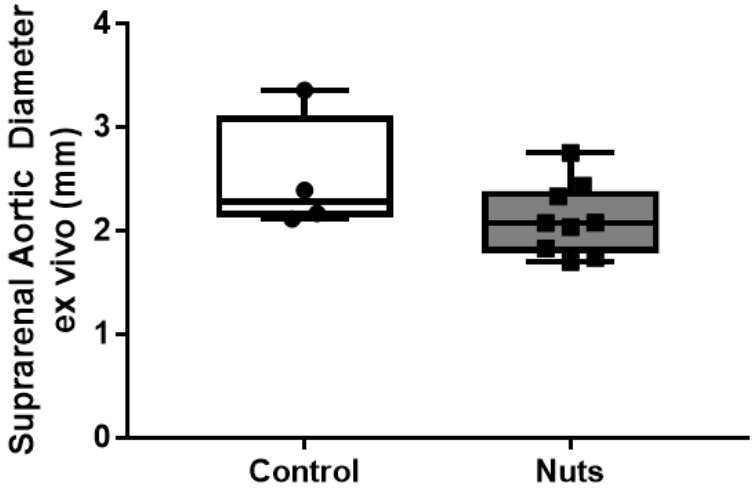

Figure 6.5. Diameter of the SRAs of mice that died of aortic rupture prior to the experimental end point (day 56). Data are presented as medians ± IQR, and were analyzed using two-tailed Mann-Whitney U tests.

6.3.2 The diet enriched with nuts reduced the severity of atherosclerosis in the brachiocephalic artery but not the aortic arch of *ApoE*$^{-/-}$ mice

The severity of atherosclerosis within the brachiocephalic artery as estimated by the intima:media area ratio was less in mice in the intervention group compared with controls (18±9.0% versus 53±12%; p=0.033; Figure 6.6A). There was no significant difference in the severity of aortic arch atherosclerosis as assessed by Sudan IV staining between the two groups (p=0.098, Figure 6.6B).

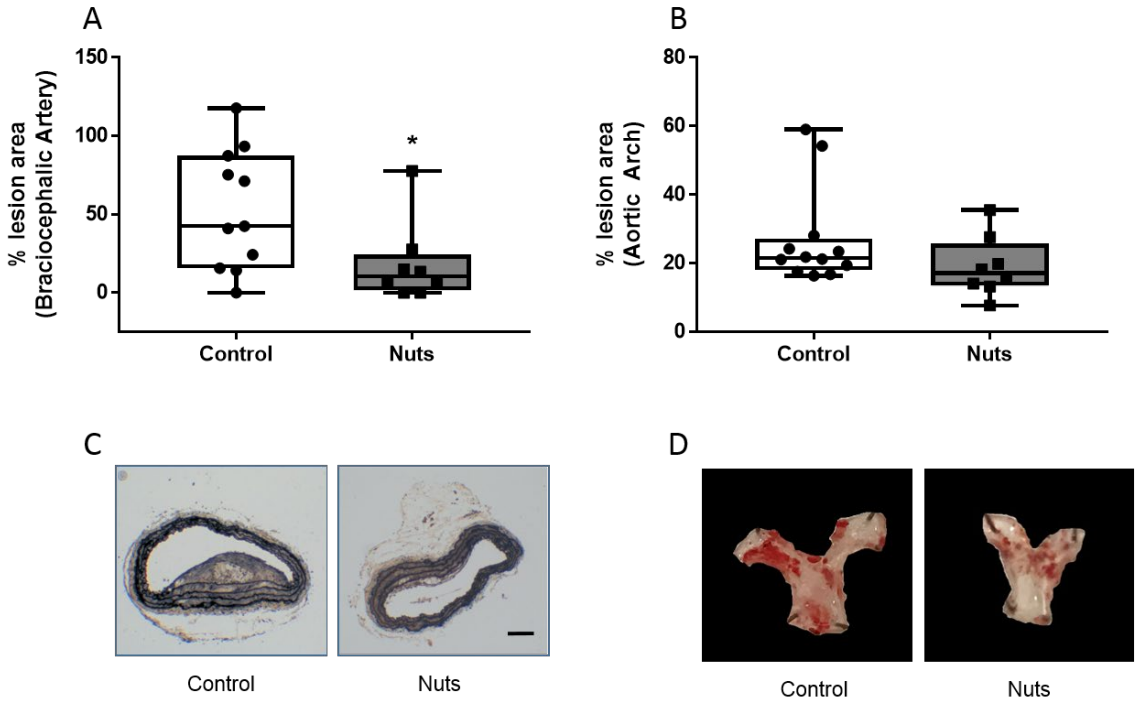

Figure 6.6. The effect of a diet enriched with nuts on atherosclerosis lesion area. Lesion area was assessed by histological assessment of cross sections of the brachiocephalic artery (A) and Sudan IV staining of the aortic arch (B). Histologically estimated intima:media area ratio was significantly less in mice receiving a diet enriched with nuts by comparison to the control group (p=0.033). (C) Representative photomicrographs of cross sections of the brachiocephalic artery from both groups. Scale bar, 100µm. (D) Representative images of *en face* Sudan IV stained aortic arches from both groups. Data are presented as medians ± IQR, and were analyzed using two-tailed Mann-Whitney U tests. * Statistically significant difference between groups (p<0.05).

6.3.3 A diet enriched with nuts did not affect blood pressure

There was no significant difference in systolic (p=0.149) or diastolic blood pressure (p=0.247) between intervention and control groups throughout the experiment (Figure 6.7). Additionally, Ang II did not cause an increase in systolic (p=0.117) or diastolic (p=0.480) blood pressure throughout the experimental period.

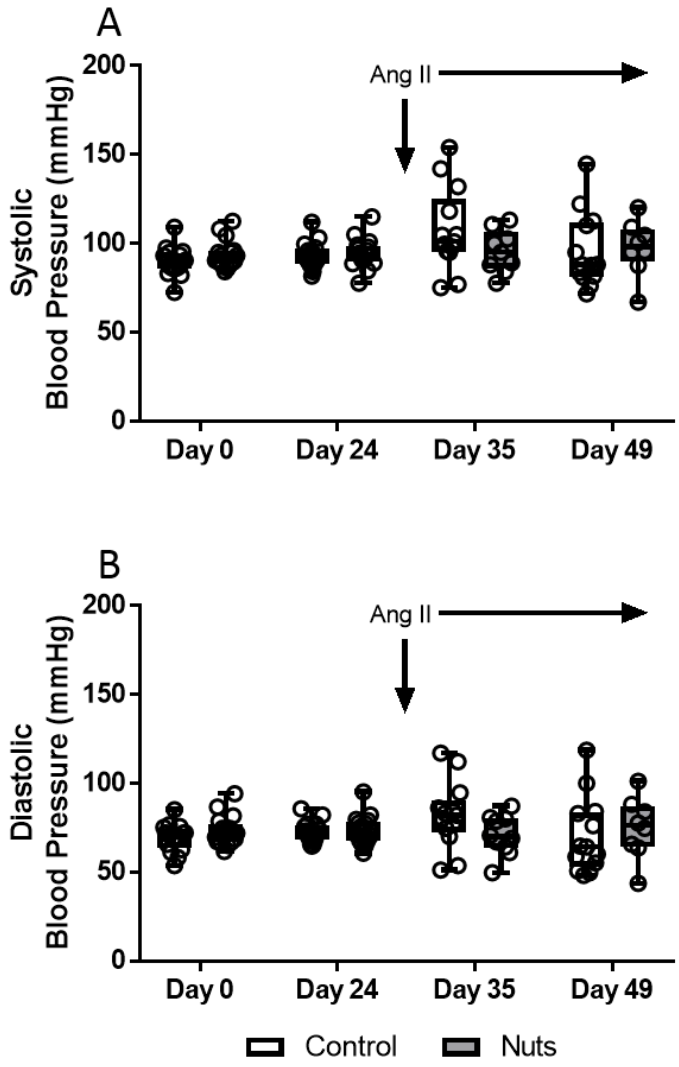

Figure 6.7. The effect of a diet enriched with nuts on blood pressure prior to and following Ang II infusion. (A) Systolic blood pressure, (B) Diastolic blood pressure. Data are presented as medians and IQR with all data points. Data were analysed using a LME model allowing for unequal variance before (day 0, 24) vs. after (day 35, 49) Ang II administration.

6.4 Discussion

The main finding of this study was that dyslipidemic mice receiving a diet enriched with nuts did not have a reduction in AAA severity following Ang II infusion. Additionally, there was no significant difference in AAA incidence or rupture between the groups. The diet enriched with nuts reduced cross sectional atherosclerosis plaque size within the brachiocephalic artery of *ApoE*$^{-/-}$ mice, but not the amount of atherosclerosis within the aortic arch.

Diets enriched with tree nuts have been previously reported to limit high fat feeding induced aortic arch atherosclerosis in male *ApoE*$^{-/-}$ mice [297], and also spontaneous aortic arch atherosclerosis development in female but not male *ApoE*$^{-/-}$ mice [304]. In this study the dietary intervention reduced the severity of atherosclerosis in the brachiocephalic artery, but not the extent of intimal atherosclerosis in the aortic arch in male *ApoE*$^{-/-}$ mice. Many of the atherosclerotic lesions found in the aortic arch were likely already present prior to dietary supplementation, as previously reported in 12 week old *ApoE*$^{-/-}$ mice, which may explain the different findings between these outcomes [259]. It is possible that a diet enriched with macadamia and pecan nuts may slow the progression of atherosclerosis but it seems unlikely it would regress existing lesions, at least in the time frame tested.

AAA has distinct pathological characteristics compared to atherosclerosis [300]. AAA are characterised by weakening and dilation of the vessel wall, thought to be stimulated by excessive extracellular matrix remodelling by proteases, such as MMPs [67, 68]. Inflammation and leukocyte recruitment have been implicated in the tissue destruction and remodelling of the vessel wall [305], often accompanied by mural thrombus and decreased smooth muscle cell density, compromising vessel wall structure and integrity [71, 72].

n-3 PUFAs and polyphenols are the main constituents of tree nuts which are thought to be beneficial against CVD [145, 206-208]. In addition to their effects on atherosclerosis, n-3 PUFA and polyphenols, such as quercetin, have both been reported to reduce AAA severity in mouse models [214, 216]. Purified n-3 PUFA (5.75g/kg/d) has been reported to reduce AAA severity in the Ang II mouse model by downregulating aortic expression of metalloproteinases 2 and 9, and decreasing expression of pro-inflammatory cytokines [214]. Purified polyphenols (60mg/kg/d) have also been reported to reduce AAA severity

in a mouse model by downregulating aortic expression of MMP-2 and MMP-9 expression, as well as increasing expression of tissue inhibitors of metalloproteinases [216].

The current study aimed to administer these active components through a dietary intervention with nuts. It is possible that the amounts of n-3 PUFAs and polyphenols in tree nuts were not high enough to induce the previously reported effects. In order to achieve the previously reported beneficial n-3 PUFA dose of 5.75g/kg/d, mice would have had to consume 50g/kg of macadamia and pecan nuts per day, which is estimated to equate to 300g/d of macadamia and pecan nuts in humans [206, 207, 214, 216]. It is unlikely that these doses would be tolerated in mice or people for long periods. To our knowledge, no human study has supplemented tree nuts at doses greater than 100g/d [306, 307]. The current study suggests that consumption of a diet enriched with tree nuts, at clinically relevant doses (estimated to be 30g/d), does not positively or negatively influence AAA development or severity in this mouse model. This finding does not negate the substantial evidence that dietary intervention with tree nuts can limit the severity of atherosclerosis. The absence of a deleterious effect of tree nuts on AAA progression is important given that patients commonly have both atherosclerosis and AAA [308]. Findings from the current study do not provide evidence to discourage consumption of nuts in AAA patients although they suggest their intake is unlikely to influence AAA progression.

The diet enriched with nuts did not significantly influence blood pressure in the current study, and Ang II did not cause an increase in blood pressure. This result is consistent with previous studies utilising the same dose of Ang II [82, 309]. No previous animal studies have investigated the effects of a diet enriched with tree nuts on blood pressure, but it has been reported that n-3 PUFA administration prevents Ang II-induced hypertension in rats [310, 311]. n-3 PUFAs have been reported to have minimal effect on blood pressure in non-hypertensive animals, however, and so it is not unexpected that a diet enriched with nuts would also have no effect on blood pressure in the current study [310, 311].

The current study has a number of strengths and limitations. Important experimental design features were included in the study such as an estimation of the required sample size, blinding of outcome assessors and the use of reproducible outcome measures. The

required sample size was calculated based on the quantification of SRA diameter, which was the primary outcome measure. Based on findings in a prior study a relatively large effect size was used in the sample size calculation [214]. Losses of mice due to aortic rupture were higher than anticipated (41% compared to a hypothesised rate of 30%). Due to both these factors the study was not adequately powered to detect a small or moderate treatment effect on the primary outcome. Thus a small or moderate effect of a diet enriched with tree nuts on experimental AAA severity cannot be excluded. The study used the most common method of inducing AAA (Ang II infusion) in male $ApoE^{-/-}$ mice. It remains unclear how findings from rodent models translate to AAA patients. There is evidence to suggest that the renin-angiotensin system is important in human AAA pathogenesis supporting the use of the Ang II model [312]. Male mice were used in the current study as they have a greater propensity for Ang II induced AAA formation [313-315]. Findings from the current study may have no relevance to AAA in women. It is also unclear whether results from rodent models can be directly translated to patients, especially when nuts are consumed for long periods, and therefore the clinical relevance of the current study should be interpreted with caution. Additionally, the mix of nuts used in the current study included macadamias and pecans because they are inexpensive and easily available but these specific nuts have been less thoroughly investigated than almonds, hazelnuts and walnuts [248, 304]. There is growing evidence to suggest that they have similar benefits to those of other tree nuts [236, 316-319]. The combination of tree nuts used in this study provide MUFA, PUFA, and polyphenol content similar to the tree nuts in the aforementioned animal and human studies, suggesting they were likely to have similar beneficial cardiovascular effects [206, 207].

In conclusion this study suggested that a diet enriched with tree nuts does not limit the incidence or severity of AAA development within a rodent experimental model. This was despite reducing the severity of atherosclerosis as assessed by histological analysis of the brachiocephalic artery. The data adds to other previous evidence suggesting that the pathogenesis, and thus effective therapies, of AAA and atherosclerosis are distinct [300].

CHAPTER 7
COLCHICINE DOES NOT REDUCE AAA GROWTH IN A NOVEL E-BAPN INDUCED MOUSE MODEL

7.1 Introduction

Surgery is the only treatment currently available for AAAs (AAA) and the identification of effective drugs to limit AAA progression and rupture is an area of intense investigation [66]. In order to test potential treatment options for AAA, a number of rodent models have been developed [78]. Most drug development research has focused on the Ang II infusion, intra-luminal elastase or adventitial calcium chloride models [78]. These models simulate some but not all aspects of human AAA and ILT are rare despite being present in the majority of patients with AAA [78]. Since these models cause an acute injury to the aorta they have been predominantly used to examine the ability of drugs to prevent AAA development, however positive results from these studies have failed to translate into clinical studies [320-322]. A novel AAA mouse model utilising E-BAPN has recently been reported that has features that are more similar to human AAA (Chapter 1.3.4)[93]. Aneurysms in this model have been reported to grow slowly for at least 100 days with some ruptures, allowing for assessment of more long term administration of interventions after aneurysm induction [93]. AAAs formed in this mouse model are true aneurysms, with many containing ILT, vascular smooth muscle cell apoptosis, extracellular matrix degradation and aortic wall infiltration by neutrophils, CD68 macrophages and $CD3^+$ T cells [93, 323].

Inflammasomes are cytosolic multiprotein units that can trigger an inflammatory response under certain conditions [222]. The NLRP3 inflammasome is a key pro-inflammatory pathway that leads to activation of caspase-1, IL-1β and interleukin-18 (IL-18) [222, 223]. Aortic NLRP3 expression has been reported to be higher in patients with AAA compared with autopsy controls that do not have aortic disease [228]. Blockade of the NLRP3 inflammasome has been reported to inhibit AAA formation in the Ang II mouse model [229, 324]. The effects of NLRP3 inflammasome blockade on the progression of established AAA has not yet been tested however. Colchicine, an FDA approved drug currently used for treating gout, inhibits macrophage NLRP3 inflammasome assembly [219]. Colchicine has been proposed as an anti-NLRP3 inflammasome drug to reduce the

risk of cardiovascular events and this is currently being tested in a number of clinical trials in patients with coronary artery disease [218-220, 325].

The aims of this study were to test whether the NLRP3 inflammasome was also upregulated in the new E-BAPN model of aneurysm, and secondly to assess whether colchicine, an NLRP3 inhibitor may reduce aneurysm growth in this model.

7.2 Methods

7.2.1 Mice

Mouse husbandry is described in detail in chapter 2.1. Briefly, Seven week old male C57BL/6J mice were acclimatised at James Cook University animal facilities for one week prior to beginning of experiments. All procedures were approved by the James Cook University Animal Ethics Committee (A2574).

7.2.2 Study design

When mice were eight weeks old, surgeries to induce AAAs and sham surgeries were conducted [93]. The experiments were split into two parts. In part one mice receiving E-BAPN (n=30) were compared to mice undergoing sham surgeries without E-BAPN (Sham, n=13) in order to test the effect of the E-BAPN model on NLRP3 activity and thrombus formation. In part two all mice received E-BAPN on the day of surgery (day 0, Figure 7.1) Additionally, mice received colchicine (Sigma, C9754, 0.2mg/kg/d, n=30) dissolved in water, or vehicle (n=30) via daily gavage from day 21 after surgery until the end of the experiment (day 90). Mice were assigned to two groups with similar aortic diameters (Figure 7.2) and these two groups were randomly allocated to receive vehicle or colchicine. Body weight was measured weekly. Research was reported in accordance with the ARRIVE guidelines [146].

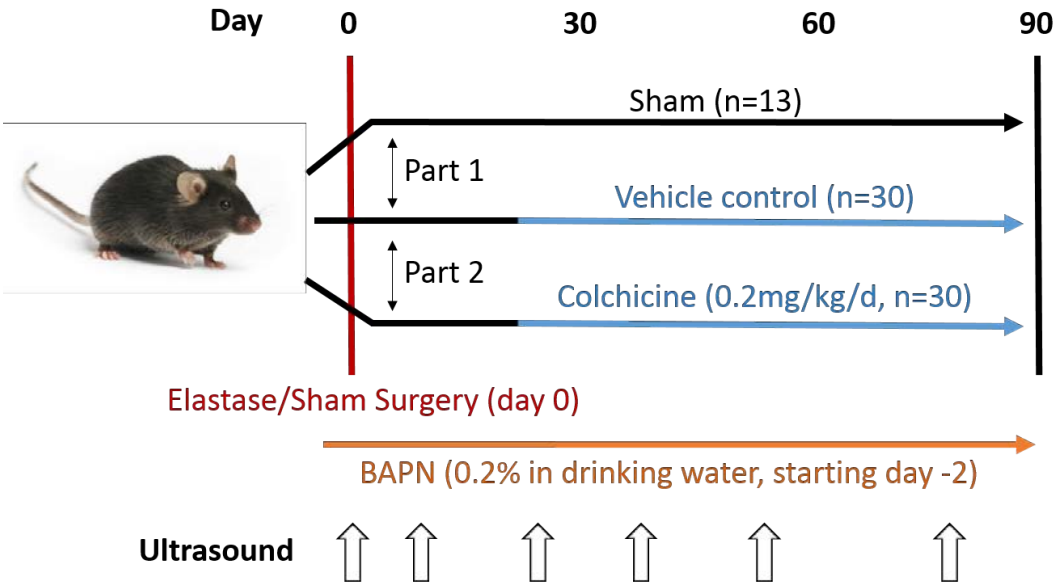

Figure 7.1. Timing of surgery, intervention and ultrasound measurements during the animal study.

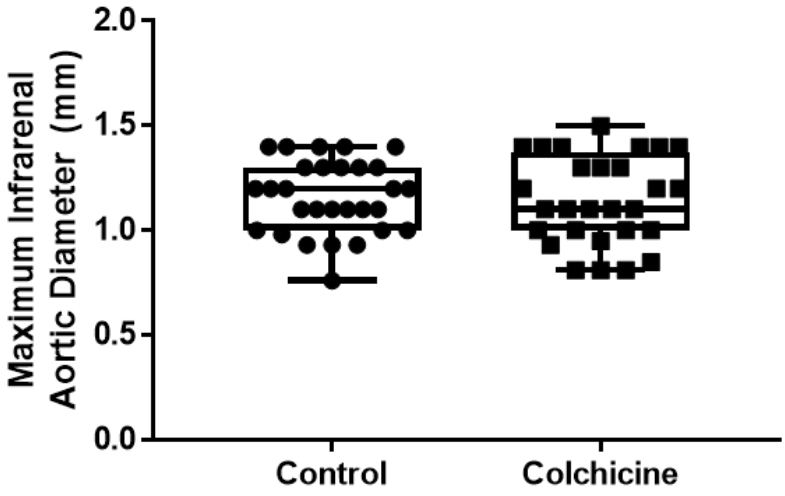

Figure 7.2. Maximum infrarenal aortic diameter in E-BAPN groups prior to randomisation to colchicine or vehicle gavage. Data are presented as medians ± IQR with individual measurements. Aortic diameters were not significantly different between randomized groups prior to initiation of interventions.

7.2.3 Induction of AAA

Mice were anaesthetised with isoflurane (Chapter 2.2) and hair was removed from the abdomen with depilatory cream prior to surgical intervention. The abdomen was then lightly cleaned with PBS followed by 70% ethanol and riodine. A 15mm vertical incision was made into the skin and abdominal cavity and the aorta and vena cava were located. The connective tissue sheath surrounding the aorta and vena cava were blunt dissected to reveal the IRA. Elastase (Sigma, E1250; 20µL, 10.3mg/mL) was applied to a 5mm x 1.5mm portion of the IRA by placing a swab containing elastase directly onto the IRA for six minutes. Elastase was not applied to the top one quarter (2mm below the left renal artery), or the bottom 1mm (just above the femoral artery branches) of the IRA. Following the application of elastase the exposed IRA was gently rinsed with PBS to clear residual elastase, the abdominal muscle and skin incisions were closed using 4/0 nylon monofilament sutures (Riverlon, 662BL), and riodine and vapour permeable surgical spray (Opsite, 66004978) were applied.

7.2.4 Intervention and vehicle control groups

The intervention group received colchicine dissolved in PBS via daily gavage at 0.2mg/kg, while control mice received PBS without colchicine as a daily gavage. Daily oral gavage was chosen to mimic daily oral dosing in humans. This dose of colchicine in mice translates to approximately a 1mg/d dose in humans, which is a currently acceptable dose for use in the treatment of gout [326], and has been the most commonly used dose in randomized controlled trials assessing the effects of colchicine on CVDs [327].

7.2.5 Ultrasound assessment of infrarenal aortic diameter

The maximum diameter of the IRA was measured using ultrasound as previously described (Chapter 2.3). Diameters were measured at baseline (day 0), and 7, 21, 28, 42, 63 and 80 days after AAA induction (Figure 7.1). Observers were blinded to experimental groups at the time of analysis.

7.2.6 Morphometric assessment of infrarenal aortic diameter

Ex vivo morphometry measurements were also performed to determine aortic diameters at the experimental end point (Chapter 2.6). Observers were blinded to intervention groups at the time of analysis.

7.2.7 Aneurysm severity

Aneurysm severity was assessed based on a modified version of a previously described protocol [93]. Briefly, aneurysms were classified into three different levels of severity as follows. (I, no aneurysm) IRAs with maximum diameters below 200% of average non-diseased controls; (II) aortas between 200-300% of non-diseased controls; (III) >300% of non-diseased controls.

7.2.8 Histological assessment of elastin degradation and collagen content

Frozen sections of the IRA were stained with Verhoeff van Giesons solution as previously described (Chapter 2.12.2 and 2.12.4). Severity of elastin degradation was graded according to the following criteria; I, no elastin degradation; II, mild fragmentation or damage; III, moderate damage; IV, severe fragmentation with sections of complete destruction of all elastic lamellae.

Additional frozen sections of IRA were stained with picrosirius red (Chapter 2.12.5). Slides were imaged on a fluorescent microscope (Zeiss, NSW) using birefringence at 200x total magnification. Five images per slide were analysed using Adobe Photoshop CC 2019. The total area of all picrosirius staining was expressed as a percentage of total IRA area on the slide (area of collagen staining/total tissue area). Observers were blinded to experimental groups at the time of analysis.

7.2.9 Measurement of tissue cytokines and caspase-1 activity

A sample of IRA tissue was lysed in radio immunoprecipitation assay buffer (Thermo Fisher Scientific, Australia), homogenised using bead homogeniser and treated with protease inhibitors (Sigma, Australia). IL-1β tissue fluorometric ELISA (Abcam, ab229440) was performed according to manufacturer instructions with 50ng/µl total protein per well. Relative caspase-1 activity was measured using a Caspase-Glo 1 Inflammasome Assay with 25ng/µl total protein from aortic samples per well (Promega, G9951), performed according to manufacturer instructions.

A sample of IRA tissue was stored in RNA Later (Invitrogen, AM7021) prior to RNA extraction. RNA extraction was performed using RNeasy mini kit (Qiagen, 74106) according to manufacturers instructions. One-step RT-PCR was performed using SYBR green kit (Qiagen, 204243, Australia). Five microliters of 2x QuantiTect SYBR Green Master Mix, 0.4µl of primer, 0.1µl of QuantiTect RT Mix, and 4.5µl of RNase-free water containing 15ng total sample RNA was added, to make a total reaction volume of 10µl.

PCR was run on a Rotor-Gene Q (Qiagen, Australia) using cycling instructions as per SYBR green kit instructions. A pilot was run using aortic samples from elastase-BAPN treated mice that received colchicine as well as vehicle controls in order to identify a housekeeping gene that did not change between interventions. One-step RT-PCR was run using beta2-microglobulin (Qiagen, QT01149547) beta-actin (Qiagen, QT00095242), 18S ribosomal RNA gene (Rn18s; Qiagen, QT02448075), and Glyceraldehyde 3-phosphate dehydrogenase (Qiagen, QT01658692). Rn18s was chosen as the housekeeping gene as it had the least variability between intervention groups. One-step RT-PCR was performed using SYBR green kit (Qiagen, 204243) and IL-1β (QT01048355), TNF-α (QT00104006), IFN- γ (QT01038821), and IL-18 (QT00171129) primers as previously described in detail [328].

7.2.10 Immunofluorescence

Slides were washed in TBS plus 0.025% Triton X-100 to allow easier coverage of slides with primary and secondary antibodies, and to reduce non-specific binding. An ImmEdge hydrophobic barrier pen (Vector, H-4000) was used to outline tissue sections to allow application of serum and antibodies. Tissues were blocked in 10% goat serum with 1% bovine serum albumin in TBS for two hours prior to staining. Frozen sections were incubated with anti-mouse CD3 (3µg/ml, Abcam, ab5690) or CD68 (5ug/ml, ab125212) primary antibodies (Abcam, Vic) and visualised with Alexa-fluor 488 conjugated anti-primary secondary antibodies (Abcam, Vic) based on previously described protocols [329]. Slides were mounted and coverslipped using slowfade gold antifade mountant with 4′,6-diamidino-2-phenylindole (DAPI, Invitrogen, Vic).Slides were imaged on a fluorescent microscope (Zeiss, NSW) at 200x total magnification. Five images per slide were analysed using Adobe Photoshop CC 2019. The total area of Alexa-fluor 488 staining was expressed as a percentage of total IRA area on the slide (area of CD3 or CD68 staining/total tissue area). Observers were blinded to experimental groups at time of analysis.

7.2.11 Sample size calculations

The objective of part 1 of the study was to assess NLRP3 inflammasome activation in the late stages of the E-BAPN model and therefore the required sample size for sham mice was estimated based on aortic tissue IL-1β in vehicle versus Ang II-infused AAA mice (Vehicle 32 ± 14pg/100µg protein, Ang II 164 ± 115pg/100µg protein, mean ± SD) [227]. The power was set to 0.8 and alpha value was set to 0.05. Based on these values, 8 mice

were required at experimental endpoint in order to detect a statistically significant difference in aortic tissue IL-1β concentration. The sample size for intervention and vehicle control mice was calculated in order to detect a clinically relevant intervention effect of 20% aneurysm growth (based on control mice having 800 ± 160% aneurysms at endpoint)[93, 330]. The desired power was set to 0.8 and the alpha value was set to 0.05. Based on these values, a minimum required sample size of 17 mice per group was estimated for control and intervention mice at endpoint. Sample sizes were increased by 30% to account for potential losses prior to endpoint.

7.2.12 Statistical analyses

Data were analysed as described in chapter 2.15. Specifically, *ex vivo* aortic diameter, TNF-α, IFN- γ and IL-18 RNA expression were compared using two-tailed t-tests as data were normally distributed. Aortic tissue IL-1β protein and RNA *expression*, Caspase-1 activity, and percentage of tissue stained with CD3, CD68 and picrosirius red were compared using Mann-Whitney U tests as these data were not normally distributed. Incidence of AAA development and ILT presence was compared using Fisher's exact test and AAA rupture was compared using Mantel-Cox (Log-rank) test. Ultrasound data was analysed using LME models. Aortic diameter was set as a fixed effect, and variation between individual mice was set as a random effect. Differences were considered statistically significant when *p*-values were <0.05.

7.3 Results

7.3.1 Characteristics of the E-BAPN model

IRA diameters of mice receiving E-BAPN were significantly greater than those of sham operated mice from day 7 (p=0.012) and onward (p<0.001) as measured by ultrasound; and on day 90 measured by *ex vivo* morphometry (p<0.001, Figure 7.3A and B). After 100 days, AAAs were present in 22 (96%) mice receiving E-BAPN and no AAAs were observed from the sham mice (Figure 7.3C, p<0.001). Aortic elastin degradation was present in all (100%) mice receiving E-BAPN but no elastin degradation was detected in sham mice (Figure 7.3D). 17 mice (23%) from the experimental groups died between the start of the experiment and sacrifice. Six mice died due to rupture, including three in the SRA and three in the IRA. In mice that had SRA rupture, aneurysms were still present in the IRA as opposed to the SRA. 11 mice died due to causes unrelated to aneurysm rupture (Table 7.1).

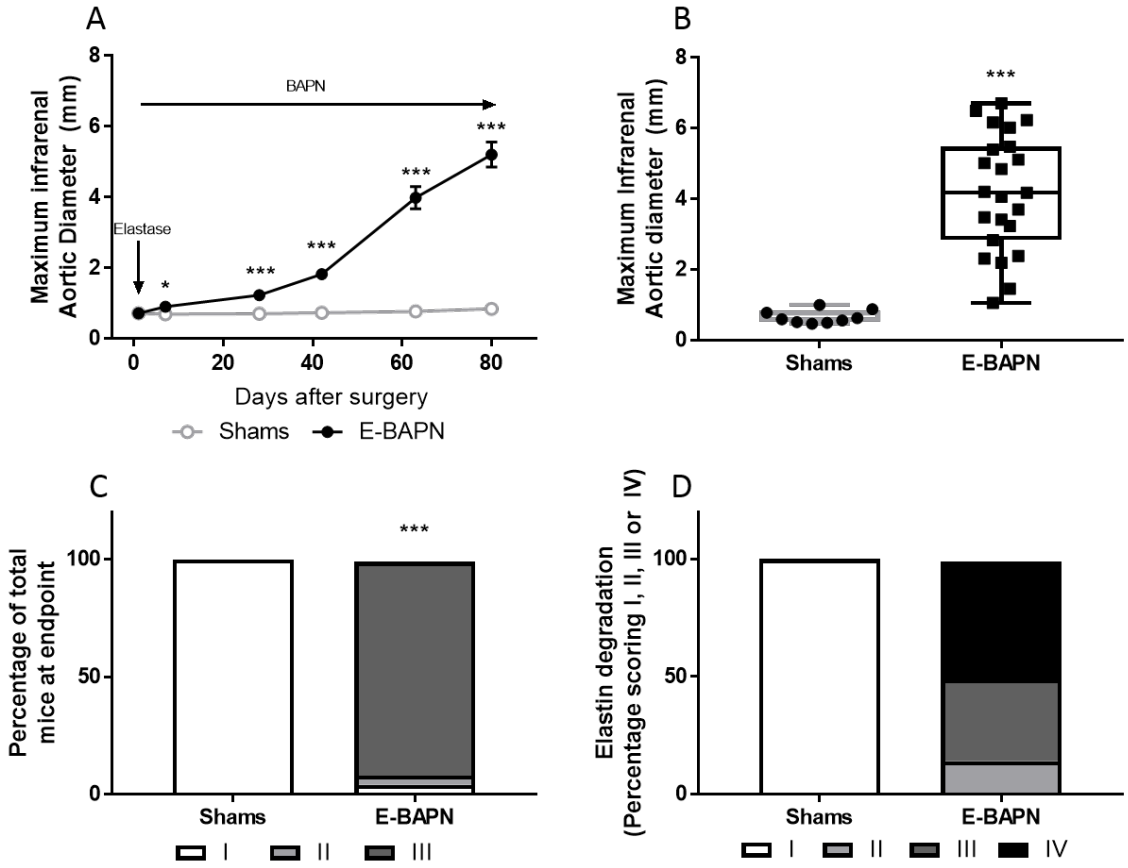

Figure 7.3. The effect of E-BAPN on infrarenal aortic diameter and structure. (A) Infrarenal aortic diameter in mice receiving E-BAPN and sham controls measured by ultrasound. Data were log transformed during statistical analysis to conform to model assumptions however raw values are shown. (B) Maximum infrarenal aortic diameter in mice receiving E-BAPN and sham controls measured *ex vivo* at the experimental endpoint. (C) Percentage of mice with different severity of aneurysm. I, no aneurysm; II, aortas between 200-300% of non-diseased controls; III, >300% of non-diseased controls. (D) Percentage of mice with different severity of aortic elastin degradation. I, no elastin degradation; II, mild fragmentation or damage; III, moderate damage; IV, severe fragmentation with sections of complete destruction of all elastic lamellae. * Mice receiving E-BAPN had significantly larger infrarenal aortic diameters from day 7. *** Mice receiving E-BAPN had significantly larger infrarenal aortic diameter from day 28 until the end of the experimental period ($p<0.001$), and significantly higher aneurysm presence ($p<0.001$). E-BAPN n=23, sham n=10 on day 90.

Table 7.1. Deaths during experimental period.

Day of death	Group	AAA diameter (mm)	Rupture site
6	Not assigned	0.7	N/A
16	Not assigned	1.1	Infrarenal
17	Not assigned	1.4	Suprarenal
22	E + BAPN	1.6	Suprarenal
23	E + BAPN	1.6	N/A
40	E + BAPN	4.4	Infrarenal
59	Colchicine	4.6	N/A
61	Colchicine	1.6	N/A
62	Colchicine	2.5	N/A
64	Colchicine	4.7	N/A
67	Colchicine	5.6	Infrarenal
74	E+BAPN	4.5	N/A
77	E +BAPN	4.0	N/A
79	E +BAPN	5.1	Suprarenal
80	Sham	0.7	N/A
81	Sham	0.7	N/A
82	Colchicine	5.7	N/A

Values measured from *ex vivo* images of dissected aortas.
N/A; Death was not related to aortic rupture.

7.3.2 Tissue Caspase-1 activity and IL-1β concentration

Aortic Caspase-1 activity was higher in mice receiving E-BAPN compared with sham controls (p<0.001, figure 7.4A). Aortic concentrations of IL-1β were greater in mice receiving E-BAPN compared with sham controls (p=0.048, figure 7.4B).

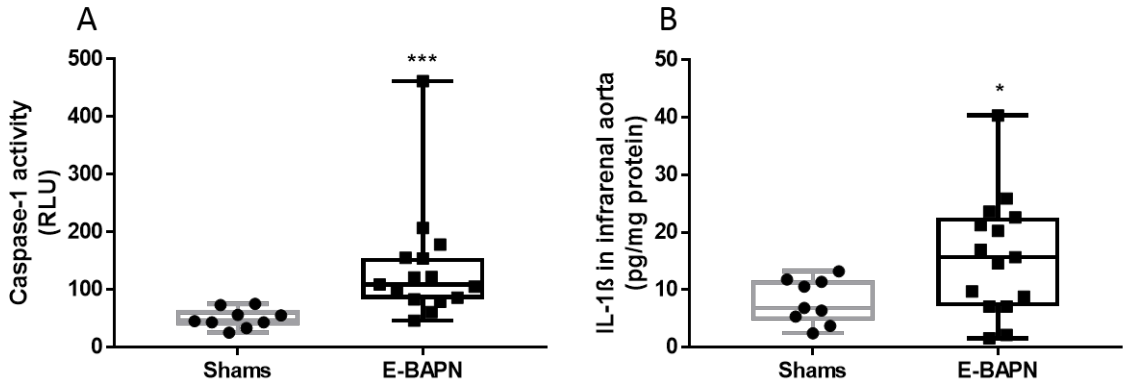

Figure 7.4. The effect of E-BAPN on the NLRP3 inflammasome. (A) Relative Caspase-1 activity within the IRA of E-BAPN treated mice and sham controls. (B) IL-1β protein concentration within the IRA of E-BAPN treated mice and sham controls. E-BAPN treated mice had significantly higher infrarenal aortic Caspase-1 activity (p<0.001, ***) and IL-1β concentration (p<0.05, *) compared with sham controls. E-BAPN n=23, sham n=10 on day 90. RLU, relative luminosity units.

7.3.3 Colchicine administration did not reduce the growth of established AAAs

There was no significant difference in AAA diameter increase in the mice administered colchicine compared to controls (p=0.527, Figure 7.5A). There were no differences in *ex vivo* AAA diameters between mice receiving colchicine and controls on day 90 (p=0.561, Figure 7.5B, Figure 7.6). AAAs were present in 21 (95%) mice receiving colchicine compared with 22 (96%) in the control group (Figure 7.5C, p=0.999). Elastin degradation was present in all control mice and mice receiving colchicine (Figure 7.5D). Aneurysm rupture occurred in one mouse from the colchicine group (4%) and three mice from the control group (10%, p=0.394, Figure 7.5E). Of mice reaching experimental endpoint, ILT were present in 14 of 23 (61%) control mice and 9 of 22 (41%) mice receiving colchicine (Figure 7.5F, p=0.238).

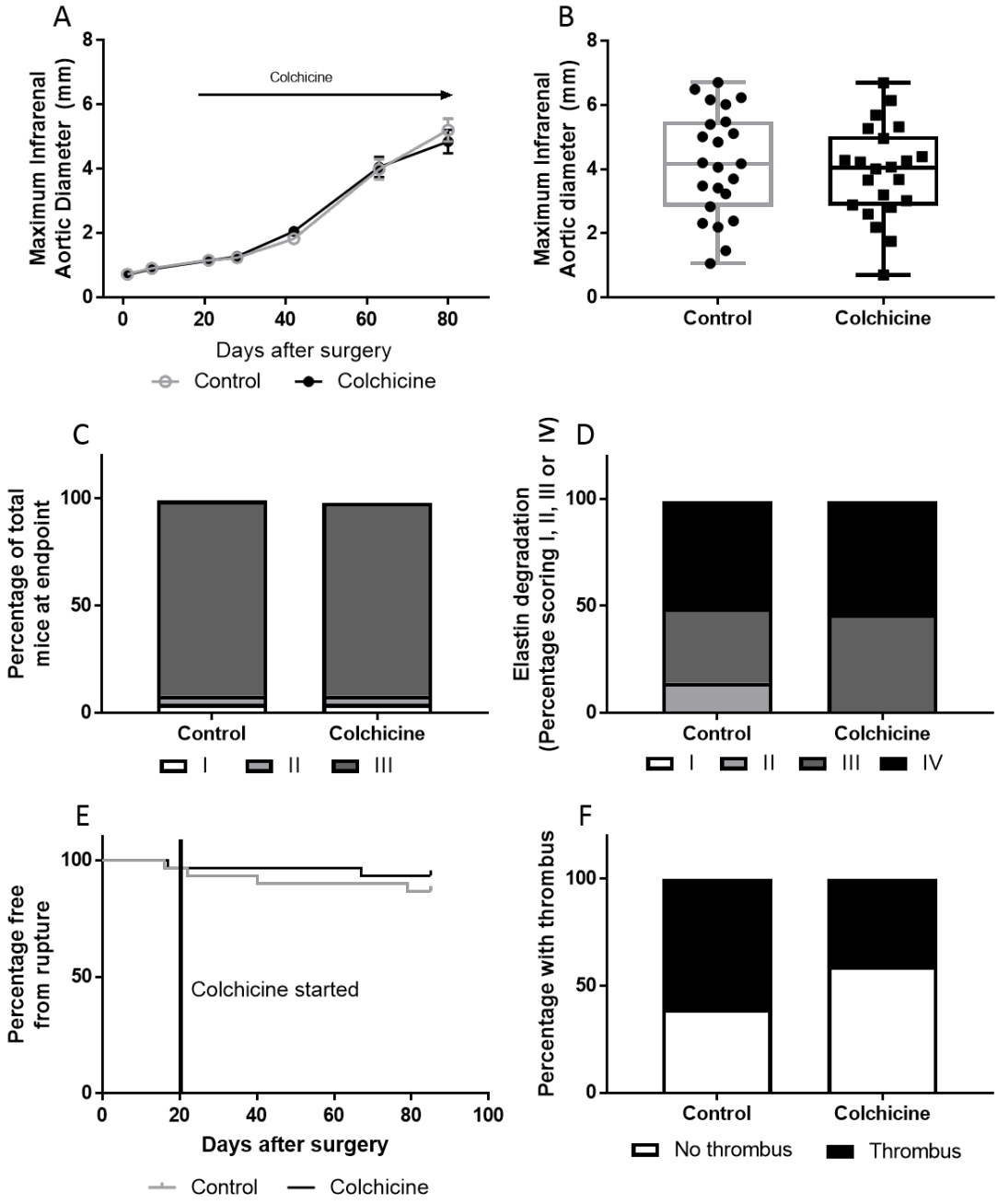

Figure 7.5. The effect of oral colchicine administration on AAA incidence, severity and rupture rates. (A) Maximum infrarenal aortic diameter measured by ultrasound. Data were log transformed during statistical analysis to conform to model assumptions however raw values are shown. (B) Maximum diameter of the IRA as measured by morphometry at the end of the experiment (day 90). (C) Percentage of mice with different severity of AAA. I, no aneurysm; II, 200-300% normal diameter; III, >300% normal diameter. (D) Percentage of mice with different severity of elastin degradation. I, no elastin degradation; II, mild fragmentation or damage; III, moderate damage; IV, severe fragmentation with sections of complete destruction of all elastic lamellae. E) Percentage of mice free from aneurysm rupture. F) Percentage of mice with and without ILT. Control n=23, colchicine n=22 on day 90.

E-BAPN with Vehicle

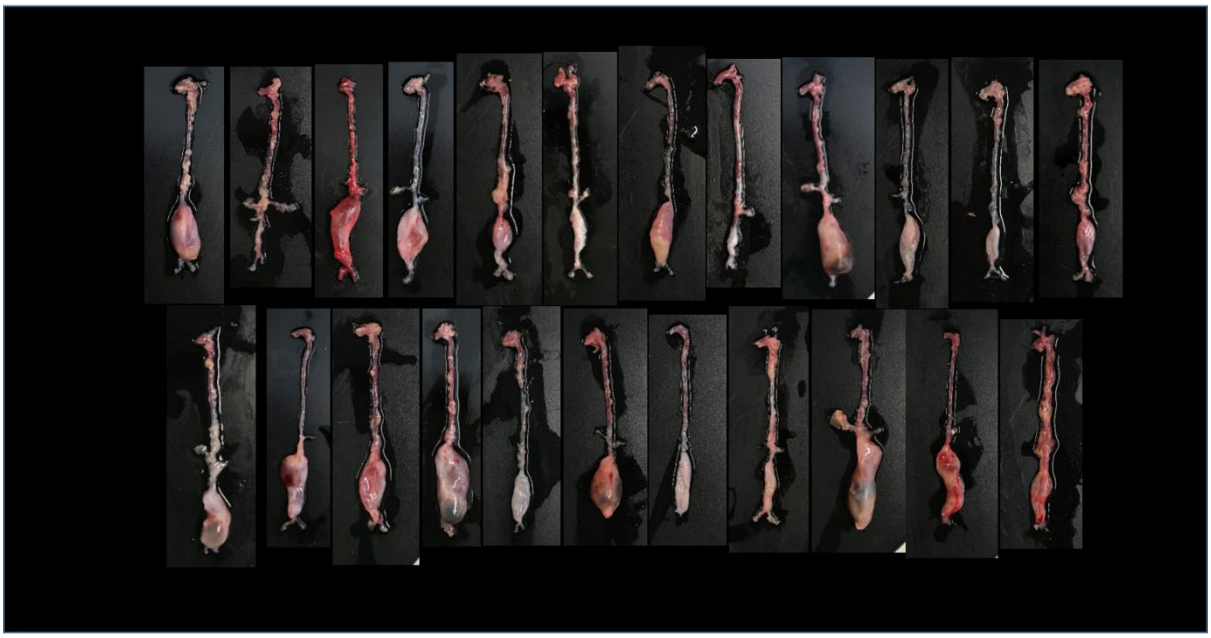

E-BAPN with Colchicine

Figure 7.6. Ex vivo images of E-BAPN treated aortas from vehicle and colchicine intervention groups.

7.3.4 Colchicine administration reduced Caspase-1 activity but did not reduce tissue inflammatory cytokine concentrations or RNA expression

Infrarenal aortic Caspase-1 activity was significantly lower in mice receiving colchicine compared with vehicle controls (p=0.047, Figure 7.7A). Infrarenal aortic IL-1β protein (p=0.174, figure 7.7B) and IL-1β (p=0.397), TNF-α (p=0.380), IFN- γ (p=0.346), and IL-18 RNA expression (p=0.828, Figure 7.7C) were not reduced in mice receiving colchicine. Infrarenal aortic CD3 T cells (p=0.406), CD68 macrophages (p=0.478) and collagen (p=0.068, Figure 7.7D) were not significantly different between mice receiving colchicine and controls.

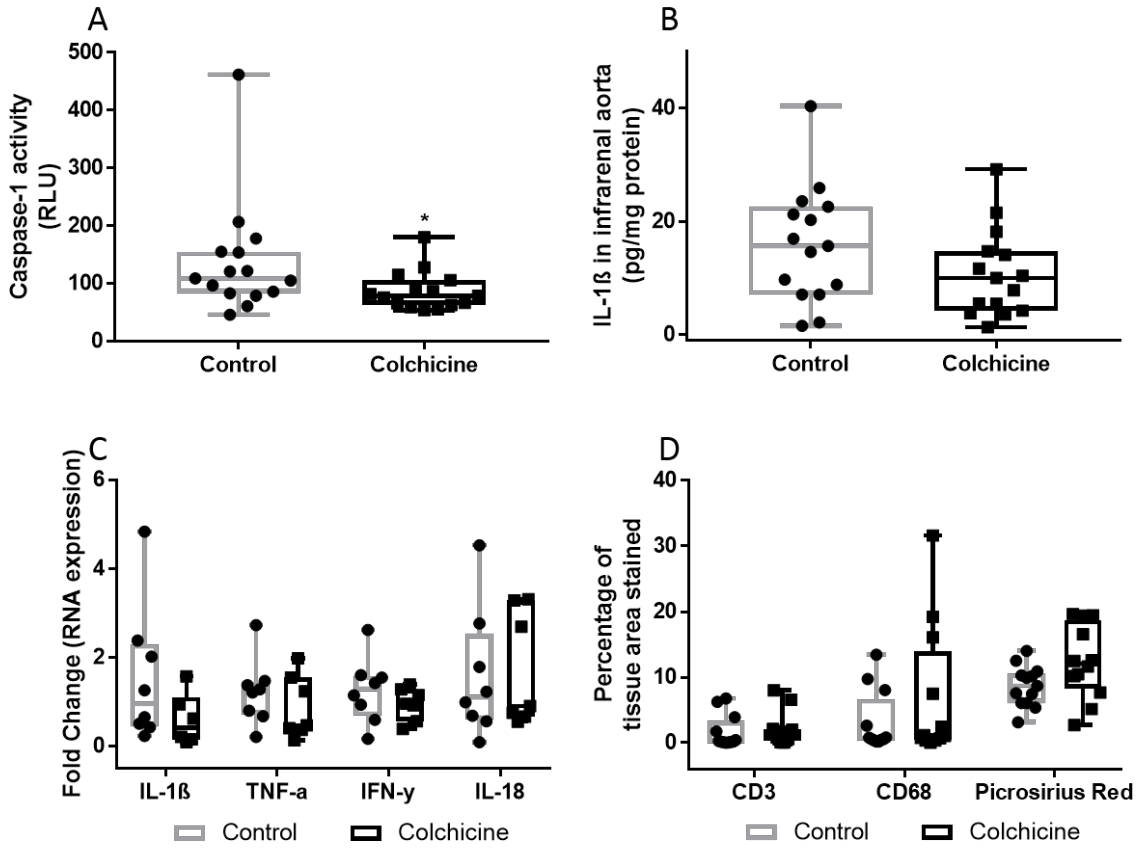

Figure 7.7. The effect of oral colchicine intervention on tissue cytokines and inflammatory cell markers related to the NLRP3 inflammasome. (A) Relative Caspase-1 activity within the IRA of mice receiving colchicine intervention compared with controls. (B) IL-1β protein concentration within the IRA of mice receiving colchicine intervention compared with controls. (C) IL-1β, TNF-α, IFN- γ and IL-18 RNA expression within the IRA in mice receiving colchicine compared with controls. (D) Percentage of tissue stained with CD3, CD68 and picrosirius red birefringence (as markers of T cells, macrophages and collagen, respectively). * Mice receiving colchicine had significantly lower infrarenal aortic caspase-1 activity at experimental endpoint ($p<0.05$). Control n=23, colchicine intervention n=22 on day 90. RLU, relative luminometer units.

7.4 Discussion

The application of E-BAPN created continually growing and evolving aneurysms with ILT, comparable to those published previously [93]. In this study it is shown that, similar to other AAA mouse models and patients, activity of the NLRP3 inflammasome mediator Caspase-1 is elevated leading to increases in IL-1β concentrations within aneurysmal tissue. Treatment with colchicine, an inhibitor of NLRP3 inflammasome activation, significantly reduced Caspase-1 activity however this did not result in downstream decreases in aortic IL-1β concentration and did not reduce aneurysm growth.

Topical elastase application causes fragmentation of one or multiple layers of the elastic lamina within the aorta, compromising aortic integrity and increasing lumen size as occurs in patients [331, 332]. BAPN inhibits cross-linking of elastin and collagen fibers which models the deterioration of aortic repair that occurs in aging human patients [93]. This reduces aortic wall thickness, stability and elasticity causing aortic expansion and an increased risk of aortic rupture. Within this study elastase degraded IRA elastin layers in all mice with varying severities. BAPN administration allowed for continual growth throughout the 90 day experimental period similar to results reported previously [93]. Continual growth over a long time period allows the use of interventions on pre-established aneurysms to measure aneurysm growth which has been difficult with previous animal models [78].

ILT are a key feature of AAA in patients and ILT presence and size has been correlated with early rupture and increased AAA growth rates [75, 333, 334]. Most ILT associated with AAA are comprised of three distinct layers with the luminal layer containing migrating cytokines and inflammatory cells, primarily T cells and macrophages [94]. In this study the presence of ILT within the E-BAPN model correlates with larger aneurysm size. There is focal accumulation of CD3 (T cell) and CD68 (macrophages) primarily within the ILT. The distinctive layers of the ILT appear to be indistinguishable.

The NLRP3 inflammasome is activated by interaction between NLRP3, apoptosis-associated speck-like protein containing a caspase recruitment domain (ASC), and pro-caspase-1 to produce activated caspase-1, which in turn leads to increased IL-1β and IL-18 [222, 223]. The NLRP3 inflammasome is elevated in AAA patients and in other mouse AAA models and blockade of the NLRP3 has been reported to reduce AAA formation in the Ang II infusion mouse model [228, 229, 324]. Data from the current

study suggest that inflammasome activation also occurs in the E-BAPN model as both Caspase-1 activity and aortic IL-1β concentrations are elevated. The NLRP3 inhibitor colchicine reduced Caspase-1 activity at experimental endpoint after 70 days of daily oral gavage however it had no effect on downstream aortic IL-1β concentrations and did not reduce aneurysm growth.

Low-dose colchicine (0.5-1mg/d, comparable to current study based on body surface area translation) is currently being investigated in clinical trials as a preventative and treatment for atherosclerosis as it reduces chronic inflammation [335]. This dose is considerably lower than the doses used for acute gout (up to 4.8mg/d) due to diarrhoea and vomiting that is caused by these high doses and the requirement of chronic treatment for CVD [336]. It is possible that the dose used in the current study is too low to significantly reduce tissue IL-1β concentrations in the E-BAPN mouse model and too low to reduce aneurysm growth, despite causing a small but significant reduction in caspase-1 activity. It is also possible that NLRP3-independent pathways may be activated that can increase IL-1β concentrations.

This low dose of colchicine, effective in atherosclerosis, appears not to be effective in reducing growth of AAA in an E-BAPN mouse model. This supports other studies that highlight potential differences between atherosclerosis and AAA regarding risk factors and effective treatments [14, 15].

The study and the E-BAPN model used has a number of patient relevant design features that increase the strength of this study, as well as some notable limitations. Aneurysms are true dilating aneurysms as opposed to dissecting aneurysms, can rupture, occur in the IRA, contain ILT, T cells and macrophages, and have decreased smooth muscle cells and collagen deposition all of which are features of human AAA [93, 94, 337]. Additionally colchicine was administered 21 days after surgery allowing aneurysms to become established prior to intervention. The current low dose of colchicine was chosen to minimise side effects and did not significantly reduce tissue IL-1β concentrations. A higher dose of colchicine may potentially supress IL-1B and have different effects. The use of BAPN inhibits cross-linking of elastin and collagen and currently no intervention has worked in this model [93, 338]. It is unclear whether this effect is too strong and whether a drug that is not a direct antagonist to lysyl oxidase inhibitors can be effective. Future studies may need to discontinue BAPN administration once aneurysms are

established in order to lower the chance of false negatives. Aortic IL-1β concentration and Caspase-1 activity were measured at the experimental endpoint in order to assess whether there was long-term NLRP3 activation. In the original study, aortic IL-1β concentration had decreased to baseline levels by 28 days after surgery as the acute inflammatory response subsided. It is currently unclear when IL-1β and Caspase-1 levels increase beyond day 28 and for how long beyond day 90 these may stay elevated.

The E-BAPN model shows evidence of NLRP3 inflammasome activation and accumulation of inflammatory cells within the ILT as occurs in patients. Despite this, intervention with colchicine, an inhibitor of the NLRP3 inflammasome, did not reduce AAA diameter or inflammation in the E-BAPN model.

CHAPTER 8
GENERAL DISCUSSION AND CONCLUSIONS

8.1 Summary of main findings

Diseases of the peripheral arteries are the cause of substantial and increasing mortality and morbidity globally, however currently there are no effective pharmacological treatments available. Multiple interventions have been reported to improve hind limb ischemia and reduce aneurysm diameter in mouse studies, however these treatments have failed to be translated in clinical trials (Chapter 1.4). Within this thesis multiple therapeutic interventions were selected based on promising results from recent pre-clinical studies and were investigated in patient focused animal models. A systematic review and meta-analysis revealed that the flavonoids, specifically the flavonol subclass, were effective at reducing atherosclerosis lesion area (Chapter 4). Of these flavonols, quercetin is the most commonly researched and previous studies suggest it may have additional effects that make it beneficial in PAD (Chapter 1.5.1). However, supplementation with quercetin did not improve blood flow or exercise performance in a novel two-stage surgical model of HLI and IC, despite previously reported beneficial effects on blood flow in acute HLI models [60] (Chapter 5). Prevention of AAA development was not achieved with a diet of macadamia and pecan nuts, which are high in polyphenol content including quercetin (Chapter 6). However, the diet did reduce atherosclerotic plaque formation in the BCA, consistent with what was reported in previous studies (Chapter 4) [248, 296, 297]. Treatment of pre-established aneurysm and prevention of further growth was not achieved with oral administration of colchicine, an FDA approved anti-inflammatory drug that has been reported to reduce atherosclerosis severity in patients (Chapter 7) [218-220, 325]. The research conducted in this thesis suggests that the three interventions studied may not be suitable in the disease models tested despite prior *in vitro* and *in vivo* studies showing promising results. The findings summarized above highlight that the specific method of disease induction, timing of treatment and experimental design used can dictate whether an intervention is effective or not and can therefore have a profound impact on clinical translatability of results.

8.2 Impact of experimental design on study results and the importance of clinical relevance

A key consideration within this thesis has been the impact of experimental design of preclinical studies on the results, interpretations and translational potential of a study. This consideration is important when assessing the aforementioned differences between the response of interventions to atherosclerosis and other PADs as study design may be a potential reason for these differences. Positive results for interventions in animal studies are ubiquitous and yet minimal pharmaceutical interventions show any success in clinical trials (Chapter 1.4). Positive results in animal studies can be beneficial to extend current understanding of disease (to identify relevant pathways in a disease model) however these results can become misleading when translated for clinical use. In this thesis it is argued that animal studies with a patient relevant design may limit the rate of false positive results, such as those highlighted above, and improve the success rate of clinical trials for peripheral artery diseases.

Many experiment and model specific design considerations have been made for the studies within this thesis in an attempt to improve the clinical relevance of the included animal studies. These considerations may have reduced the efficacy of the interventions used compared with previous studies. In chapter 5, elderly mice were used. Older mice are less responsive to interventions that stimulate angiogenesis [293] and therefore quercetin may have had a reduced effect on these mice compared with younger mice [60]. The two-stage HLI model reduced abrupt, pro-angiogenic changes in shear stress, making recovery of blood flow more difficult [46, 58]. The aforementioned study design features limit the potential for quercetin administration to have a beneficial effect, however these factors are also a limitation for most patients. In chapter 7, a recently developed E-BAPN AAA model was used to test colchicine intervention. The E-BAPN model produces large non-resolving true infrarenal aneurysms that contain ILT, which are features common in human AAA. The non-resolving aneurysms allow for longer term administration of treatment interventions, compared with previous models which were more suitable to study of preventions due to AAA that resolve early or cause other side effects that limit duration of studies (Chapter 1.3.4). These studies within this thesis may potentially provide a more accurate depiction of the effects of these drugs in PADs, and limit the chance of false positive results.

An example of the impact of experimental design on results is the finding that quercetin pre-treatment has previously reduced acute HLI in young mice, however quercetin treatment failed to reduce established and sustained HLI in elderly mice at similar doses in the current study (Chapter 5). Similarly, NLRP3 knockout mice were reported to have a reduced propensity to develop AAA and reduced AAA diameter following Ang II administration [227], and pre-treatment with an NLRP3 inhibitor was reported to reduce the severity of Ang II-induced AAA development [229]. However, inhibition of NLRP3 activation did not influence the growth rate of already developed AAAs (Chapter 7). These data suggest that quercetin and colchicine treatment in patients may be insufficient to treat PAD and AAA respectively in patients similar to the myriad of other drugs that have failed clinical trials. The key design considerations leading to the disparity in results above are the potency of treatment and the window of time that the treatment is administered. Specifically, knockout models are potent and serve a role in mechanistic studies to inform of whether blocking a pathway may influence disease, but these results are rarely translatable. Pre-treatment models serve to test whether diseases can be prevented and are potentially translatable provided that the treatment used is cheap, readily available, easy to administer and can be taken for a long period of time without negative side effects. A treatment model is the most translatable, as a large majority of patients seek treatment once a disease is already established. Similar to clinical trials, these studies rarely show positive effects due to the complications associated with treating pre-established disease [339].

It is important to minimise false positive results in animal studies if they are to inform potential drugs for use in clinical trials, however it is unclear whether the models within this study may also be prone to more false negative results by consequence. That is, there is a possibility that the drugs studied in this thesis may be beneficial in human studies despite not having beneficial effects in these animal models. Currently it is difficult to effectively test whether these disease models are prone to false negative results due to there being a lack of treatments that are beneficial in patients to serve as a reference. Exercise intervention is beneficial for patients with PAD [27] and the two-stage stable HLI model has also been responsive to exercise [340]. This suggests that the novel HLI model may indeed be receptive to at least some treatment interventions that are effective in humans. The use of the lysyl oxidase inhibitor, BAPN, inhibits elastin and collagen cross-linking which models the deterioration of aortic repair that occurs in aging human

patients [93]. However, it is possible that this inhibition is too severe and it may limit the likelihood that drugs may have an effect on aneurysm growth. No drugs have shown efficacy in treating established AAA in patients and therefore it is not possible to determine whether or not the E-BAPN model is prone to false negative results.

8.3 Thesis strengths and limitations

The systematic review and meta-analysis conducted in chapter 4 examined specific study design features by utilising a quality assessment tool. This tool was modified from a previously published quality assessment tool [268], and further developed based on design features that are required for clinical studies, such as those outlined in the Cochrane risk of bias assessment [341] and the ARRIVE guidelines for pre-clinical studies [146]. Specifically, study design considerations such as randomized group allocation, sample size calculations, justification of intervention dose, intra-observer and inter-observer reproducibility measures, and blinding of treatment interventions were assessed. The median score of studies included in the quality assessment in chapter 4 was 59%, suggesting a moderate study quality.

Many of the experimental design features identified as important in the study quality assessment have been incorporated into the studies included within this thesis. All studies within the thesis included ethics approval statements, randomized group allocation, reporting of key study characteristics, sample size calculations and justification of the drug dose used. Blinding to treatment groups at the time of analysis occurred for most relevant outcome measures within the studies. Blinding to treatment groups for analysis of the primary outcome occurred for chapter 6 and 7. Intra-observer and inter-observer reproducibility measurements were performed for quantitative outcome measures where analysis could be influenced by subjective bias. Training effects prevented reproducibility measurements from being taken for distance travelled in a TMT and so these results were supported with open field assessment of voluntary exercise [342] (Chapter 5).

The concentration of the drug administered was not measured in the plasma for any of the studies included within the thesis. However, the doses of quercetin (Chapter 5), nuts (Chapter 6) and colchicine (Chapter 7) used have previously been reported to have pharmacological effects [153, 174-177, 185, 291, 335]. Indeed, the studies included within the thesis found that quercetin increased plasma nitric oxide, nuts reduced

atherosclerosis lesion area and colchicine reduced caspase-1 activity, suggesting that these drug doses were sufficient to have a pharmacological effect.

8.4 Implications and future research

There are a number of implications and potential avenues of future research brought up by the results of this thesis. The interventions used in this thesis did not significantly alter the primary outcome despite favorable results found in different disease models. It cannot be excluded that the negative results are due to the specific animal models used despite considerations taken in choosing these models and the robust study design used. There are potentially major implications if this research is interpreted as concrete evidence for the lack of efficacy of these drugs in light of a potential false negative result. If quercetin, dietary intervention with nuts or colchicine are effective in their disease targets in humans but not in the animal models examined, there is a risk of missing potentially life-altering therapeutics. Conversely, if these results are ignored, large amounts of money, time and resources may be wasted on drugs that may not be of any benefit to patients.

A pilot randomized controlled trial published shortly after the completion of the studies utilising quercetin in the two-stage HLI model suggested that resveratrol, a related polyphenol with similar sirtuin 1 activator properties, did not improve walking performance in older patients with IC [343]. This is supportive of the results from chapter 5 and suggests that quercetin indeed may not be a beneficial treatment for IC, although it is difficult to determine the likelihood beyond extrapolations from this related study. If further animal studies are to be performed, a longer duration of treatment may be required. This is potentially achievable with the current two-stage HLI model due to reduced blood flow recovery, although this model has currently not been tested for longer than 35 days after the two-stage surgical procedure (Chapter 5)[59].

The 56-day dietary intervention with tree nuts, including 28 days prior to Ang II treatment, did not reduce AAA formation (Chapter 6). It is possible that a longer duration of dietary intervention prior to Ang II treatment will have led to more beneficial effects, although a longer duration was not required for nuts to reduce the formation of atherosclerotic plaques (Chapter 6). Current clinical research supports dietary nut intake for the prevention of lower limb PAD, myocardial infarction and hypertension [153, 202]. The results from this thesis therefore will not influence current recommendations for

dietary nut intake as no negative consequences for nut supplementation in AAA were identified.

Colchicine is an anti-inflammatory agent and appears to be beneficial for the treatment of atherosclerosis [344, 345], and there are ongoing clinical trials assessing its efficacy in this disease. AAA is a chronic inflammatory disease and therefore an anti-inflammatory such as colchicine is a prime candidate for AAA treatment. Despite this, results from this thesis suggest that colchicine has no significant effect on AAA growth (Chapter 7), not unlike findings of from chapter 6 on the effects of dietary nut supplementation. The animal experiments in chapter 7 did not test the effects of colchicine on atherosclerosis, however, so it is not possible to conclude whether or not the dose regimen used would have reduced severity or increased stability of atherosclerotic plaques. Due to the limited data on the effects of colchicine and related drugs in AAA, and the evidence of the involvement of the NLRP3 in human AAA [228], results from this one study are not enough to rule out an effect of colchicine in AAA. Therapeutics have not been tested in the elastase-BAPN mouse model previously, and it is difficult to discern how likely it is for this model to respond to interventions. Therefore a similar colchicine regimen should be tested in other similar animal models including the Ang II model to be interpreted alongside this study.

8.5 Conclusions

Lower limb PAD and AAA are two often concurrent diseases that both reduce quality of life and increase mortality. In this thesis, animal models of these PADs were used that included clinically relevant design features in order to better determine whether promising interventions may be worth investigating in clinical trials. The studies suggest that, despite these interventions working in other *in vitro* and *in vivo* models, none reduced disease severity in the animal models used. These results emphasise the impact of experimental design and animal models on study results and their translatability to patients.

REFERENCES

1. Bergiers, S., B. Vaes, and J. Degryse, *To screen or not to screen for peripheral arterial disease in subjects aged 80 and over in primary health care: a cross-sectional analysis from the BELFRAIL study.* BMC Fam Pract, 2011. **12**: p. 39.
2. Moxon, J.V., et al., *Comparison of the serum lipidome in patients with abdominal aortic aneurysm and peripheral artery disease.* Circ Cardiovasc Genet, 2014. **7**(1): p. 71-9.
3. Shah, N., et al., *Sleep apnea is independently associated with peripheral arterial disease in the Hispanic Community Health Study/Study of Latinos.* Arterioscler Thromb Vasc Biol, 2015. **35**(3): p. 710-5.
4. Sieminski, D.J. and A.W. Gardner, *The relationship between free-living daily physical activity and the severity of peripheral arterial occlusive disease.* Vasc Med, 1997. **2**(4): p. 286-91.
5. Hernandez, H., et al., *Quantification of Daily Physical Activity and Sedentary Behavior of Claudicating Patients.* Ann Vasc Surg, 2019. **55**: p. 112-121.
6. Wu, A., et al., *Lower Extremity Peripheral Artery Disease and Quality of Life Among Older Individuals in the Community.* J Am Heart Assoc, 2017. **6**(1).
7. Gardner, A.W., et al., *Predictors of health-related quality of life in patients with symptomatic peripheral artery disease.* J Vasc Surg, 2018. **68**(4): p. 1126-1134.
8. Morris, D.R., et al., *Association of lower extremity performance with cardiovascular and all-cause mortality in patients with peripheral artery disease: a systematic review and meta-analysis.* J Am Heart Assoc, 2014. **3**(4).
9. Kniemeyer, H.W., et al., *Treatment of Ruptured Abdominal Aortic Aneurysm, a Permanent Challenge or a Waste of Resources? Prediction of Outcome Using a Multi-organ-dysfunction Score.* Eur J Vac Endovasc, 2000. **19**(2): p. 190-196.
10. Assar, A. and C. Zarins, *Ruptured abdominal aortic aneurysm: a surgical emergency with many clinical presentations.* Postgrad Med, 2009. **85**(1003): p. 268-273.
11. Gray, C., et al., *Screening for Peripheral Arterial Disease and Carotid Artery Disease in Patients With Abdominal Aortic Aneurysm.* Angiology, 2016. **67**(4): p. 346-9.
12. Chun, K.C., et al., *Risk factors associated with the diagnosis of abdominal aortic aneurysm in patients screened at a regional Veterans Affairs health care system.* Ann Vasc Surg, 2014. **28**(1): p. 87-92.
13. Sukhija, R., et al., *Prevalence of coronary artery disease, lower extremity peripheral arterial disease, and cerebrovascular disease in 110 men with an abdominal aortic aneurysm.* Am J Cardiol, 2004. **94**(10): p. 1358-1359.
14. Golledge, J. and P. Norman, *Atherosclerosis and abdominal aortic aneurysm: Cause, response or common risk factors?* Arteriosclerosis, thrombosis, and vascular biology, 2010. **30**(6): p. 1075-1077.
15. Phie, J., et al., *A diet enriched with tree nuts reduces severity of atherosclerosis but not abdominal aneurysm in angiotensin II-infused apolipoprotein E deficient mice.* Atherosclerosis, 2018.
16. Aboyans, V., et al., *2017 ESC Guidelines on the Diagnosis and Treatment of Peripheral Arterial Diseases, in collaboration with the European Society for Vascular Surgery (ESVS).* Eur J Vasc Endovasc Surg, 2018. **55**: p. 305-368.
17. Golledge, J., et al., *Risk of major amputation in patients with intermittent claudication undergoing early revascularization.* Br J Surg, 2018. **105**(6): p. 699-708.
18. Katz, D.A., B. Littenberg, and J.L. Cronenwett, *Management of small abdominal aortic aneurysms. Early surgery vs watchful waiting.* JAMA, 1992. **268**(19): p. 2678-86.

19. Norgren, L., et al., *Inter-society consensus for the management of peripheral arterial disease (TASC II).* Eur J Vasc Endovasc Surg, 2007. **33**(1): p. S1-S75.
20. Hiatt, W.R., et al., *Pathogenesis of the limb manifestations and exercise limitations in peripheral artery disease.* Circ Res, 2015. **116**(9): p. 1527-39.
21. Endemann, D.H. and E.L. Schiffrin, *Endothelial dysfunction.* Clin J Am Soc Nephrol, 2004. **15**(8): p. 1983-1992.
22. Yoboue, E.D. and A. Devin, *Reactive oxygen species-mediated control of mitochondrial biogenesis.* Int J Biochem Cell Biol, 2012. **2012**.
23. Brevetti, G., et al., *Inflammation in peripheral artery disease.* Circulation, 2010. **122**(18): p. 1862-1875.
24. Vranic, M. *What is Claudication?* 2020.
25. Grenon, S.M., et al., *Walking disability in patients with peripheral artery disease is associated with arterial endothelial function.* J Vasc Surg, 2014. **59**(4): p. 1025-34.
26. Gaenzer, H., et al., *Flow-mediated vasodilation of the femoral and brachial artery induced by exercise in healthy nonsmoking and smoking men.* J Am Coll Cardiol, 2001. **38**(5): p. 1313-1319.
27. Hamburg, N.M. and G.J. Balady, *Exercise rehabilitation in peripheral artery disease: functional impact and mechanisms of benefits.* Circulation, 2011. **123**(1): p. 87-97.
28. Baum, O., et al., *Capillary ultrastructure and mitochondrial volume density in skeletal muscle in relation to reduced exercise capacity of patients with intermittent claudication.* Am J Physiol Regul Integr Comp Physiol, 2016. **310**(10): p. R943-51.
29. McDermott, M.M., et al., *Peripheral artery disease, calf skeletal muscle mitochondrial DNA copy number, and functional performance.* Vasc Med, 2018. **23**(4): p. 340-348.
30. Highsmith, E.W., et al., *Mitochondrial Aging and Physical Decline: Insights From Three Generations of Women.* J Gerontol A Biol Sci Med Sci, 2015. **70**(11): p. 1409-1417.
31. Hebert, S.L., et al., *Mitochondrial Aging and Physical Decline: Insights From Three Generations of Women.* J Gerontol A Biol Sci Med Sci, 2015. **70**(11): p. 1409-17.
32. White, S.H., et al., *Walking performance is positively correlated to calf muscle fiber size in peripheral artery disease subjects, but fibers show aberrant mitophagy: an observational study.* J Transl Med, 2016. **14**(1): p. 284.
33. Kwon, S.-G., et al., *Acid evoked thermal hyperalgesia involves peripheral P2Y1 receptor mediated TRPV1 phosphorylation in a rodent model of thrombus induced ischemic pain.* Molecular pain, 2014. **10**(1): p. 1.
34. Brass, E.P., W.R. Hiatt, and S. Green, *Skeletal muscle metabolic changes in peripheral arterial disease contribute to exercise intolerance: a point-counterpoint discussion.* Vascular medicine, 2004. **9**(4): p. 293-301.
35. Parr, B., T.D. Noakes, and E.W. Derman, *Factors predicting walking intolerance in patients with peripheral arterial disease and intermittent claudication.* S Afr Med J, 2008. **98**(12): p. 958-62.
36. Svensson, C.I., *Interleukin-6: a local pain trigger?* Arthritis Res Ther, 2010. **12**(5): p. 145-145.
37. Manjavachi, M.N., et al., *Mechanisms involved in IL-6-induced muscular mechanical hyperalgesia in mice.* Pain, 2010. **151**(2): p. 345-355.
38. Nylaende, M., et al., *Markers of vascular inflammation are associated with the extent of atherosclerosis assessed as angiographic score and treadmill walking distances in patients with peripheral arterial occlusive disease.* Vasc Med, 2006. **11**(1): p. 21-8.
39. Aboyans, V., et al., *Editor's Choice - 2017 ESC Guidelines on the Diagnosis and Treatment of Peripheral Arterial Diseases, in collaboration with the European*

Society for Vascular Surgery (ESVS). Eur J Vasc Endovasc Surg, 2018. **55**(3): p. 305-368.
40. Poredos, P. and M.K. Jezovnik, *Do the Effects of Secondary Prevention of Cardiovascular Events in PAD Patients Differ from Other Atherosclerotic Disease?* International journal of molecular sciences, 2015. **16**(7): p. 14477-14489.
41. Golledge, J., et al., *Meta-analysis of clinical trials examining the benefit of structured home exercise in patients with peripheral artery disease.* Br J Surg, 2019. **106**(4): p. 319-331.
42. Fokkenrood, H.J., et al., *Supervised exercise therapy versus non-supervised exercise therapy for intermittent claudication.* Cochrane Database Syst Rev, 2013(8): p. Cd005263.
43. Dawson, D.L., et al., *A comparison of cilostazol and pentoxifylline for treating intermittent claudication.* Am J Med, 2000. **109**(7): p. 523-30.
44. Hiatt, W.R., S.R. Money, and E.P. Brass, *Long-term safety of cilostazol in patients with peripheral artery disease: the CASTLE study (Cilostazol: A Study in Long-term Effects).* J Vasc Surg, 2008. **47**(2): p. 330-336.
45. Brass, E.P., *Intermittent claudication: new targets for drug development.* Drugs, 2013. **73**(10): p. 999-1014.
46. Krishna, S.M., S.M. Omer, and J. Golledge, *Evaluation of the clinical relevance and limitations of current pre-clinical models of peripheral artery disease.* Clin Sci (Lond), 2016. **130**(3): p. 127-50.
47. Niiyama, H., et al., *Murine model of hindlimb ischemia.* Journal of visualized experiments : JoVE, 2009(23): p. 1035.
48. Shireman, P.K. and M.P. Quinones, *Differential necrosis despite similar perfusion in mouse strains after ischemia.* J Surg Res, 2005. **129**(2): p. 242-50.
49. Suhara, M., et al., *Targeting ability of self-assembled nanomedicines in rat acute limb ischemia model is affected by size.* J Control Release, 2018. **286**: p. 394-401.
50. Goto, T., et al., *Search for appropriate experimental methods to create stable hind-limb ischemia in mouse.* Tokai J Exp Clin Med, 2006. **31**(3): p. 128-32.
51. Cen, Y., et al., *Denervation in Femoral Artery-Ligated Hindlimbs Diminishes Ischemic Recovery Primarily via Impaired Arteriogenesis.* PloS one, 2016. **11**(5): p. e0154941-e0154941.
52. Scholz, D., et al., *Contribution of Arteriogenesis and Angiogenesis to Postocclusive Hindlimb Perfusion in Mice.* J Mol Cell Cardiol, 2002. **34**(7): p. 775-787.
53. Chalothorn, D., et al., *Collateral density, remodeling, and VEGF-A expression differ widely between mouse strains.* Physiol Genomics, 2007. **30**(2): p. 179-91.
54. Westvik, T.S., et al., *Limb ischemia after iliac ligation in aged mice stimulates angiogenesis without arteriogenesis.* J Vasc Surg, 2009. **49**(2): p. 464-473.
55. McClung, J.M., et al., *Subacute limb ischemia induces skeletal muscle injury in genetically susceptible mice independent of vascular density.* J Vasc Surg, 2016. **64**(4): p. 1101-1111.e2.
56. Padgett, M.E., et al., *Methods for Acute and Subacute Murine Hindlimb Ischemia.* J Vis Exp, 2016(112).
57. Tang, G.L., et al., *The effect of gradual or acute arterial occlusion on skeletal muscle blood flow, arteriogenesis, and inflammation in rat hindlimb ischemia.* J Vasc Surg, 2005. **41**(2): p. 312-20.
58. Yang, Y., et al., *Cellular and molecular mechanism regulating blood flow recovery in acute versus gradual femoral artery occlusion are distinct in the mouse.* J Vasc Surg, 2008. **48**(6): p. 1546-1558.

59. Krishna, S.M., et al., *Development of a two-stage lower limb ischemia mouse model to better simulate human peripheral artery disease.* Sci Rep (In Press), 2020.
60. Sumi, M., et al., *Quercetin glucosides promote ischemia-induced angiogenesis, but do not promote tumor growth.* Life Sci, 2013. **93**(22): p. 814-9.
61. Park, B., et al., *Endothelial nitric oxide synthase affects both early and late collateral arterial adaptation and blood flow recovery after induction of hind limb ischemia in mice.* Journal of vascular surgery, 2010. **51**(1): p. 165-173.
62. Yu, J., et al., *Endothelial nitric oxide synthase is critical for ischemic remodeling, mural cell recruitment, and blood flow reserve.* Proceedings of the National Academy of Sciences, 2005. **102**(31): p. 10999-11004.
63. Wahlberg, E., *Angiogenesis and arteriogenesis in limb ischemia.* Journal of vascular surgery, 2003. **38**(1): p. 198-203.
64. Murrant, C.L., *Structural and functional limitations of the collateral circulation in peripheral artery disease.* The Journal of physiology, 2008. **586**(24): p. 5845-5845.
65. Shireman, P.K. and M.P. Quinones, *Differential Necrosis Despite Similar Perfusion in Mouse Strains after Ischemia1.* Journal of Surgical Research, 2005. **129**(2): p. 242-250.
66. Kuivaniemi, H., et al., *Understanding the pathogenesis of abdominal aortic aneurysms.* Expert review of cardiovascular therapy, 2015. **13**(9): p. 975-987.
67. Thompson, R.W. and W.C. Parks, *Role of matrix metalloproteinases in abdominal aortic aneurysms.* Ann N Y Acad Sci, 1996. **800**: p. 157-74.
68. Carmeliet, P., et al., *Urokinase-generated plasmin activates matrix metalloproteinases during aneurysm formation.* Nat Genet, 1997. **17**(4): p. 439-44.
69. Moran, C.S., J.H. Campbell, and G.R. Campbell, *Induction of smooth muscle cell nitric oxide synthase by human leukaemia inhibitory factor: effects in vitro and in vivo.* J Vasc Res, 1997. **34**(5): p. 378-85.
70. Liao, S., et al., *Accelerated replicative senescence of medial smooth muscle cells derived from abdominal aortic aneurysms compared to the adjacent inferior mesenteric artery.* J Surg Res, 2000. **92**(1): p. 85-95.
71. Lopez-Candales, A., et al., *Decreased vascular smooth muscle cell density in medial degeneration of human abdominal aortic aneurysms.* Am J Pathol, 1997. **150**(3): p. 993-1007.
72. Vorp, D.A., et al., *Association of intraluminal thrombus in abdominal aortic aneurysm with local hypoxia and wall weakening.* J Vasc Surg, 2001. **34**(2): p. 291-9.
73. Behr-Rasmussen, C., et al., *Mural thrombus and the progression of abdominal aortic aneurysms: a large population-based prospective cohort study.* Eur J Vasc Endovasc Surg, 2014. **48**(3): p. 301-7.
74. Martufi, G., et al., *Local Quantification of Wall Thickness and Intraluminal Thrombus Offer Insight into the Mechanical Properties of the Aneurysmal Aorta.* Ann Biomed Eng, 2015. **43**(8): p. 1759-71.
75. Haller, S.J., et al., *Intraluminal thrombus is associated with early rupture of abdominal aortic aneurysm.* J Vasc Surg, 2018. **67**(4): p. 1051-1058.e1.
76. Vorp, D.A., et al., *Association of intraluminal thrombus in abdominal aortic aneurysm with local hypoxia and wall weakening.* Journal of Vascular Surgery, 2001. **34**(2): p. 291-299.
77. Campbell, E.J. and M.S. Wald, *Hypoxic injury to human alveolar macrophages accelerates release of previously bound neutrophil elastase: implications for lung connective tissue injury including pulmonary emphysema.* American Review of Respiratory Disease, 1983. **127**(5): p. 631-635.

78. Golledge, J., *Abdominal aortic aneurysm: update on pathogenesis and medical treatments.* Nat Rev Cardiol, 2019. **16**(4): p. 225-242.
79. Jackson, R.S., D.C. Chang, and J.A. Freischlag, *Comparison of long-term survival after open vs endovascular repair of intact abdominal aortic aneurysm among Medicare beneficiaries.* JAMA, 2012. **307**(15): p. 1621-1628.
80. Greenhalgh, R.M., *Comparison of endovascular aneurysm repair with open repair in patients with abdominal aortic aneurysm (EVAR trial 1), 30-day operative mortality results: randomised controlled trial.* The Lancet. **364**(9437): p. 843-848.
81. van Marrewijk, C., et al., *Significance of endoleaks after endovascular repair of abdominal aortic aneurysms: the EUROSTAR experience.* Journal of vascular surgery, 2002. **35**(3): p. 461-473.
82. Daugherty, A., M.W. Manning, and L.A. Cassis, *Angiotensin II promotes atherosclerotic lesions and aneurysms in apolipoprotein E–deficient mice.* The Journal of clinical investigation, 2000. **105**(11): p. 1605-1612.
83. Al-Thani, H. and A. El-Menyar, *Abdominal aortic aneurysms and coronary artery disease in a small country with high cardiovascular burden.* ISRN cardiology, 2014. **2014**: p. 825461-825461.
84. Trachet, B., et al., *Angiotensin II infusion into ApoE-/- mice: a model for aortic dissection rather than abdominal aortic aneurysm?* Cardiovasc Res, 2017. **113**(10): p. 1230-1242.
85. Rateri, D.L., et al., *Prolonged infusion of angiotensin II in apoE(-/-) mice promotes macrophage recruitment with continued expansion of abdominal aortic aneurysm.* Am J Pathol, 2011. **179**(3): p. 1542-8.
86. Daugherty, A., et al., *Angiotensin II infusion promotes ascending aortic aneurysms: attenuation by CCR2 deficiency in apoE-/- mice.* Clinical science, 2010. **118**(11): p. 681-689.
87. Azuma, J., et al., *Creation of murine experimental abdominal aortic aneurysms with elastase.* Journal of visualized experiments : JoVE, 2009(29): p. 1280.
88. Bartoli, M.A., et al., *In Vivo Assessment of Murine Elastase-induced Abdominal Aortic Aneurysm with High Resolution Magnetic Resonance Imaging.* European Journal of Vascular and Endovascular Surgery, 2012. **44**(5): p. 475-481.
89. Busch, A., et al., *Four Surgical Modifications to the Classic Elastase Perfusion Aneurysm Model Enable Haemodynamic Alterations and Extended Elastase Perfusion.* European Journal of Vascular and Endovascular Surgery, 2018. **56**(1): p. 102-109.
90. Yamanouchi, D., et al., *Accelerated aneurysmal dilation associated with apoptosis and inflammation in a newly developed calcium phosphate rodent abdominal aortic aneurysm model.* Journal of Vascular Surgery, 2012. **56**(2): p. 455-461.
91. Bhamidipati, C.M., et al., *Development of a novel murine model of aortic aneurysms using peri-adventitial elastase.* Surgery, 2012. **152**(2): p. 238-246.
92. Wang, Y., S. Krishna, and J. Golledge, *The calcium chloride-induced rodent model of abdominal aortic aneurysm.* Atherosclerosis, 2013. **226**(1): p. 29-39.
93. Lu, G., et al., *A novel chronic advanced stage abdominal aortic aneurysm murine model.* J Vasc Surg, 2017. **66**(1): p. 232-242.e4.
94. Piechota-Polanczyk, A., et al., *The Abdominal Aortic Aneurysm and Intraluminal Thrombus: Current Concepts of Development and Treatment.* Frontiers in cardiovascular medicine, 2015. **2**: p. 19-19.
95. Bergoeing, M.P., et al., *Cigarette smoking increases aortic dilatation without affecting matrix metalloproteinase-9 and -12 expression in a modified mouse model of aneurysm formation.* J Vasc Surg, 2007. **45**(6): p. 1217-1227.

96. Campa, J.S., R.M. Greenhalgh, and J.T. Powell, *Elastin degradation in abdominal aortic aneurysms.* Atherosclerosis, 1987. **65**(1-2): p. 13-21.
97. Busch, A., et al., *Extra-and intraluminal elastase induce morphologically distinct abdominal aortic aneurysms in mice and thus represent specific subtypes of human disease.* Journal of vascular research, 2016. **53**(1-2): p. 49-57.
98. Longo, G.M., et al., *MMP-12 has a role in abdominal aortic aneurysms in mice.* Surgery, 2005. **137**(4): p. 457-62.
99. Xiong, W., et al., *Membrane-type 1 matrix metalloproteinase regulates macrophage-dependent elastolytic activity and aneurysm formation in vivo.* J Biol Chem, 2009. **284**(3): p. 1765-71.
100. Watanabe, K., et al., *Group X secretory PLA2 in neutrophils plays a pathogenic role in abdominal aortic aneurysms in mice.* Am J Physiol Heart Circ Physiol, 2012. **302**(1): p. H95-104.
101. Longo, G.M., et al., *Matrix metalloproteinases 2 and 9 work in concert to produce aortic aneurysms.* J Clin Invest, 2002. **110**(5): p. 625-32.
102. Carrell, T., A. Smith, and K. Burnand, *Experimental techniques and models in the study of the development and treatment of abdominal aortic aneurysm.* British journal of surgery, 1999. **86**(3): p. 305-312.
103. Oakes, J.M., et al., *Nicotine and the renin-angiotensin system.* Am J Physiol Regul Integr Comp Physiol, 2018. **315**(5): p. R895-r906.
104. Busse, L.W., et al., *The effect of angiotensin II on blood pressure in patients with circulatory shock: a structured review of the literature.* Crit Care, 2017. **21**(1): p. 324.
105. Kristensen, K.E., et al., *Angiotensin-converting enzyme inhibitors and angiotensin II receptor blockers in patients with abdominal aortic aneurysms: nation-wide cohort study.* Arterioscler Thromb Vasc Biol, 2015. **35**(3): p. 733-40.
106. Ren, W., et al., *beta-Aminopropionitrile monofumarate induces thoracic aortic dissection in C57BL/6 mice.* Sci Rep, 2016. **6**: p. 28149.
107. Gao, Y.X., et al., *[Establishment of beta-aminopropionitrile-induced aortic dissection model in C57Bl/6J mice].* Zhonghua Xin Xue Guan Bing Za Zhi, 2018. **46**(2): p. 137-142.
108. Meijer, C.A., et al., *Doxycycline for stabilization of abdominal aortic aneurysms: a randomized trial.* Ann Intern Med, 2013. **159**(12): p. 815-23.
109. Koga, J., T. Matoba, and K. Egashira, *Anti-inflammatory Nanoparticle for Prevention of Atherosclerotic Vascular Diseases.* J Atheroscler Thromb, 2016. **23**(7): p. 757-65.
110. Zhang, M.J., et al., *Resolvin D2 Enhances Postischemic Revascularization While Resolving Inflammation.* Circulation, 2016. **134**(9): p. 666-680.
111. Shaikh, I.A., et al., *Overexpression of Thioredoxin1 enhances functional recovery in a mouse model of hind limb ischemia.* J Surg Res, 2017. **216**: p. 158-168.
112. Hsieh, K.F., et al., *Arginine administration increases circulating endothelial progenitor cells and attenuates tissue injury in a mouse model of hind limb ischemia/reperfusion.* Nutrition, 2018. **55-56**: p. 29-35.
113. Dai, X., et al., *Sitagliptin-mediated preservation of endothelial progenitor cell function via augmenting autophagy enhances ischaemic angiogenesis in diabetes.* J Cell Mol Med, 2018. **22**(1): p. 89-100.
114. Valatsou, A., et al., *Beneficial Effects of Sildenafil on Tissue Perfusion and Inflammation in a Murine Model of Limb Ischemia and Atherosclerosis.* Curr Vasc Pharmacol, 2017. **15**(3): p. 282-287.
115. Lachmann, N. and S. Nikol, *Therapeutic angiogenesis for peripheral artery disease: stem cell therapy.* Vasa, 2007. **36**(4): p. 241-51.

116. Zhu, Q., et al., *Extracellular Vesicles Secreted by Human Urine-Derived Stem Cells Promote Ischemia Repair in a Mouse Model of Hind-Limb Ischemia.* Cell Physiol Biochem, 2018. **47**(3): p. 1181-1192.
117. Ju, C., et al., *Transplantation of Cardiac Mesenchymal Stem Cell-Derived Exosomes for Angiogenesis.* J Cardiovasc Transl Res, 2018. **11**(5): p. 429-437.
118. Ghoshal, S. and C.D. Loftin, *Cyclooxygenase-2 inhibition attenuates abdominal aortic aneurysm progression in hyperlipidemic mice.* PLoS One, 2012. **7**(11): p. e44369.
119. Kristo, F., et al., *Pharmacological inhibition of BLT1 diminishes early abdominal aneurysm formation.* Atherosclerosis, 2010. **210**(1): p. 107-13.
120. Moran, C.S., et al., *Resveratrol Inhibits Growth of Experimental Abdominal Aortic Aneurysm Associated With Upregulation of Angiotensin-Converting Enzyme 2.* Arterioscler Thromb Vasc Biol, 2017. **37**(11): p. 2195-2203.
121. Moran, C.S., et al., *Modulation of Kinin B2 Receptor Signaling Controls Aortic Dilatation and Rupture in the Angiotensin II-Infused Apolipoprotein E-Deficient Mouse.* Arterioscler Thromb Vasc Biol, 2016. **36**(5): p. 898-907.
122. Rouer, M., et al., *Rapamycin limits the growth of established experimental abdominal aortic aneurysms.* Eur J Vasc Endovasc Surg, 2014. **47**(5): p. 493-500.
123. Yoshimura, K., et al., *Regression of abdominal aortic aneurysm by inhibition of c-Jun N-terminal kinase in mice.* Ann N Y Acad Sci, 2006. **1085**: p. 74-81.
124. Huang, X.F., et al., *Ginkgo biloba extracts prevent aortic rupture in angiotensin II-infused hypercholesterolemic mice.* Acta Pharmacol Sin, 2019. **40**(2): p. 192-198.
125. Lai, C.H., et al., *Recombinant adeno-associated virus vector carrying the thrombomodulin lectin-like domain for the treatment of abdominal aortic aneurysm.* Atherosclerosis, 2017. **262**: p. 62-70.
126. Moran, C.S., et al., *Parenteral administration of factor Xa/IIa inhibitors limits experimental aortic aneurysm and atherosclerosis.* Sci Rep, 2017. **7**: p. 43079.
127. Owens, A.P., 3rd, et al., *Platelet Inhibitors Reduce Rupture in a Mouse Model of Established Abdominal Aortic Aneurysm.* Arterioscler Thromb Vasc Biol, 2015. **35**(9): p. 2032-2041.
128. Lai, C.H., et al., *Targeting vascular smooth muscle cell dysfunction with xanthine derivative KMUP-3 inhibits abdominal aortic aneurysm in mice.* Atherosclerosis, 2020. **297**: p. 16-24.
129. Park, S.M., et al., *Comparison of Efficacy between Ramipril and Carvedilol on Limiting the Expansion of Abdominal Aortic Aneurysm in Mouse Model.* J Cardiovasc Pharmacol Ther, 2018: p. 1074248418798631.
130. Seto, S.W., et al., *Aliskiren limits abdominal aortic aneurysm, ventricular hypertrophy and atherosclerosis in an apolipoprotein-E-deficient mouse model.* Clin Sci (Lond), 2014. **127**(2): p. 123-34.
131. Police, S.B., et al., *Weight loss in obese C57BL/6 mice limits adventitial expansion of established angiotensin II-induced abdominal aortic aneurysms.* Am J Physiol Heart Circ Physiol, 2010. **298**(6): p. H1932-8.
132. Bridge, K., et al., *Inhibition of plasmin-mediated TAFI activation may affect development but not progression of abdominal aortic aneurysms.* PLoS One, 2017. **12**(5): p. e0177117.
133. Li, G., et al., *Ulinastatin Inhibits the Formation and Progression of Experimental Abdominal Aortic Aneurysms.* J Vasc Res, 2020. **57**(2): p. 58-64.
134. Xie, X., et al., *Doxycycline does not influence established abdominal aortic aneurysms in angiotensin II-infused mice.* PLoS One, 2012. **7**(9): p. e46411.

135. Fu, X.M., et al., *Intravenous administration of mesenchymal stem cells prevents angiotensin II-induced aortic aneurysm formation in apolipoprotein E-deficient mouse.* J Transl Med, 2013. **11**: p. 175.
136. Yamawaki-Ogata, A., et al., *Therapeutic potential of bone marrow-derived mesenchymal stem cells in formed aortic aneurysms of a mouse model.* Eur J Cardiothorac Surg, 2014. **45**(5): p. e156-65.
137. Yamawaki-Ogata, A., et al., *Bone marrow-derived mesenchymal stromal cells regress aortic aneurysm via the NF-kB, Smad3 and Akt signaling pathways.* Cytotherapy, 2017. **19**(10): p. 1167-1175.
138. Blose, K.J., et al., *Periadventitial adipose-derived stem cell treatment halts elastase-induced abdominal aortic aneurysm progression.* Regen Med, 2014. **9**(6): p. 733-41.
139. Yoshimura, K., et al., *Current Status and Perspectives on Pharmacologic Therapy for Abdominal Aortic Aneurysm.* Current drug targets, 2018. **19**(11): p. 1265-1275.
140. Petrinec, D., et al., *Doxycycline inhibition of aneurysmal degeneration in an elastase-induced rat model of abdominal aortic aneurysm: preservation of aortic elastin associated with suppressed production of 92 kD gelatinase.* J Vasc Surg, 1996. **23**(2): p. 336-46.
141. Yu, M., et al., *Thermosensitive Hydrogel Containing Doxycycline Exerts Inhibitory Effects on Abdominal Aortic Aneurysm Induced By Pancreatic Elastase in Mice.* Adv Healthc Mater, 2017. **6**(22).
142. Mata, K.M., et al., *Interference of doxycycline pretreatment in a model of abdominal aortic aneurysms.* Cardiovasc Pathol, 2015. **24**(2): p. 110-20.
143. Manning, M.W., L.A. Cassis, and A. Daugherty, *Differential effects of doxycycline, a broad-spectrum matrix metalloproteinase inhibitor, on angiotensin II-induced atherosclerosis and abdominal aortic aneurysms.* Arterioscler Thromb Vasc Biol, 2003. **23**(3): p. 483-8.
144. Xiong, F., et al., *Inhibition of AAA in a rat model by treatment with ACEI perindopril.* J Surg Res, 2014. **189**(1): p. 166-73.
145. Phie, J., et al., *Flavonols reduce aortic atherosclerosis lesion area in apolipoprotein E deficient mice: A systematic review and meta-analysis.* PLoS One, 2017. **12**(7): p. e0181832.
146. Kilkenny, C., et al., *Animal research: reporting in vivo experiments: the ARRIVE guidelines.* British journal of pharmacology, 2010. **160**(7): p. 1577-1579.
147. Leung, V., et al., *ARRIVE has not ARRIVEd: Support for the ARRIVE (Animal Research: Reporting of in vivo Experiments) guidelines does not improve the reporting quality of papers in animal welfare, analgesia or anesthesia.* PloS one, 2018. **13**(5): p. e0197882.
148. Garelnabi, M., H. Mahini, and T. Wilson, *Quercetin intake with exercise modulates lipoprotein metabolism and reduces atherosclerosis plaque formation.* J Int Soc Sports Nutr, 2014. **11**: p. 22.
149. Filho, A.W., et al., *Quercetin: further investigation of its antinociceptive properties and mechanisms of action.* Arch Pharm Res, 2008. **31**(6): p. 713-21.
150. Davis, J.M., et al., *The dietary flavonoid quercetin increases VO(2max) and endurance capacity.* Int J Sport Nutr Exerc Metab, 2010. **20**(1): p. 56-62.
151. Azevedo, M.I., et al., *The antioxidant effects of the flavonoids rutin and quercetin inhibit oxaliplatin-induced chronic painful peripheral neuropathy.* Mol Pain, 2013. **9**: p. 53.
152. Crozier, A., et al., *Quantitative analysis of the flavonoid content of commercial tomatoes, onions, lettuce, and celery.* Journal of Agricultural and Food Chemistry, 1997. **45**(3): p. 590-595.

153. Ruiz-Canela, M., et al., *Association of Mediterranean diet with peripheral artery disease: the PREDIMED randomized trial.* JAMA, 2014. **311**(4): p. 415-7.
154. Stewart, R.A., et al., *Dietary patterns and the risk of major adverse cardiovascular events in a global study of high-risk patients with stable coronary heart disease.* Eur Heart J, 2016. **37**(25): p. 1993-2001.
155. Hayek, T., et al., *Reduced progression of atherosclerosis in apolipoprotein E-deficient mice following consumption of red wine, or its polyphenols quercetin or catechin, is associated with reduced susceptibility of LDL to oxidation and aggregation.* Arteriosclerosis, Thrombosis & Vascular Biology, 1997. **17**(11): p. 2744-52.
156. Loke, W.M., et al., *Specific dietary polyphenols attenuate atherosclerosis in apolipoprotein E-knockout mice by alleviating inflammation and endothelial dysfunction.* Arteriosclerosis, Thrombosis & Vascular Biology, 2010. **30**(4): p. 749-57.
157. Kita, T., et al., *Role of oxidized LDL in atherosclerosis.* Ann N Y Acad Sci, 2001. **947**: p. 199-205; discussion 205-6.
158. Bentzon, J.F., et al., *Red wine does not reduce mature atherosclerosis in apolipoprotein E-deficient mice.* Circulation, 2001. **103**(12): p. 1681-7.
159. Motoyama, K., et al., *Atheroprotective and plaque-stabilizing effects of enzymatically modified isoquercitrin in atherogenic apoE-deficient mice.* Nutrition, 2009. **25**(4): p. 421-7.
160. Xiao, H.B., et al., *Kaempferol regulates OPN-CD44 pathway to inhibit the atherogenesis of apolipoprotein E deficient mice.* Toxicology & Applied Pharmacology, 2011. **257**(3): p. 405-11.
161. Krettek, A., et al., *Enhanced expression of CD44 variants in human atheroma and abdominal aortic aneurysm: possible role for a feedback loop in endothelial cells.* Am J Pathol, 2004. **165**(5): p. 1571-81.
162. Donnini, S., et al., *Divergent effects of quercetin conjugates on angiogenesis.* Br J Nutr, 2006. **95**(5): p. 1016-23.
163. Hardie, D.G., *Sensing of energy and nutrients by AMP-activated protein kinase.* Am J Clin Nutr, 2011. **93**(4): p. 891s-6.
164. Jackson, S.J. and R.C. Venema, *Quercetin inhibits eNOS, microtubule polymerization, and mitotic progression in bovine aortic endothelial cells.* J Nutr, 2006. **136**(5): p. 1178-84.
165. Kim, J.D., et al., *Chemical structure of flavonols in relation to modulation of angiogenesis and immune-endothelial cell adhesion.* J Nutr Biochem, 2006. **17**(3): p. 165-76.
166. Li, F., et al., *Quercetin inhibits vascular endothelial growth factor-induced choroidal and retinal angiogenesis in vitro.* Ophthalmic Res, 2015. **53**(3): p. 109-16.
167. Scoditti, E., et al., *Mediterranean diet polyphenols reduce inflammatory angiogenesis through MMP-9 and COX-2 inhibition in human vascular endothelial cells: a potentially protective mechanism in atherosclerotic vascular disease and cancer.* Arch Biochem Biophys, 2012. **527**(2): p. 81-9.
168. Shen, Y., et al., *Quercetin and its metabolites improve vessel function by inducing eNOS activity via phosphorylation of AMPK.* Biochem Pharmacol, 2012. **84**(8): p. 1036-44.
169. Wilson, W.J. and L. Poellinger, *The dietary flavonoid quercetin modulates HIF-1 alpha activity in endothelial cells.* Biochem Biophys Res Commun, 2002. **293**(1): p. 446-50.

170. Khoo, N.K., et al., *Activation of vascular endothelial nitric oxide synthase and heme oxygenase-1 expression by electrophilic nitro-fatty acids.* Free Radic Biol Med, 2010. **48**(2): p. 230-9.
171. Ziello, J.E., I.S. Jovin, and Y. Huang, *Hypoxia-Inducible Factor (HIF)-1 Regulatory Pathway and its Potential for Therapeutic Intervention in Malignancy and Ischemia.* The Yale Journal of Biology and Medicine, 2007. **80**(2): p. 51-60.
172. Hoeben, A., et al., *Vascular endothelial growth factor and angiogenesis.* Pharmacological reviews, 2004. **56**(4): p. 549-580.
173. Short, K.R., et al., *Impact of aerobic exercise training on age-related changes in insulin sensitivity and muscle oxidative capacity.* Diabetes, 2003. **52**(8): p. 1888-1896.
174. Davis, J.M., et al., *Quercetin increases brain and muscle mitochondrial biogenesis and exercise tolerance.* Am J Physiol Regul Integr Comp Physiol, 2009. **296**(4): p. R1071-7.
175. Mukai, R., et al., *Preventive effect of dietary quercetin on disuse muscle atrophy by targeting mitochondria in denervated mice.* J Nutr Biochem, 2016. **31**: p. 67-76.
176. Liu, P., et al., *Quercetin ameliorates hypobaric hypoxia-induced memory impairment through mitochondrial and neuron function adaptation via the PGC-1alpha pathway.* Restor Neurol Neurosci, 2015. **33**(2): p. 143-57.
177. Kim, C.S., et al., *Quercetin reduces obesity-induced hepatosteatosis by enhancing mitochondrial oxidative metabolism via heme oxygenase-1.* Nutr Metab (Lond), 2015. **12**: p. 33.
178. Rayamajhi, N., et al., *Quercetin induces mitochondrial biogenesis through activation of HO-1 in HepG2 cells.* Oxid Med Cell Longev, 2013. **2013**: p. 154279.
179. Jimenez, R., et al., *Quercetin and its metabolites inhibit the membrane NADPH oxidase activity in vascular smooth muscle cells from normotensive and spontaneously hypertensive rats.* Food Funct, 2015. **6**(2): p. 409-14.
180. Datla, S.R., et al., *Induction of heme oxygenase-1 in vivo suppresses NADPH oxidase derived oxidative stress.* Hypertension, 2007. **50**(4): p. 636-42.
181. Brevetti, G., et al., *Endothelial dysfunction in peripheral arterial disease is related to increase in plasma markers of inflammation and severity of peripheral circulatory impairment but not to classic risk factors and atherosclerotic burden.* J Vasc Surg, 2003. **38**(2): p. 374-9.
182. Brevetti, G., et al., *In concomitant coronary and peripheral arterial disease, inflammation of the affected limbs predicts coronary artery endothelial dysfunction.* Atherosclerosis, 2008. **201**(2): p. 440-6.
183. Henagan, T.M., et al., *Dietary quercetin supplementation in mice increases skeletal muscle PGC1alpha expression, improves mitochondrial function and attenuates insulin resistance in a time-specific manner.* PLoS One, 2014. **9**(2): p. e89365.
184. Liang, H. and W.F. Ward, *PGC-1alpha: a key regulator of energy metabolism.* Adv Physiol Educ, 2006. **30**(4): p. 145-51.
185. Kwon, S.M., et al., *Exercise, but not quercetin, ameliorates inflammation, mitochondrial biogenesis, and lipid metabolism in skeletal muscle after strenuous exercise by high-fat diet mice.* J Exerc Nutrition Biochem, 2014. **18**(1): p. 51-60.
186. Ruiz, L.M., et al., *Quercetin Affects Erythropoiesis and Heart Mitochondrial Function in Mice.* Oxid Med Cell Longev, 2015. **2015**: p. 836301.
187. Casuso, R.A., et al., *Oral quercetin supplementation hampers skeletal muscle adaptations in response to exercise training.* Scand J Med Sci Sports, 2014. **24**(6): p. 920-7.
188. Le, N.H., et al., *Quercetin protects against obesity-induced skeletal muscle inflammation and atrophy.* Mediators Inflamm, 2014. **2014**: p. 834294.

189. Casuso, R.A., et al., *The combination of oral quercetin supplementation and exercise prevents brain mitochondrial biogenesis.* Genes Nutr, 2014. **9**(5): p. 420.
190. Askari, G., et al., *Does quercetin and vitamin C improve exercise performance, muscle damage, and body composition in male athletes?* J Res Med Sci, 2012. **17**(4): p. 328-31.
191. Askari, G., et al., *The effects of quercetin supplementation on body composition, exercise performance and muscle damage indices in athletes.* Int J Prev Med, 2013. **4**(1): p. 21-6.
192. Nieman, D.C., et al., *Quercetin's influence on exercise performance and muscle mitochondrial biogenesis.* Med Sci Sports Exerc, 2010. **42**(2): p. 338-45.
193. Daneshvar, P., et al., *Effect of eight weeks of quercetin supplementation on exercise performance, muscle damage and body muscle in male badminton players.* Int J Prev Med, 2013. **4**(Suppl 1): p. S53-7.
194. Cureton, K.J., et al., *Dietary quercetin supplementation is not ergogenic in untrained men.* J Appl Physiol (1985), 2009. **107**(4): p. 1095-104.
195. Scholten, S.D., et al., *Effects of vitamin D and quercetin, alone and in combination, on cardiorespiratory fitness and muscle function in physically active male adults.* Open Access J Sports Med, 2015. **6**: p. 229-39.
196. Menshikova, E.V., et al., *Effects of exercise on mitochondrial content and function in aging human skeletal muscle.* The Journals of Gerontology Series A: Biological Sciences and Medical Sciences, 2006. **61**(6): p. 534-540.
197. Valerio, D.A., et al., *Quercetin reduces inflammatory pain: inhibition of oxidative stress and cytokine production.* J Nat Prod, 2009. **72**(11): p. 1975-9.
198. Civi, S., et al., *Effects of quercetin on chronic constriction nerve injury in an experimental rat model.* Acta Neurochir (Wien), 2016. **158**(5): p. 959-65.
199. Anjaneyulu, M. and K. Chopra, *Quercetin, a bioflavonoid, attenuates thermal hyperalgesia in a mouse model of diabetic neuropathic pain.* Prog Neuropsychopharmacol Biol Psychiatry, 2003. **27**(6): p. 1001-5.
200. Calixto-Campos, C., et al., *Quercetin reduces Ehrlich tumor-induced cancer pain in mice.* Anal Cell Pathol (Amst), 2015. **2015**: p. 285708.
201. Ren, K. and R. Torres, *Role of interleukin-1beta during pain and inflammation.* Brain Res Rev, 2009. **60**(1): p. 57-64.
202. Sauder, K.A., et al., *Pistachio nut consumption modifies systemic hemodynamics, increases heart rate variability, and reduces ambulatory blood pressure in well-controlled type 2 diabetes: a randomized trial.* J Am Heart Assoc, 2014. **3**(4).
203. West, S.G., et al., *Effects of diets high in walnuts and flax oil on hemodynamic responses to stress and vascular endothelial function.* J Am Coll Nutr, 2010. **29**(6): p. 595-603.
204. Jiang, R., et al., *Nut and seed consumption and inflammatory markers in the multi-ethnic study of atherosclerosis.* Am J Epidemiol, 2006. **163**(3): p. 222-31.
205. Wu, L., et al., *Walnut-enriched diet reduces fasting non-HDL-cholesterol and apolipoprotein B in healthy Caucasian subjects: a randomized controlled cross-over clinical trial.* Metabolism, 2014. **63**(3): p. 382-91.
206. Bolling, B.W., et al., *Tree nut phytochemicals: composition, antioxidant capacity, bioactivity, impact factors. A systematic review of almonds, Brazils, cashews, hazelnuts, macadamias, pecans, pine nuts, pistachios and walnuts.* Nutrition research reviews, 2011. **24**(02): p. 244-275.
207. Kornsteiner, M., K.-H. Wagner, and I. Elmadfa, *Tocopherols and total phenolics in 10 different nut types.* Food Chemistry, 2006. **98**(2): p. 381-387.

208. Ros, E. and J. Mataix, *Fatty acid composition of nuts--implications for cardiovascular health.* Br J Nutr, 2006. **96 Suppl 2**: p. S29-35.
209. Kornsteiner-Krenn, M., K.-H. Wagner, and I. Elmadfa, *Phytosterol content and fatty acid pattern of ten different nut types.* Int J Vitam Nutr Res, 2013. **83**(5): p. 263-270.
210. Grundy, S.M., *Comparison of monounsaturated fatty acids and carbohydrates for lowering plasma cholesterol.* New England Journal of Medicine, 1986. **314**(12): p. 745-748.
211. Mensink, R. and M. Katan, *Effect of monounsaturated fatty acids versus complex carbohydrates on high-density lipoproteins in healthy men and women.* The Lancet, 1987. **329**(8525): p. 122-125.
212. Calder, P.C., *n− 3 polyunsaturated fatty acids, inflammation, and inflammatory diseases.* The American journal of clinical nutrition, 2006. **83**(6): p. S1505-1519S.
213. Siscovick, D.S., et al., *Dietary intake and cell membrane levels of long-chain n-3 polyunsaturated fatty acids and the risk of primary cardiac arrest.* Jama, 1995. **274**(17): p. 1363-1367.
214. Yoshihara, T., et al., *Omega 3 Polyunsaturated Fatty Acids Suppress the Development of Aortic Aneurysms Through the Inhibition of Macrophage-Mediated Inflammation.* Circ J, 2015. **79**(7): p. 1470-8.
215. Meyer, B.J., *Australians are not Meeting the Recommended Intakes for Omega-3 Long Chain Polyunsaturated Fatty Acids: Results of an Analysis from the 2011-2012 National Nutrition and Physical Activity Survey.* Nutrients, 2016. **8**(3): p. 111.
216. Wang, L., et al., *Quercetin, a flavonoid with anti-inflammatory activity, suppresses the development of abdominal aortic aneurysms in mice.* Eur J Pharmacol, 2012. **690**(1-3): p. 133-41.
217. Strittmatter, S.M., *Overcoming drug development bottlenecks with repurposing: old drugs learn new tricks.* Nature medicine, 2014. **20**(6): p. 590-591.
218. Solomon, D.H., et al., *Effects of colchicine on risk of cardiovascular events and mortality among patients with gout: a cohort study using electronic medical records linked with Medicare claims.* Ann Rheum Dis, 2016. **75**(9): p. 1674-9.
219. Demidowich, A.P., et al., *Colchicine to decrease NLRP3-activated inflammation and improve obesity-related metabolic dysregulation.* Medical hypotheses, 2016. **92**: p. 67-73.
220. Hemkens, L.G., et al., *Colchicine for prevention of cardiovascular events.* Cochrane Database Syst Rev, 2016(1): p. Cd011047.
221. Sun, W., et al., *Macrophage inflammasome mediates hyperhomocysteinemia-aggravated abdominal aortic aneurysm.* J Mol Cell Cardiol, 2015. **81**: p. 96-106.
222. Latz, E., T.S. Xiao, and A. Stutz, *Activation and regulation of the inflammasomes.* Nature reviews. Immunology, 2013. **13**(6): p. 397-411.
223. van de Veerdonk, F.L., et al., *Inflammasome activation and IL-1beta and IL-18 processing during infection.* Trends Immunol, 2011. **32**(3): p. 110-6.
224. Alvarez, S. and M.A. Munoz-Fernandez, *TNF-Alpha may mediate inflammasome activation in the absence of bacterial infection in more than one way.* PLoS One, 2013. **8**(8): p. e71477.
225. Eigenbrod, T., K.A. Bode, and A.H. Dalpke, *Early inhibition of IL-1beta expression by IFN-gamma is mediated by impaired binding of NF-kappaB to the IL-1beta promoter but is independent of nitric oxide.* J Immunol, 2013. **190**(12): p. 6533-41.
226. Kopitar-Jerala, N., *The Role of Interferons in Inflammation and Inflammasome Activation.* Frontiers in immunology, 2017. **8**: p. 873-873.

227. Usui, F., et al., *Inflammasome activation by mitochondrial oxidative stress in macrophages leads to the development of angiotensin II-induced aortic aneurysm.* Arterioscler Thromb Vasc Biol, 2015. **35**(1): p. 127-36.
228. Gonzalez-Hidalgo, C., et al., *Differential mRNA expression of inflammasome genes NLRP1 and NLRP3 in abdominal aneurysmal and occlusive aortic disease.* Ther Adv Cardiovasc Dis, 2018. **12**(4): p. 123-129.
229. Wu, D., et al., *NLRP3 (Nucleotide Oligomerization Domain-Like Receptor Family, Pyrin Domain Containing 3)-Caspase-1 Inflammasome Degrades Contractile Proteins: Implications for Aortic Biomechanical Dysfunction and Aneurysm and Dissection Formation.* Arterioscler Thromb Vasc Biol, 2017. **37**(4): p. 694-706.
230. Qiao, J., et al., *NLRP3 regulates platelet integrin alphaIIbbeta3 outside-in signaling, hemostasis and arterial thrombosis.* Haematologica, 2018. **103**(9): p. 1568-1576.
231. Cohen, A.B., et al., *A controlled trial of colchicine to reduce the elastase load in the lungs of ex-cigarette smokers with chronic obstructive pulmonary disease.* Am Rev Respir Dis, 1991. **143**(5 Pt 1): p. 1038-43.
232. Ercolani, L. and W.E. Schulte, *Metabolic and morphologic effects of colchicine on human T-lymphocyte expression of Fcμ, and Fcγ receptors.* Cellular Immunology, 1983. **77**(2): p. 222-232.
233. Perico, N., et al., *Colchicine interferes with L-selectin and leukocyte function-associated antigen-1 expression on human T lymphocytes and inhibits T cell activation.* J Am Soc Nephrol, 1996. **7**(4): p. 594-601.
234. Cronstein, B.N., et al., *Colchicine alters the quantitative and qualitative display of selectins on endothelial cells and neutrophils.* J Clin Invest, 1995. **96**(2): p. 994-1002.
235. Sheward, W.J., et al., *Circadian control of mouse heart rate and blood pressure by the suprachiasmatic nuclei: behavioral effects are more significant than direct outputs.* PloS one, 2010. **5**(3): p. e9783.
236. Hudthagosol, C., et al., *Pecans Acutely Increase Plasma Postprandial Antioxidant Capacity and Catechins and Decrease LDL Oxidation in Humans–3.* The Journal of nutrition, 2010. **141**(1): p. 56-62.
237. Nakayama, H., et al., *Chronic intake of onion extract containing quercetin improved postprandial endothelial dysfunction in healthy men.* J Am Coll Nutr, 2013. **32**(3): p. 160-4.
238. Krishna, S.M., et al. *Anionic nanoliposomes reduced atherosclerosis progression in Low Density Lipoprotein Receptor (LDLR) deficient mice fed a high fat diet*. J Cell Physiol, 2018.
239. Fink, G.D., *Does Tail-Cuff Plethysmography Provide a Reliable Estimate of Central Blood Pressure in Mice?* Journal of the American Heart Association, 2017. **6**(6): p. e006554.
240. WHO. *Cardiovascular Diseases*. 2015 [cited 2016 accessed 20 June 2018]; Available from: http://www.who.int/mediacentre/factsheets/fs317/en/.
241. Farnier, M. and J. Davignon, *Current and future treatment of hyperlipidemia: the role of statins.* The American Journal of Cardiology, 1998. **82**(4, Supplement 2): p. 3J-10J.
242. Law, M., J. Morris, and N. Wald, *Use of blood pressure lowering drugs in the prevention of cardiovascular disease: meta-analysis of 147 randomised trials in the context of expectations from prospective epidemiological studies.* Bmj, 2009. **338**: p. b1665.
243. Schömig, A., et al., *A randomized comparison of antiplatelet and anticoagulant therapy after the placement of coronary-artery stents.* New England Journal of Medicine, 1996. **334**(17): p. 1084-1089.

244. Hu, F.B. and W.C. Willett, *Optimal diets for prevention of coronary heart disease.* Jama, 2002. **288**(20): p. 2569-78.
245. Katcher, H.I., et al., *The effects of a whole grain–enriched hypocaloric diet on cardiovascular disease risk factors in men and women with metabolic syndrome.* The American journal of clinical nutrition, 2008. **87**(1): p. 79-90.
246. Keys, A., et al., *The diet and 15-year death rate in the seven countries study.* American journal of epidemiology, 1986. **124**(6): p. 903-915.
247. Vincent-Baudry, S., et al., *The Medi-RIVAGE study: reduction of cardiovascular disease risk factors after a 3-mo intervention with a Mediterranean-type diet or a low-fat diet.* The American journal of clinical nutrition, 2005. **82**(5): p. 964-971.
248. Estruch, R., et al., *Primary prevention of cardiovascular disease with a Mediterranean diet.* New England Journal of Medicine, 2013. **368**(14): p. 1279-1290.
249. Ramirez-Tortosa, M.C., et al., *Extra-virgin olive oil increases the resistance of LDL to oxidation more than refined olive oil in free-living men with peripheral vascular disease.* Journal of Nutrition, 1999. **129**(12): p. 2177-83.
250. Harnly, J.M., et al., *Flavonoid content of US fruits, vegetables, and nuts.* Journal of agricultural and food chemistry, 2006. **54**(26): p. 9966-9977.
251. King, A.M.Y. and G. Young, *Characteristics and Occurrence of Phenolic Phytochemicals.* Journal of the American Dietetic Association, 1999. **99**(2): p. 213-218.
252. Cook, N.C. and S. Samman, *Flavonoids—Chemistry, metabolism, cardioprotective effects, and dietary sources.* The Journal of Nutritional Biochemistry, 1996. **7**(2): p. 66-76.
253. Hooper, L., et al., *Flavonoids, flavonoid-rich foods, and cardiovascular risk: a meta-analysis of randomized controlled trials.* Am J Clin Nutr, 2008. **88**(1): p. 38-50.
254. Belinky, P.A., et al., *The antioxidative effects of the isoflavan glabridin on endogenous constituents of LDL during its oxidation.* Atherosclerosis, 1998. **137**(1): p. 49-61.
255. Lai, M.Y., et al., *Comparison of metabolic pharmacokinetics of baicalin and baicalein in rats.* The Journal of Pharmacy and Pharmacology, 2003. **55**(2): p. 205-9.
256. Makino, T., et al., *Enzymatically modified isoquercitrin, alpha-oligoglucosyl quercetin 3-O-glucoside, is absorbed more easily than other quercetin glycosides or aglycone after oral administration in rats.* Biol Pharm Bull, 2009. **32**(12): p. 2034-40.
257. de Pascual-Teresa, S., D.A. Moreno, and C. García-Viguera, *Flavanols and anthocyanins in cardiovascular health: a review of current evidence.* International journal of molecular sciences, 2010. **11**(4): p. 1679-1703.
258. Meir, K.S. and E. Leitersdorf, *Atherosclerosis in the Apolipoprotein E–Deficient Mouse A Decade of Progress.* Arteriosclerosis, thrombosis, and vascular biology, 2004. **24**(6): p. 1006-1014.
259. Nakashima, Y., et al., *ApoE-deficient mice develop lesions of all phases of atherosclerosis throughout the arterial tree.* Arteriosclerosis, thrombosis, and vascular biology, 1994. **14**(1): p. 133-140.
260. Cherubini, A., et al., *Role of antioxidants in atherosclerosis: epidemiological and clinical update.* Curr Pharm Des, 2005. **11**(16): p. 2017-32.
261. Corti, R., et al., *Effects of lipid-lowering by simvastatin on human atherosclerotic lesions a longitudinal study by high-resolution, noninvasive magnetic resonance imaging.* Circulation, 2001. **104**(3): p. 249-252.
262. Zeng, P., et al., *Apigenin Attenuates Atherogenesis through Inducing Macrophage Apoptosis via Inhibition of AKT Ser473 Phosphorylation and Downregulation of Plasminogen Activator Inhibitor-2.* Oxid Med Cell Longev, 2015. **2015**: p. 379538.

263. Liao, P., et al., *Baicalin and geniposide attenuate atherosclerosis involving lipids regulation and immunoregulation in ApoE-/- mice.* European Journal of Pharmacology, 2014. **740**: p. 488-95.
264. Auclair, S., et al., *Catechin reduces atherosclerotic lesion development in apo E-deficient mice: a transcriptomic study.* Atherosclerosis, 2009. **204**(2): p. e21-7.
265. Rosenblat, M., et al., *Macrophage enrichment with the isoflavan glabridin inhibits NADPH oxidase-induced cell-mediated oxidation of low density lipoprotein. A possible role for protein kinase C.* Journal of Biological Chemistry, 1999. **274**(20): p. 13790-9.
266. Shen, Y., et al., *Dietary quercetin attenuates oxidant-induced endothelial dysfunction and atherosclerosis in apolipoprotein E knockout mice fed a high-fat diet: a critical role for heme oxygenase-1.* Free Radical Biology & Medicine, 2013. **65**: p. 908-15.
267. Lin, W., et al., *Quercetin protects against atherosclerosis by inhibiting dendritic cell activation.* Mol Nutr Food Res, 2017.
268. Omer, S.M., et al., *The efficacy of extraembryonic stem cells in improving blood flow within animal models of lower limb ischaemia.* Heart, 2016. **102**(1): p. 69-74.
269. Xiao, L., et al., *Quercetin attenuates high fat diet-induced atherosclerosis in apolipoprotein E knockout mice: A critical role of NADPH oxidase.* Food and Chemical Toxicology, 2017. **105**: p. 22-33.
270. Chanet, A., et al., *Naringin, the major grapefruit flavonoid, specifically affects atherosclerosis development in diet-induced hypercholesterolemia in mice.* Journal of Nutritional Biochemistry, 2012. **23**(5): p. 469-77.
271. Luo, Y., et al., *Isorhamnetin attenuates atherosclerosis by inhibiting macrophage apoptosis via PI3K/AKT activation and HO-1 induction.* PLoS ONE [Electronic Resource], 2015. **10**(3): p. e0120259.
272. Sun, G.B., et al., *Inhibitory effects of myricitrin on oxidative stress-induced endothelial damage and early atherosclerosis in ApoE-/- mice.* Toxicology & Applied Pharmacology, 2013. **271**(1): p. 114-26.
273. Qin, M., et al., *Myricitrin attenuates endothelial cell apoptosis to prevent atherosclerosis: An insight into PI3K/Akt activation and STAT3 signaling pathways.* Vascular Pharmacology, 2015. **70**: p. 23-34.
274. Liu, L., et al., *Oral administration of baicalin and geniposide induces regression of atherosclerosis via inhibiting dendritic cells in ApoE-knockout mice.* International Immunopharmacology, 2014. **20**(1): p. 197-204.
275. Wang, B., et al., *Baicalin and geniposide inhibit the development of atherosclerosis by increasing Wnt1 and inhibiting dickkopf-related protein-1 expression.* J Geriatr Cardiol, 2016. **13**(10): p. 846-854.
276. Schierwagen, R., et al., *Seven weeks of Western diet in apolipoprotein-E-deficient mice induce metabolic syndrome and non-alcoholic steatohepatitis with liver fibrosis.* Scientific reports, 2015. **5**: p. 12931.
277. Jeon, S.M., S.A. Lee, and M.S. Choi, *Antiobesity and vasoprotective effects of resveratrol in apoE-deficient mice.* J Med Food, 2014. **17**(3): p. 310-6.
278. Fuhrman, B., et al., *Licorice extract and its major polyphenol glabridin protect low-density lipoprotein against lipid peroxidation: in vitro and ex vivo studies in humans and in atherosclerotic apolipoprotein E-deficient mice.* American Journal of Clinical Nutrition, 1997. **66**(2): p. 267-75.
279. Meir, K.S. and E. Leitersdorf, *Atherosclerosis in the apolipoprotein E–deficient mouse.* Arteriosclerosis, thrombosis, and vascular biology, 2004. **24**(6): p. 1006-1014.
280. Tokede, O.A., J.M. Gaziano, and L. Djousse, *Effects of cocoa products/dark chocolate on serum lipids: a meta-analysis.* Eur J Clin Nutr, 2011. **65**(8): p. 879-86.

281. Hanasaki, Y., S. Ogawa, and S. Fukui, *The correlation between active oxygens scavenging and antioxidative effects of flavonoids.* Free Radic Biol Med, 1994. **16**(6): p. 845-50.
282. Wu, B.J., et al., *Antioxidants protect from atherosclerosis by a heme oxygenase-1 pathway that is independent of free radical scavenging.* Journal of Experimental Medicine, 2006. **203**(4): p. 1117-27.
283. Dower, J.I., et al., *Supplementation of the Pure Flavonoids Epicatechin and Quercetin Affects Some Biomarkers of Endothelial Dysfunction and Inflammation in (Pre)Hypertensive Adults: A Randomized Double-Blind, Placebo-Controlled, Crossover Trial.* J Nutr, 2015. **145**(7): p. 1459-63.
284. Chyu, K.Y., et al., *Differential effects of green tea-derived catechin on developing versus established atherosclerosis in apolipoprotein E-null mice.* Circulation, 2004. **109**(20): p. 2448-2453.
285. Blankenberg, S., et al., *Plasma concentrations and genetic variation of matrix metalloproteinase 9 and prognosis of patients with cardiovascular disease.* Circulation, 2003. **107**(12): p. 1579-1585.
286. Chen, Y.C., J. Rivera, and K. Peter, *Tandem Stenosis to Induce Atherosclerotic Plaque Instability in the Mouse.* Methods Mol Biol, 2015. **1339**: p. 333-8.
287. Reagan-Shaw, S., M. Nihal, and N. Ahmad, *Dose translation from animal to human studies revisited.* Faseb j, 2008. **22**(3): p. 659-61.
288. Allison, M.A., et al., *Ethnic-specific prevalence of peripheral arterial disease in the United States.* Am J Prev Med, 2007. **32**(4): p. 328-33.
289. Pell, J.P., *Impact of intermittent claudication on quality of life. The Scottish Vascular Audit Group.* Eur J Vasc Endovasc Surg, 1995. **9**(4): p. 469-72.
290. Kressler, J., M. Millard-Stafford, and G.L. Warren, *Quercetin and endurance exercise capacity: a systematic review and meta-analysis.* Med Sci Sports Exerc, 2011. **43**(12): p. 2396-404.
291. Hollinger, K., et al., *Long-term quercetin dietary enrichment decreases muscle injury in mdx mice.* Clinical Nutrition, 2015. **34**(3): p. 515-522.
292. Sanchez, M., et al., *Quercetin downregulates NADPH oxidase, increases eNOS activity and prevents endothelial dysfunction in spontaneously hypertensive rats.* J Hypertens, 2006. **24**(1): p. 75-84.
293. Derbré, F., et al., *Age associated low mitochondrial biogenesis may be explained by lack of response of PGC-1α to exercise training.* Age, 2012. **34**(3): p. 669-679.
294. Hirsch, A.T., et al., *A call to action: women and peripheral artery disease: a scientific statement from the American Heart Association.* Circulation, 2012. **125**(11): p. 1449-1472.
295. Hjermann, I., et al., *Effect of diet and smoking intervention on the incidence of coronary heart disease: report from the Oslo Study Group of a randomised trial in healthy men.* The Lancet, 1981. **318**(8259): p. 1303-1310.
296. Surra, J.C., et al., *In comparison with palm oil, dietary nut supplementation delays the progression of atherosclerotic lesions in female apoE-deficient mice.* Br J Nutr, 2013. **109**(2): p. 202-9.
297. Nergiz-Unal, R., et al., *Atheroprotective effect of dietary walnut intake in ApoE-deficient mice: involvement of lipids and coagulation factors.* Thromb Res, 2013. **131**(5): p. 411-7.
298. Sakalihasan, N., R. Limet, and O.D. Defawe, *Abdominal aortic aneurysm.* Lancet, 2005. **365**(9470): p. 1577-89.

299. Thompson, R.W., et al., *Pathophysiology of abdominal aortic aneurysms: insights from the elastase-induced model in mice with different genetic backgrounds.* Ann N Y Acad Sci, 2006. **1085**: p. 59-73.
300. Golledge, J. and P.E. Norman, *Atherosclerosis and abdominal aortic aneurysm: cause, response, or common risk factors?* 2010.
301. Tilson, M.D., *Aortic aneurysms and atherosclerosis.* Circulation, 1992. **85**(1): p. 378-9.
302. Singh, K., et al., *Prevalence of and risk factors for abdominal aortic aneurysms in a population-based study: The Tromsø Study.* American journal of epidemiology, 2001. **154**(3): p. 236-244.
303. Daugherty, A. and L. Cassis, *Angiotensin II and abdominal aortic aneurysms.* Current hypertension reports, 2004. **6**(6): p. 442-446.
304. Surra, J.C., et al., *In comparison with palm oil, dietary nut supplementation delays the progression of atherosclerotic lesions in female apoE-deficient mice.* British Journal of Nutrition, 2013. **109**(2): p. 202-9.
305. Shah, P.K., *Inflammation, metalloproteinases, and increased proteolysis: an emerging pathophysiological paradigm in aortic aneurysm.* Circulation, 1997. **96**(7): p. 2115-7.
306. de Souza, R.G.M., et al., *Nuts and Human Health Outcomes: A Systematic Review.* Nutrients, 2017. **9**(12): p. 1311.
307. Ruisinger, J.F., et al., *Statins and almonds to lower lipoproteins (the STALL Study).* J Clin Lipidol, 2015. **9**(1): p. 58-64.
308. Matthews, E., et al., *Meta-analysis of the association between peripheral artery disease and growth of abdominal aortic aneurysms.* British Journal of Surgery, 2017.
309. Berk, B.C., J. Haendeler, and J. Sottile, *Angiotensin II, atherosclerosis, and aortic aneurysms.* The Journal of clinical investigation, 2000. **105**(11): p. 1525-1526.
310. Niazi, Z.R., et al., *EPA:DHA 6:1 prevents angiotensin II-induced hypertension and endothelial dysfunction in rats: role of NADPH oxidase- and COX-derived oxidative stress.* Hypertens Res, 2017. **40**(12): p. 966-975.
311. Frenoux, J.-M.R., et al., *A polyunsaturated fatty acid diet lowers blood pressure and improves antioxidant status in spontaneously hypertensive rats.* The Journal of nutrition, 2001. **131**(1): p. 39-45.
312. Lu, H., et al., *Involvement of the renin-angiotensin system in abdominal and thoracic aortic aneurysms.* Clin Sci (Lond), 2012. **123**(9): p. 531-43.
313. Villard, C. and R. Hultgren, *Abdominal aortic aneurysm: Sex differences.* Maturitas, 2018. **109**: p. 63-69.
314. Starr, J.E. and V. Halpern, *Abdominal aortic aneurysms in women.* Journal of Vascular Surgery, 2013. **57**(4, Supplement): p. 3S-10S.
315. Brown, P.M., D.T. Zelt, and B. Sobolev, *The risk of rupture in untreated aneurysms: the impact of size, gender, and expansion rate.* J Vasc Surg, 2003. **37**(2): p. 280-4.
316. Curb, J.D., et al., *Serum lipid effects of a high–monounsaturated fat diet based on macadamia nuts.* Archives of Internal Medicine, 2000. **160**(8): p. 1154-1158.
317. Quinn, L. and H. Tang, *Antioxidant properties of phenolic compounds in macadamia nuts.* Journal of the American Oil Chemists' Society, 1996. **73**(11): p. 1585-1588.
318. Hiraoka-Yamamoto, J., et al., *Serum lipid effects of a monounsaturated (palmitoleic) fatty acid-rich diet based on macadamia nuts in healthy, young Japanese women.* Clinical and Experimental Pharmacology and Physiology, 2004. **31**(s2).
319. Morgan, W.A. and B.J. Clayshulte, *Pecans lower low density lipoprotein cholesterol in people with normal lipid levels.* Journal of the American Dietetic Association, 2000. **100**(3): p. 312-318.

320. Golledge, J., et al., *Lack of an effective drug therapy for abdominal aortic aneurysm.* J Intern Med, 2019.
321. Daugherty, A. and L.A. Cassis, *Mouse models of abdominal aortic aneurysms.* Arterioscler Thromb Vasc Biol, 2004. **24**(3): p. 429-34.
322. Golledge, J., *Abdominal aortic aneurysm: update on pathogenesis and medical treatments.* Nat Rev Cardiol, 2018.
323. Forester, N.D., et al., *Functional characterization of T cells in abdominal aortic aneurysms.* Immunology, 2005. **115**(2): p. 262-270.
324. Lamkanfi, M., et al., *Glyburide inhibits the Cryopyrin/Nalp3 inflammasome.* J Cell Biol, 2009. **187**(1): p. 61-70.
325. Fiolet, A.T., et al., *Colchicine in stable coronary artery disease.* Clinical therapeutics, 2019. **41**(1): p. 30-40.
326. Emmerson, B.T., *The management of gout.* New England Journal of Medicine, 1996. **334**(7): p. 445-451.
327. Verma, S., et al., *Colchicine in cardiac disease: a systematic review and meta-analysis of randomized controlled trials.* BMC Cardiovasc Disord, 2015. **15**: p. 96.
328. Biros, E., et al., *Downregulation of transforming growth factor, beta receptor 2 and Notch signaling pathway in human abdominal aortic aneurysm.* Atherosclerosis, 2012. **221**(2): p. 383-386.
329. Krishna, S.M., et al., *A peptide antagonist of thrombospondin-1 promotes abdominal aortic aneurysm progression in the angiotensin II–infused apolipoprotein-E–deficient mouse.* Arteriosclerosis, thrombosis, and vascular biology, 2015. **35**(2): p. 389-398.
330. Page, P., *Beyond statistical significance: clinical interpretation of rehabilitation research literature.* International journal of sports physical therapy, 2014. **9**(5): p. 726-736.
331. Villard, C., et al., *Differences in Elastin and Elastolytic Enzymes between Men and Women with Abdominal Aortic Aneurysm.* Aorta (Stamford, Conn.), 2014. **2**(5): p. 179-185.
332. Bhamidipati, C.M., et al., *Development of a novel murine model of aortic aneurysms using peri-adventitial elastase.* Surgery, 2012. **152**(2): p. 238-246.
333. Parr, A., et al., *Thrombus volume is associated with cardiovascular events and aneurysm growth in patients who have abdominal aortic aneurysms.* Journal of vascular surgery, 2011. **53**(1): p. 28-35.
334. Mower, W.R., W.J. Quiñones, and S.S. Gambhir, *Effect of intraluminal thrombus on abdominal aortic aneurysm wall stress.* Journal of Vascular Surgery, 1997. **26**(4): p. 602-608.
335. Nidorf, S.M., et al., *Low-dose colchicine for secondary prevention of cardiovascular disease.* J Am Coll Cardiol, 2013. **61**(4): p. 404-410.
336. Terkeltaub, R.A., et al., *High versus low dosing of oral colchicine for early acute gout flare: Twenty-four-hour outcome of the first multicenter, randomized, double-blind, placebo-controlled, parallel-group, dose-comparison colchicine study.* Arthritis Rheum, 2010. **62**(4): p. 1060-8.
337. Dale, M.A., M.K. Ruhlman, and B.T. Baxter, *Inflammatory cell phenotypes in AAAs: their role and potential as targets for therapy.* Arteriosclerosis, thrombosis, and vascular biology, 2015. **35**(8): p. 1746-1755.
338. Craighead, D.H., et al., *Acute lysyl oxidase inhibition alters microvascular function in normotensive but not hypertensive men and women.* Am J Physiol Heart Circ Physiol, 2018. **314**(3): p. H424-h433.
339. Hackam, D.G., *Translating animal research into clinical benefit.* BMJ (Clinical research ed.), 2007. **334**(7586): p. 163-164.

340. Mohamed Omer, S., *A new mouse model of peripheral artery disease: development, validation and assessment of a potential intervention and a therapeutic target*. 2019, James Cook University.
341. Higgins, J.P., et al., *The Cochrane Collaboration's tool for assessing risk of bias in randomised trials.* Bmj, 2011. **343**: p. d5928.
342. Knab, A.M., et al., *Repeatability of exercise behaviors in mice.* Physiology & behavior, 2009. **98**(4): p. 433-440.
343. McDermott, M.M., et al., *Effect of resveratrol on walking performance in older people with peripheral artery disease: the RESTORE randomized clinical trial.* JAMA cardiology, 2017. **2**(8): p. 902-907.
344. Spartalis, M., et al., *The Beneficial Therapy with Colchicine for Atherosclerosis via Anti-inflammation and Decrease in Hypertriglyceridemia.* Cardiovasc Hematol Agents Med Chem, 2018. **16**(2): p. 74-80.
345. Tardif, J.C., et al., *Efficacy and Safety of Low-Dose Colchicine after Myocardial Infarction.* N Engl J Med, 2019.

APPENDIX

A. Copyright permission from publishers to use my primary authored material

1. PloS ONE

2. Atherosclerosis

B. LME model raw outputs

Below are summaries for all LME output. Full outputs and rationale for all LME model analyses can be found on the Tropical Data Hub (https://tropicaldatahub.org/, DOI: 10.25903/5e2541346b21b)

1. LME model analysis of suprarenal aortic diameter as measured by ultrasound in mice receiving control diet or a diet enriched with tree nuts

```
## Linear mixed-effects model fit by REML
##  Data: James.US.data
##         AIC       BIC   logLik
##   -147.6421 -105.8716 87.82105
##
## Random effects:
##  Formula: ~1 | Mouse.number
##         (Intercept)  Residual
## StdDev:  0.02206586 0.1175192
##
## Fixed effects: log.SRA ~ Time.f * Treatment
##                            Value  Std.Error  DF   t-value p-value
## (Intercept)           0.4446628 0.02900067 114 15.332843  0.0000
## Time.f23             -0.0465863 0.04030875 114 -1.155735  0.2502
## Time.f34              0.0077178 0.04167352 114  0.185196  0.8534
## Time.f41              0.0439416 0.04339179 114  1.012670  0.3134
## Time.f48             -0.0183617 0.04339179 114 -0.423160  0.6730
## Time.f54             -0.0493740 0.04443008 114 -1.111274  0.2688
## TreatmentT           -0.0022149 0.04101315  32 -0.054006  0.9573
## Time.f23:TreatmentT -0.0481214 0.05700519 114 -0.844158  0.4003
## Time.f34:TreatmentT  0.0220756 0.06179881 114  0.357218  0.7216
## Time.f41:TreatmentT -0.0521528 0.06399056 114 -0.815007  0.4168
## Time.f48:TreatmentT -0.0017302 0.06671329 114 -0.025935  0.9794
## Time.f54:TreatmentT  0.0973844 0.06739196 114  1.445045  0.1512
##  Correlation:
##                      (Intr) Tm.f23 Tm.f34 Tm.f41 Tm.f48 Tm.f54 TrtmnT
## Time.f23             -0.695
## Time.f34             -0.672  0.484
## Time.f41             -0.646  0.464  0.451
## Time.f48             -0.646  0.464  0.451  0.436
## Time.f54             -0.630  0.454  0.441  0.426  0.426
## TreatmentT           -0.707  0.491  0.475  0.456  0.456  0.446
## Time.f23:TreatmentT  0.491 -0.707 -0.342 -0.328 -0.328 -0.321 -0.695
## Time.f34:TreatmentT  0.453 -0.326 -0.674 -0.304 -0.304 -0.297 -0.641
## Time.f41:TreatmentT  0.438 -0.315 -0.306 -0.678 -0.295 -0.289 -0.619
## Time.f48:TreatmentT  0.420 -0.302 -0.293 -0.283 -0.650 -0.277 -0.594
## Time.f54:TreatmentT  0.416 -0.299 -0.291 -0.281 -0.281 -0.659 -0.588
##                     T.23:T T.34:T T.41:T T.48:T
## Time.f23
## Time.f34
## Time.f41
## Time.f48
## Time.f54
## TreatmentT
```

```
## Time.f23:TreatmentT
## Time.f34:TreatmentT  0.461
## Time.f41:TreatmentT  0.445  0.415
## Time.f48:TreatmentT  0.427  0.398  0.387
## Time.f54:TreatmentT  0.423  0.393  0.382  0.368
##
## Standardized Within-Group Residuals:
##         Min          Q1         Med          Q3         Max
## -2.78994218 -0.56353271  0.04935935  0.63057577  2.50258277
##
## Number of Observations: 158
## Number of Groups: 34
```

```
anova(mouse.US.lme3)
```

```
##                   numDF denDF   F-value p-value
## (Intercept)           1   114 1789.2240  <.0001
## Time.f                5   114    2.4574  0.0373
## Treatment             1    32    0.0656  0.7994
## Time.f:Treatment      5   114    1.2011  0.3132
```

```
#LME model was performed on Log transformed data as this greatly improved
the qqnorm plot and residual versus fit of the models
```

2. LME model analysis of systolic blood pressure in mice receiving control diet or a diet enriched with tree nuts

```
## Linear mixed-effects model fit by REML
##  Data: James.BP.data
##        AIC      BIC    logLik
##   830.8527 859.8347 -404.4263
##
## Random effects:
##  Formula: ~1 | Mouse.number
##         (Intercept) Residual
## StdDev:    4.074523 6.848228
##
## Variance function:
##  Structure: Different standard deviations per stratum
##  Formula: ~1 | AngII.Effect
##  Parameter estimates:
##    FALSE     TRUE
## 1.000000 2.768527
## Fixed effects: BP.Systolic ~ Time.f * Treatment
##                          Value Std.Error DF  t-value p-value
## (Intercept)          89.91900  1.987796 71 45.23554  0.0000
## Time.f24              3.12021  2.394468 71  1.30309  0.1968
## Time.f35             17.93535  5.542767 71  3.23581  0.0018
## Time.f49              6.19055  5.552359 71  1.11494  0.2686
## TreatmentT            3.82609  2.772476 32  1.38003  0.1771
## Time.f24:TreatmentT  -2.47315  3.354238 71 -0.73732  0.4634
## Time.f35:TreatmentT -19.45527  8.356151 71 -2.32826  0.0228
## Time.f49:TreatmentT  -2.38143  8.896915 71 -0.26767  0.7897
##  Correlation:
##                      (Intr) Tm.f24 Tm.f35 Tm.f49 TrtmnT T.24:T T.35:T
## Time.f24             -0.625
## Time.f35             -0.266  0.221
## Time.f49             -0.271  0.225  0.099
## TreatmentT           -0.717  0.448  0.191  0.194
## Time.f24:TreatmentT   0.446 -0.714 -0.158 -0.160 -0.617
## Time.f35:TreatmentT   0.176 -0.147 -0.663 -0.066 -0.246  0.203
## Time.f49:TreatmentT   0.169 -0.140 -0.062 -0.624 -0.233  0.193  0.082
##
## Standardized Within-Group Residuals:
##        Min         Q1        Med         Q3        Max
## -1.9484134 -0.5298036 -0.1322914  0.4827106  2.6270456
##
## Number of Observations: 111
## Number of Groups: 34
```

```
anova(mouse.BP.lme1s)
```

```
##                   numDF denDF  F-value p-value
## (Intercept)           1    71 7662.280  <.0001
## Time.f                3    71    2.034  0.1168
## Treatment             1    32    0.710  0.4057
## Time.f:Treatment      3    71    1.832  0.1492
```

```
#Log transformation of data and exclusion of outliers did not markedly imp
rove the qqnorm or residual versus fit of the data. Model fit was improved
most by allowing for different standard deviations per stratum, due to the
difference in variation between mice receiving Ang II versus mice not rece
iving Ang II.
```

3. LME model analysis of diastolic blood pressure in mice receiving control diet or a diet enriched with tree nuts

```
## Linear mixed-effects model fit by REML
##  Data: James.BP.data
##       AIC     BIC   logLik
##   820.846 849.828 -399.423
##
## Random effects:
##  Formula: ~1 | Mouse.number
##         (Intercept) Residual
## StdDev:    2.500323  7.15849
##
## Variance function:
##  Structure: Different standard deviations per stratum
##  Formula: ~1 | AngII.Effect
##  Parameter estimates:
##    FALSE     TRUE
## 1.000000 2.483678
## Fixed effects: BP.Diastolic ~ Time.f * Treatment
##                          Value Std.Error DF  t-value p-value
## (Intercept)          69.25738  1.894895 71 36.54945  0.0000
## Time.f24              3.23281  2.497446 71  1.29445  0.1997
## Time.f35             12.81476  5.252723 71  2.43964  0.0172
## Time.f49              1.21599  5.257573 71  0.23128  0.8178
## TreatmentT            4.17399  2.640591 32  1.58070  0.1238
## Time.f24:TreatmentT  -3.11517  3.502276 71 -0.88947  0.3768
## Time.f35:TreatmentT -15.69855  7.900781 71 -1.98696  0.0508
## Time.f49:TreatmentT  -0.15056  8.396411 71 -0.01793  0.9857
##  Correlation:
##                      (Intr) Tm.f24 Tm.f35 Tm.f49 TrtmnT T.24:T T.35:T
## Time.f24             -0.681
## Time.f35             -0.322  0.244
## Time.f49             -0.324  0.246  0.118
## TreatmentT           -0.718  0.489  0.231  0.233
## Time.f24:TreatmentT  0.486 -0.713 -0.174 -0.175 -0.674
## Time.f35:TreatmentT  0.214 -0.162 -0.665 -0.079 -0.298  0.225
## Time.f49:TreatmentT  0.203 -0.154 -0.074 -0.626 -0.282  0.212  0.097
##
## Standardized Within-Group Residuals:
##         Min          Q1         Med          Q3         Max
## -1.84677300 -0.57878818 -0.06922858  0.55420846  2.71868717
##
## Number of Observations: 111
## Number of Groups: 34
```

```
anova(mouse.BP.lmedbps)
```

```
##                   numDF denDF  F-value p-value
## (Intercept)           1    71 5988.529  <.0001
## Time.f                3    71    0.832  0.4807
## Treatment             1    32    1.089  0.3045
## Time.f:Treatment      3    71    1.409  0.2472
```

```
#Log transformation of data and exclusion of outliers did not markedly imp
rove the qqnorm or residual versus fit of the data. Model fit was improved
most by allowing for different standard deviations per stratum, due to the
difference in variation between mice receiving Ang II versus mice not rece
iving Ang II.
```

4. LME model analysis of body weight in mice receiving control diet or a diet enriched with tree nuts

```
## Linear mixed-effects model fit by REML
##  Data: James.BW.data
##   Subset: divsd.resids1 > -2 & divsd.resids1 < 2
##        AIC      BIC    logLik
##   1614.317 1879.752 -749.1586
##
## Random effects:
##  Formula: ~1 | Mouse.number
##         (Intercept)  Residual
## StdDev:    1.725751 0.5509257
##
## Fixed effects: BW ~ Time.f * Treatment
##                          Value Std.Error  DF  t-value p-value
## (Intercept)         25.424766 0.4421801 686 57.49866  0.0000
## Time.f3              0.462660 0.1981260 686  2.33518  0.0198
## Time.f5              0.581116 0.1954181 686  2.97371  0.0030
## Time.f7              0.492881 0.1954181 686  2.52219  0.0119
## Time.f9              0.804646 0.1954181 686  4.11756  0.0000
## Time.f11             1.298763 0.1954181 686  6.64608  0.0000
## Time.f13             1.368910 0.1981260 686  6.90929  0.0000
## Time.f15             1.363469 0.1954181 686  6.97719  0.0000
## Time.f17             1.658927 0.1983935 686  8.36180  0.0000
## Time.f19             1.828175 0.1954181 686  9.35520  0.0000
## Time.f21             1.954072 0.1983934 686  9.84948  0.0000
## Time.f23             1.581116 0.1954181 686  8.09094  0.0000
## Time.f25             2.069352 0.1954181 686 10.58936  0.0000
## Time.f27             1.307535 0.1983876 686  6.59081  0.0000
## Time.f29             2.239022 0.1984783 686 11.28094  0.0000
## Time.f31             2.661509 0.2019057 686 13.18194  0.0000
## Time.f33             2.094267 0.2015465 686 10.39098  0.0000
## Time.f35             2.734937 0.2099502 686 13.02660  0.0000
## Time.f37             2.859685 0.2147549 686 13.31604  0.0000
## Time.f39             3.611348 0.2100201 686 17.19525  0.0000
## Time.f41             3.447506 0.2148310 686 16.04753  0.0000
## Time.f43             3.511348 0.2100201 686 16.71910  0.0000
## Time.f45             3.827115 0.2264737 686 16.89872  0.0000
## Time.f47             3.573525 0.2264686 686 15.77934  0.0000
## Time.f49             3.334425 0.2100201 686 15.87669  0.0000
## Time.f51             3.680579 0.2100201 686 17.52489  0.0000
## Time.f53             3.283921 0.2148321 686 15.28599  0.0000
## Time.f55             3.475588 0.2148321 686 16.17816  0.0000
## TreatmentT           0.981116 0.6233510  32  1.57394  0.1253
## Time.f3:TreatmentT   0.231457 0.2737920 686  0.84538  0.3982
## Time.f5:TreatmentT   0.389472 0.2718389 686  1.43273  0.1524
## Time.f7:TreatmentT   0.874071 0.2739865 686  3.19020  0.0015
## Time.f9:TreatmentT   0.718884 0.2718389 686  2.64452  0.0084
## Time.f11:TreatmentT  0.524291 0.2739689 686  1.91369  0.0561
## Time.f13:TreatmentT  0.660502 0.2737920 686  2.41242  0.0161
## Time.f15:TreatmentT  0.690835 0.2739689 686  2.52158  0.0119
## Time.f17:TreatmentT  0.529308 0.2739856 686  1.93188  0.0538
## Time.f19:TreatmentT  0.626129 0.2739689 686  2.28540  0.0226
```

```
## Time.f21:TreatmentT  0.810634 0.2739855 686  2.95867  0.0032
## Time.f23:TreatmentT  0.713001 0.2718389 686  2.62288  0.0089
## Time.f25:TreatmentT  0.630648 0.2718389 686  2.31993  0.0206
## Time.f27:TreatmentT  0.605061 0.2760911 686  2.19153  0.0287
## Time.f29:TreatmentT  0.318134 0.2761824 686  1.15190  0.2498
## Time.f31:TreatmentT  0.443070 0.2810292 686  1.57660  0.1153
## Time.f33:TreatmentT  0.874502 0.2943332 686  2.97113  0.0031
## Time.f35:TreatmentT  0.405813 0.3107090 686  1.30609  0.1920
## Time.f37:TreatmentT  0.945877 0.3083733 686  3.06731  0.0022
## Time.f39:TreatmentT  0.694214 0.3050949 686  2.27540  0.0232
## Time.f41:TreatmentT  0.238056 0.3084263 686  0.77184  0.4405
## Time.f43:TreatmentT  0.625379 0.3266227 686  1.91468  0.0559
## Time.f45:TreatmentT  0.375554 0.3289879 686  1.14154  0.2540
## Time.f47:TreatmentT  0.329425 0.3374350 686  0.97626  0.3293
## Time.f49:TreatmentT  0.399346 0.3379402 686  1.18171  0.2377
## Time.f51:TreatmentT  0.390433 0.3379402 686  1.15533  0.2484
## Time.f53:TreatmentT  0.071248 0.3210849 686  0.22190  0.8245
## Time.f55:TreatmentT -0.107918 0.3210849 686 -0.33611  0.7369
##
## Standardized Within-Group Residuals:
##         Min          Q1         Med          Q3         Max
## -4.42824903 -0.51286072  0.02922378  0.61075966  4.35480859
##
## Number of Observations: 774
## Number of Groups: 34
```

```
anova(mouse.BW.lme2)
```

```
##                  numDF denDF  F-value p-value
## (Intercept)          1   686 8945.688  <.0001
## Time.f              27   686  102.571  <.0001
## Treatment            1    32    6.464  0.0160
## Time.f:Treatment    27   686    1.459  0.0636
```

```
#Best model fit was achieved after exclusion of outliers of + or - 2 stand
ard deviations
```

5. LME model analysis of food consumption in mice receiving control diet or a diet enriched with tree nuts

```
## Linear mixed-effects model fit by REML
##  Data: James.Food.data
##         AIC      BIC   logLik
##   -64.93848 122.7656 88.46924
##
## Random effects:
##  Formula: ~1 | Mouse.number
##         (Intercept)  Residual
## StdDev:   0.1185192 0.1201745
##
## Fixed effects: log.Consumption ~ Time.f * Treatment
##                            Value  Std.Error  DF   t-value p-value
## (Intercept)           1.2898925 0.06965094 198 18.519384  0.0000
## Time.f5               0.0060499 0.07600502 198  0.079598  0.9366
## Time.f7              -0.0711737 0.07600502 198 -0.936434  0.3502
## Time.f9              -0.0081305 0.07600502 198 -0.106974  0.9149
## Time.f11             -0.0071024 0.07600502 198 -0.093446  0.9256
## Time.f13             -0.0301239 0.07600502 198 -0.396340  0.6923
## Time.f15             -0.0062747 0.07600502 198 -0.082557  0.9343
## Time.f17              0.0128573 0.07600502 198  0.169164  0.8658
## Time.f19              0.0751426 0.07600502 198  0.988653  0.3240
## Time.f21              0.0099272 0.07600502 198  0.130612  0.8962
## Time.f23              0.1178015 0.07600502 198  1.549917  0.1228
## Time.f25              0.1308587 0.07600502 198  1.721711  0.0867
## Time.f27              0.1241286 0.07600502 198  1.633163  0.1040
## Time.f29              0.0048332 0.07600502 198  0.063590  0.9494
## Time.f31              0.2115292 0.07600502 198  2.783095  0.0059
## Time.f33              0.1753570 0.07600502 198  2.307176  0.0221
## Time.f35              0.0628546 0.07844356 198  0.801271  0.4239
## Time.f37              0.1215065 0.07377773 198  1.646927  0.1012
## Time.f39              0.2027796 0.07377773 198  2.748521  0.0065
## Time.f41              0.2275993 0.07377773 198  3.084932  0.0023
## Time.f43              0.1091302 0.07377773 198  1.479176  0.1407
## Time.f45              0.1936745 0.07377773 198  2.625108  0.0093
## Time.f47              0.0169342 0.07377773 198  0.229530  0.8187
## Time.f49              0.1180535 0.07377773 198  1.600124  0.1112
## Time.f51              0.1156309 0.07377773 198  1.567287  0.1186
## Time.f53              0.1355269 0.07377773 198  1.836962  0.0677
## Time.f55              0.0825683 0.07377773 198  1.119150  0.2644
## TreatmentT            0.0627124 0.10358301  13  0.605431  0.5553
## Time.f5:TreatmentT   -0.0324361 0.11400753 198 -0.284508  0.7763
## Time.f7:TreatmentT    0.0024031 0.11400753 198  0.021078  0.9832
## Time.f9:TreatmentT   -0.0344672 0.11400753 198 -0.302324  0.7627
## Time.f11:TreatmentT -0.0778900 0.11400753 198 -0.683201  0.4953
## Time.f13:TreatmentT  0.0205445 0.11400753 198  0.180203  0.8572
## Time.f15:TreatmentT -0.0001971 0.11400753 198 -0.001729  0.9986
## Time.f17:TreatmentT -0.0251009 0.11400753 198 -0.220169  0.8260
## Time.f19:TreatmentT -0.0090513 0.11400753 198 -0.079392  0.9368
## Time.f21:TreatmentT  0.0112175 0.11400753 198  0.098393  0.9217
## Time.f23:TreatmentT -0.0366283 0.11400753 198 -0.321279  0.7483
## Time.f25:TreatmentT -0.0636479 0.11400753 198 -0.558278  0.5773
```

```
## Time.f27:TreatmentT -0.0309241 0.11400753 198 -0.271246  0.7865
## Time.f29:TreatmentT -0.1532232 0.11400753 198 -1.343974  0.1805
## Time.f31:TreatmentT -0.1516728 0.11400753 198 -1.330375  0.1849
## Time.f33:TreatmentT -0.1081485 0.11400753 198 -0.948608  0.3440
## Time.f35:TreatmentT -0.0211188 0.11564751 198 -0.182614  0.8553
## Time.f37:TreatmentT -0.0532492 0.10959483 198 -0.485873  0.6276
## Time.f39:TreatmentT -0.0102640 0.10959483 198 -0.093654  0.9255
## Time.f41:TreatmentT -0.0850806 0.10959483 198 -0.776320  0.4385
## Time.f43:TreatmentT -0.0345069 0.10885587 198 -0.316996  0.7516
## Time.f45:TreatmentT -0.0830427 0.10885587 198 -0.762868  0.4464
## Time.f47:TreatmentT -0.0549836 0.11036723 198 -0.498188  0.6189
## Time.f49:TreatmentT -0.2056301 0.11036723 198 -1.863145  0.0639
## Time.f51:TreatmentT -0.0479623 0.11036723 198 -0.434571  0.6643
## Time.f53:TreatmentT -0.0524931 0.11036723 198 -0.475622  0.6349
## Time.f55:TreatmentT -0.1531251 0.11036723 198 -1.387414  0.1669
##
## Standardized Within-Group Residuals:
##         Min          Q1         Med          Q3         Max
## -2.23408607 -0.41435881 -0.02724344  0.37390832  5.41553764
##
## Number of Observations: 265
## Number of Groups: 15
```

```
anova(mouse.Food.lme3)
```

```
##                   numDF denDF   F-value p-value
## (Intercept)           1   198 1819.3895  <.0001
## Time.f               26   198    3.7804  <.0001
## Treatment             1    13    0.0018  0.9664
## Time.f:Treatment     26   198    0.5296  0.9716
```

```
#Log transforming data greatly improves the qqnorm plot and fit of the mod
el.
```

6. LME model analysis of distance travelled measured by treadmill test in mice receiving control diet or a diet containing quercetin

```
## Linear mixed-effects model fit by REML
##  Data: James.TMT.data
##        AIC      BIC    logLik
##   535.8661 567.3411 -257.9331
##
## Random effects:
##  Formula: ~1 | Mouse.number
##         (Intercept)  Residual
## StdDev:   0.6985269 0.8575158
##
## Fixed effects: log.Distance ~ Time.f * Treatment
##                          Value Std.Error  DF   t-value p-value
## (Intercept)          4.307168 0.2358036 129 18.265914  0.0000
## Time.f10             0.501639 0.2585508 129  1.940196  0.0545
## Time.f20             1.026995 0.2585508 129  3.972122  0.0001
## Time.f30             1.084197 0.2585508 129  4.193363  0.0001
## TreatmentT           0.140787 0.3298320  43  0.426845  0.6716
## Time.f10:TreatmentT  0.159205 0.3616497 129  0.440220  0.6605
## Time.f20:TreatmentT -0.039674 0.3616497 129 -0.109703  0.9128
## Time.f30:TreatmentT -0.212081 0.3616497 129 -0.586427  0.5586
##  Correlation:
##                     (Intr) Tm.f10 Tm.f20 Tm.f30 TrtmnT T.10:T T.20:T
## Time.f10            -0.548
## Time.f20            -0.548  0.500
## Time.f30            -0.548  0.500  0.500
## TreatmentT          -0.715  0.392  0.392  0.392
## Time.f10:TreatmentT  0.392 -0.715 -0.357 -0.357 -0.548
## Time.f20:TreatmentT  0.392 -0.357 -0.715 -0.357 -0.548  0.500
## Time.f30:TreatmentT  0.392 -0.357 -0.357 -0.715 -0.548  0.500  0.500
##
## Standardized Within-Group Residuals:
##         Min          Q1         Med          Q3         Max
## -2.82486898 -0.50913474  0.06043225  0.63378506  1.64397887
##
## Number of Observations: 180
## Number of Groups: 45
```

```
anova(mouse.TMT.lme1b)
```

```
##                  numDF denDF   F-value p-value
## (Intercept)          1   129 1688.4381  <.0001
## Time.f               3   129   13.4650  <.0001
## Treatment            1    43    0.2317  0.6327
## Time.f:Treatment     3   129    0.3556  0.7852
```

```
#Log transformation drastically improved qqnorm and residuals vs fit plots
.
```

7. LME model analysis of blood flow measured by laser Doppler perfusion imaging in mice receiving control diet or a diet containing quercetin

```
## Linear mixed-effects model fit by REML
##  Data: James.LDI.data
##         AIC       BIC   logLik
##   -105.7584 -56.12595 66.87922
##
## Random effects:
##  Formula: ~1 | Mouse.number
##         (Intercept)  Residual
## StdDev:  0.06162658 0.1646556
##
## Fixed effects: BFR ~ Time.f * Treatment
##                          Value  Std.Error  DF    t-value p-value
## (Intercept)         1.0569587 0.03832083 213  27.581833  0.0000
## Time.f2            -0.4185054 0.05028118 213  -8.323301  0.0000
## Time.f3            -0.4349669 0.05028118 213  -8.650691  0.0000
## Time.f4            -0.6183156 0.05028118 213 -12.297159  0.0000
## Time.f5            -0.5462005 0.05028118 213 -10.862922  0.0000
## Time.f6            -0.6024650 0.05028118 213 -11.981918  0.0000
## TreatmentT         -0.0005823 0.05357577  43  -0.010869  0.9914
## Time.f2:TreatmentT -0.0203797 0.07031152 213  -0.289848  0.7722
## Time.f3:TreatmentT  0.0251659 0.07031152 213   0.357921  0.7208
## Time.f4:TreatmentT -0.0075077 0.07031152 213  -0.106778  0.9151
## Time.f5:TreatmentT -0.0287410 0.07031152 213  -0.408766  0.6831
## Time.f6:TreatmentT -0.0397070 0.07031152 213  -0.564730  0.5729
##  Correlation:
##                    (Intr) Tim.f2 Tim.f3 Tim.f4 Tim.f5 Tim.f6 TrtmnT T.2
:TT
## Time.f2            -0.673
## Time.f3            -0.673  0.513
## Time.f4            -0.673  0.513  0.513
## Time.f5            -0.673  0.513  0.513  0.513
## Time.f6            -0.673  0.513  0.513  0.513  0.513
## TreatmentT         -0.715  0.481  0.481  0.481  0.481  0.481
## Time.f2:TreatmentT  0.481 -0.715 -0.367 -0.367 -0.367 -0.367 -0.672
## Time.f3:TreatmentT  0.481 -0.367 -0.715 -0.367 -0.367 -0.367 -0.672  0.
512
## Time.f4:TreatmentT  0.481 -0.367 -0.367 -0.715 -0.367 -0.367 -0.672  0.
512
## Time.f5:TreatmentT  0.481 -0.367 -0.367 -0.367 -0.715 -0.367 -0.672  0.
512
## Time.f6:TreatmentT  0.481 -0.367 -0.367 -0.367 -0.367 -0.715 -0.672  0.
512
##                    T.3:TT T.4:TT T.5:TT
## Time.f2
## Time.f3
## Time.f4
## Time.f5
## Time.f6
## TreatmentT
## Time.f2:TreatmentT
## Time.f3:TreatmentT
```

```
## Time.f4:TreatmentT  0.512
## Time.f5:TreatmentT  0.512  0.512
## Time.f6:TreatmentT  0.512  0.512  0.512
##
## Standardized Within-Group Residuals:
##        Min         Q1        Med         Q3        Max
## -2.2796770 -0.6244929 -0.1083635  0.4732391  3.7931751
##
## Number of Observations: 268
## Number of Groups: 45
```

```
anova(mouse.LDI.lme1)
```

```
##                   numDF denDF   F-value p-value
## (Intercept)           1   213 2006.5694  <.0001
## Time.f                5   213   88.2091  <.0001
## Treatment             1    43    0.2117  0.6478
## Time.f:Treatment      5   213    0.2204  0.9535
```

```
#Transformation of data and exclusion of outliers did not improve
qqnorm or residual versus fit plots. Original LME was accepted.
```

8. LME model analysis of body weight of mice receiving control diet or a diet containing quercetin

```
## Linear mixed-effects model fit by REML
##  Data: James.BW.data
##   Subset: divsd.resids1 > -3 & divsd.resids1 < 3
##       AIC     BIC    logLik
##   703.607 743.886 -339.8035
##
## Random effects:
##  Formula: ~1 | Mouse.number
##         (Intercept)  Residual
## StdDev:    1.828009 0.8008082
##
## Fixed effects: BW ~ Time.f * Treatment
##                          Value Std.Error  DF  t-value p-value
## (Intercept)          29.409091 0.4254897 169 69.11822  0.0000
## Time.f1              -0.227273 0.2414528 169 -0.94127  0.3479
## Time.f14              0.174672 0.2449870 169  0.71299  0.4768
## Time.f21              0.318182 0.2414528 169  1.31778  0.1894
## Time.f35             -0.045455 0.2414528 169 -0.18825  0.8509
## TreatmentT            0.286561 0.5951568  43  0.48149  0.6326
## Time.f1:TreatmentT   -0.033597 0.3377338 169 -0.09948  0.9209
## Time.f14:TreatmentT  -0.259405 0.3425686 169 -0.75724  0.4500
## Time.f21:TreatmentT   0.073123 0.3377338 169  0.21651  0.8289
## Time.f35:TreatmentT   0.287042 0.3400500 169  0.84412  0.3998
##  Correlation:
##                      (Intr) Tim.f1 Tm.f14 Tm.f21 Tm.f35 TrtmnT T.1:TT
## Time.f1              -0.284
## Time.f14             -0.280  0.493
## Time.f21             -0.284  0.500  0.493
## Time.f35             -0.284  0.500  0.493  0.500
## TreatmentT           -0.715  0.203  0.200  0.203  0.203
## Time.f1:TreatmentT    0.203 -0.715 -0.352 -0.357 -0.357 -0.284
## Time.f14:TreatmentT   0.200 -0.352 -0.715 -0.352 -0.352 -0.280  0.493
## Time.f21:TreatmentT   0.203 -0.357 -0.352 -0.715 -0.357 -0.284  0.500
## Time.f35:TreatmentT   0.201 -0.355 -0.350 -0.355 -0.710 -0.282  0.497
##                      T.14:T T.21:T
## Time.f1
## Time.f14
## Time.f21
## Time.f35
## TreatmentT
## Time.f1:TreatmentT
## Time.f14:TreatmentT
## Time.f21:TreatmentT   0.493
## Time.f35:TreatmentT   0.489  0.497
##
## Standardized Within-Group Residuals:
##         Min          Q1         Med          Q3         Max
## -3.27058640 -0.50434041  0.04525939  0.54097929  3.53976064
##
## Number of Observations: 222
## Number of Groups: 45
```

```r
anova(mouse.BW.lme1a)
```

```
##                   numDF denDF   F-value p-value
## (Intercept)           1   169 11359.967  <.0001
## Time.f                4   169     3.242  0.0136
## Treatment             1    43     0.294  0.5902
## Time.f:Treatment      4   169     0.654  0.6250
```

```r
#Large improvement in qqnorm and residual versus fit plots when outliers > 3 standard deviations are excluded.
```

9. LME model analysis of infrarenal aortic diameter as measured by ultrasound in mice undergoing sham surgery or mice undergoing elastase surgery with oral BAPN

```
## Linear mixed-effects model fit by REML
##  Data: James.US.data
##        AIC      BIC    logLik
##   28.43573 76.38503 -0.217863
##
## Random effects:
##  Formula: ~1 | Mouse.number
##         (Intercept)  Residual
## StdDev:  0.08544664 0.2116567
##
## Fixed effects: log.IRA ~ time.f * Treatment
##                            Value  Std.Error  DF   t-value p-value
## (Intercept)          -0.3222824 0.04167320 185  -7.73356  0.0000
## time.f7               0.2201651 0.05464952 185   4.02867  0.0001
## time.f28              0.5244373 0.05694238 185   9.20997  0.0000
## time.f42              0.9008413 0.05695337 185  15.81717  0.0000
## time.f63              1.6119979 0.05695337 185  28.30382  0.0000
## time.f80              1.9011336 0.05760902 185  33.00062  0.0000
## TreatmentS           -0.0066016 0.07387870  42  -0.08936  0.9292
## time.f7:TreatmentS   -0.2550198 0.09991249 185  -2.55243  0.0115
## time.f28:TreatmentS  -0.5374702 0.09961359 185  -5.39555  0.0000
## time.f42:TreatmentS  -0.8754869 0.09961988 185  -8.78828  0.0000
## time.f63:TreatmentS  -1.5398900 0.09961988 185 -15.45766  0.0000
## time.f80:TreatmentS  -1.7376846 0.10336631 185 -16.81094  0.0000
##  Correlation:
##                      (Intr) tim.f7 tm.f28 tm.f42 tm.f63 tm.f80 TrtmnS
## time.f7              -0.656
## time.f28             -0.629  0.480
## time.f42             -0.629  0.480  0.467
## time.f63             -0.629  0.480  0.467  0.469
## time.f80             -0.622  0.474  0.461  0.463  0.463
## TreatmentS           -0.564  0.370  0.355  0.355  0.355  0.351
## time.f7:TreatmentS    0.359 -0.547 -0.262 -0.262 -0.262 -0.259 -0.636
## time.f28:TreatmentS   0.360 -0.274 -0.572 -0.267 -0.267 -0.264 -0.638
## time.f42:TreatmentS   0.360 -0.274 -0.267 -0.572 -0.268 -0.265 -0.638
## time.f63:TreatmentS   0.360 -0.274 -0.267 -0.268 -0.572 -0.265 -0.638
## time.f80:TreatmentS   0.347 -0.264 -0.257 -0.258 -0.258 -0.557 -0.615
##                      t.7:TS t.28:T t.42:T t.63:T
## time.f7
## time.f28
## time.f42
## time.f63
## time.f80
## TreatmentS
## time.f7:TreatmentS
## time.f28:TreatmentS  0.475
## time.f42:TreatmentS  0.475  0.478
## time.f63:TreatmentS  0.475  0.478  0.479
## time.f80:TreatmentS  0.461  0.461  0.462  0.462
##
## Standardized Within-Group Residuals:
```

```
##          Min           Q1          Med           Q3          Max
## -3.615006425 -0.317850935  0.004396393  0.381744207  2.779703707
##
## Number of Observations: 239
## Number of Groups: 44
```

```
anova(mouse.US.lme3)
```

```
##                   numDF denDF  F-value p-value
## (Intercept)           1   185 150.0152  <.0001
## time.f                5   185 253.6157  <.0001
## Treatment             1    42 373.5833  <.0001
## time.f:Treatment      5   185  91.8336  <.0001
```

```
#Log transforming data greatly improved the qqnorm plot and residual versu
s fit of the model
```

10. LME model analysis of infrarenal aortic diameter as measured by ultrasound in mice undergoing elastase surgery with oral BAPN and either vehicle or colchicine gavage

```
## Linear mixed-effects model fit by REML
##  Data: James.US.data
##        AIC      BIC    logLik
##   154.7719 207.3523 -63.38595
##
## Random effects:
##  Formula: ~1 | Mouse.number
##         (Intercept)  Residual
## StdDev:  0.07298233 0.2693436
##
## Fixed effects: log.IRA ~ time.f * Treatment
##                            Value  Std.Error  DF   t-value p-value
## (Intercept)          -0.3222824 0.05094847 258 -6.325654  0.0000
## time.f7               0.2201651 0.06954422 258  3.165828  0.0017
## time.f28              0.5255064 0.07232692 258  7.265710  0.0000
## time.f42              0.9020352 0.07233152 258 12.470844  0.0000
## time.f63              1.6131918 0.07233152 258 22.302748  0.0000
## time.f80              1.9016724 0.07313996 258 26.000455  0.0000
## TreatmentT           -0.0284417 0.07205202  58 -0.394738  0.6945
## time.f7:TreatmentT   -0.0014799 0.09880226 258 -0.014979  0.9881
## time.f28:TreatmentT   0.0601250 0.10125084 258  0.593822  0.5532
## time.f42:TreatmentT   0.1496256 0.10175223 258  1.470490  0.1426
## time.f63:TreatmentT   0.0333287 0.10125414 258  0.329159  0.7423
## time.f80:TreatmentT  -0.0484155 0.10470680 258 -0.462391  0.6442
##  Correlation:
##                      (Intr) tim.f7 tm.f28 tm.f42 tm.f63 tm.f80 TrtmnT
## time.f7              -0.682
## time.f28             -0.656  0.481
## time.f42             -0.656  0.481  0.465
## time.f63             -0.656  0.481  0.465  0.467
## time.f80             -0.649  0.475  0.460  0.462  0.462
## TreatmentT           -0.707  0.483  0.464  0.464  0.464  0.459
## time.f7:TreatmentT    0.480 -0.704 -0.338 -0.338 -0.338 -0.335 -0.679
## time.f28:TreatmentT   0.469 -0.343 -0.714 -0.333 -0.333 -0.329 -0.663
## time.f42:TreatmentT   0.466 -0.342 -0.331 -0.711 -0.332 -0.328 -0.660
## time.f63:TreatmentT   0.469 -0.343 -0.333 -0.333 -0.714 -0.330 -0.663
## time.f80:TreatmentT   0.453 -0.332 -0.322 -0.322 -0.322 -0.699 -0.641
##                     t.7:TT t.28:T t.42:T t.63:T
## time.f7
## time.f28
## time.f42
## time.f63
## time.f80
## TreatmentT
## time.f7:TreatmentT
## time.f28:TreatmentT   0.484
## time.f42:TreatmentT   0.482  0.472
## time.f63:TreatmentT   0.484  0.475  0.473
## time.f80:TreatmentT   0.468  0.459  0.457  0.459
##
```

```
## Standardized Within-Group Residuals:
##         Min          Q1         Med          Q3         Max
## -4.27955460 -0.38697308  0.03040771  0.48831630  2.53587130
##
## Number of Observations: 328
## Number of Groups: 60
```

```
anova(mouse.US.lme3)
```

```
##                   numDF denDF  F-value p-value
## (Intercept)           1   258 762.4905  <.0001
## time.f                5   258 426.7133  <.0001
## Treatment             1    58   0.0102  0.9199
## time.f:Treatment      5   258   0.8333  0.5270
```

```
#Log transforming data greatly improved the qqnorm plot and residual versu
s fit of the model
```